AN EVALUATION OF LAKE AND RIVER LEVELS AS INDICATORS OF CLIMATE VARIABILITY IN TROPICAL SOUTHERN AFRICA

MAXWELL ESAU GWAZANTINI

DEPARTMENT OF GEOGRAPHY

UNIVERSITY OF ZULULAND

A thesis submitted in fulfilment of the degree of Master of Science

August 1999

TABLE OF CONTENTS

ACKNOWLEDGEMENTS

I thank the Malawian Meteorological department for making arrangements and allowing me to attend this course. Special thanks go to Prof. Mark Jury, Head of Geography Department at the University of Zululand, and the South African Water Research Commission for their support to make my study possible. I thank my family members for their patience during the period I have been away from home.

Special thanks go to the Namibia Chief Hydrologist, Mr. Van Langenhove (Namibia Water Department) for assisting in data acquisition and Mr. Rawlins (Hydrology Department-University of Zululand) for his assistance.

LIST OF FIGURES AND TABLES

Figures

Tables

ABSTRACT

Southern Africa has only a few large lakes, one of which is Lake Malawi. It forms part of the lower Zambezi River catchment and is part of the Great Rift Valley. Lake Malawi plays a significant role in socio- economic development particularly in food production, health, energy, transport, recreation, and environment. Changes in its level are related to variations in rainfall and the surrounding atmospheric circulation. Runoff is greatest in late summer following an active spell of the Inter Tropical Convergence Zone (ITCZ). This study looks at differences between years when the inflow to Lake Malawi is above and below normal using NCEP reanalysis composites. An understanding of factors governing variations of water resources will be useful to hydrologists and resource managers who deal with seasonal and inter-annual fluctuations.

To this end monthly lake level and rainfall data were analysed for variability in the period 1915 to 1995. From the lake level time series, differences in the minimum and maximum level from beginning to end of summer were calculated, then years with high inflow and low inflow were identified in the period overlapping with the NCEP reanalysis data 1958 - 1998. The Zambezi annual flows have been included to study regional coherence of climatic variability. Composites were generated during and prior to the season for sea surface temperature, outgoing longwave radiation, wind, pressure, and circulation derivatives in the area 50°S to 10°N and 30°W to 100°E.

The mean annual cycle of lake levels contains a peak in April-May and low point in November-December. The inflow index (Maximum - Minimum) is well correlated with adjacent station rainfall ($r = 0.51$ to 0.66). Spectral analysis on the inflow index indicates a cycle of 9.58 yrs in the period 1938-1976; and a lower frequency oscillation of 19.16 yrs in recent decades 1976-

1995. Secondary oscillations occur at periods of 14.5 yrs, 8.3 yrs, 5.8 yrs (ENSO) and 2.05 yrs (QBO). The 9.58 yrs cycle is consistent with that of Abu-Zeid et al (1992) for the Nile River. Composite years include: Wet 1962, 1963, 1974, 1978, 1979, 1989; and Dry 1959, 1967, 1972, 1977, 1992, 1994. Surface pressure and wind show significant anomaly patterns for wet minus mean composites. The sea surface temperature patterns alternate over the Atlantic and Indian Oceans particularly in the 30S - 40S belt south east of Africa. Patterns in the precursor seasons: Sept - Nov and Jun - Aug enable development of predictive models for Lake Malawi inflow at 3 to 6 months lead time.

CHAPTER 1.0: INTRODUCTION

1.1 Introduction

Lakes and rivers in tropical Southern Africa provide much needed water resources to the region. The availability of water varies from year to year depending on the prevailing climatic conditions. Summer rainfall is the main freshwater recharging system for the region. The potential for surplus or deficit conditions is determined by climatic anomalies, which cause shifts in the location or intensity of the Inter Tropical Convergence Zone (ITCZ). Any variation in rainfall distribution will have an impact on lake levels and river flows, and hence water resources are duly affected. The inter-annual variation of summer rainfall over Southern Africa is becoming a matter of economic importance. Southern Africa is known to be prone to extremes of drought and flood. The drought of 1991/92 season which caused a marked decline in lake levels and river flows is still a fresh memory. Many studies in the past concentrated on the climatic parameters directly. However, recent work show that some of the hydrologic responses give a sound starting point for characterising the governing climatic patterns. Some of the strongest evidence of changes in continental climates during the past years comes from the variations of inland lakes water levels(Maidment, 1993). Lake and river levels in Africa region such as Lake Malawi are useful indicators of climatic fluctuations and enable development of predictive models for managing water resources. Lake levels can change in response to local impacts such as building of dams, erosion of lake outlet or regionally over a large basin responding to a climatic signal. In this study lake level and streamflow data have been used to define the regional climatic variability and to determine climatic patterns causing wet conditions over tropical southern Africa in particular the Lake Malawi basin. The objective of study is to analyse Lake Malawi levels and regional runoff with a view to developing statistical forecast models of summer climatic and hydrological resources over southern Africa. In addition periods of abnormally low

and high lake levels and regional runoff are analysed using regional climate data sets to establish the atmospheric controls.

There are a number of water bodies that provide water supplies for various uses in the southern Africa region. These range from small streams to big lakes such as Lake Malawi, Figure 1.1. Other water bodies of economic importance include Lake Kariba, Zambezi river, Limpopo River, Okavango, Kunene, Orange River etc. The Zambezi river, for example, stretches through a distance of 2660 km with a drainage area of $1.3\ 10^6\ km^2$, with mean discharge of $2500\ m^3s^{-1}$, and is shared by Zambia, Zimbabwe, and Mozambique (Liebaert, 1997). The SADC region covers about 7 million km^2 with geographic and climatic conditions varying from subtropical rainfed vegetation to the oldest desert in the world, the Namib. Most of the countries are either semi arid or arid and thus have limited water resources. Water resources play a significant role in socio-economic development particularly in food production, health, energy and environment. A big proportion of the regions electricity is hydro-generated with a capacity of more than 10^4Mw (Liebaert, 1997). Freshwater fisheries and maritime industries and shipping are important activities on Malawi, Kariba, and near Cabora Bassa. Many surface water resources constitute international boundaries such as Cunene, Ruvuma, Okavango Zambezi etc.

1.1.1 Motivation

Inter-annual rainfall variation is becoming a matter of economic importance since crop irrigation, electric power, water resources, tourism resorts, fishing, etc depend on freshwater inputs from rain-producing weather systems such as the ITCZ and its associated air masses. Summer rainfall over southern Africa varies from year to year with a coefficient of variation of >20 percent, depending on locality. Rainfall in the northern Malawi may be is abundant when conditions are dry in the south, and vice versa. Rainfall and the resultant runoff distribution contribute to

variations in lake levels over the catchment, which will be analyzed with gridded data sets. Lake Malawi is one of the proxy indicators of climate variation (Mason et al, 1991). As expected its levels respond to changes in precipitation over the lake basin. The focus here is the interpretation of lake level changes as climatic variations with a view to formulating predictive models important for water resource management

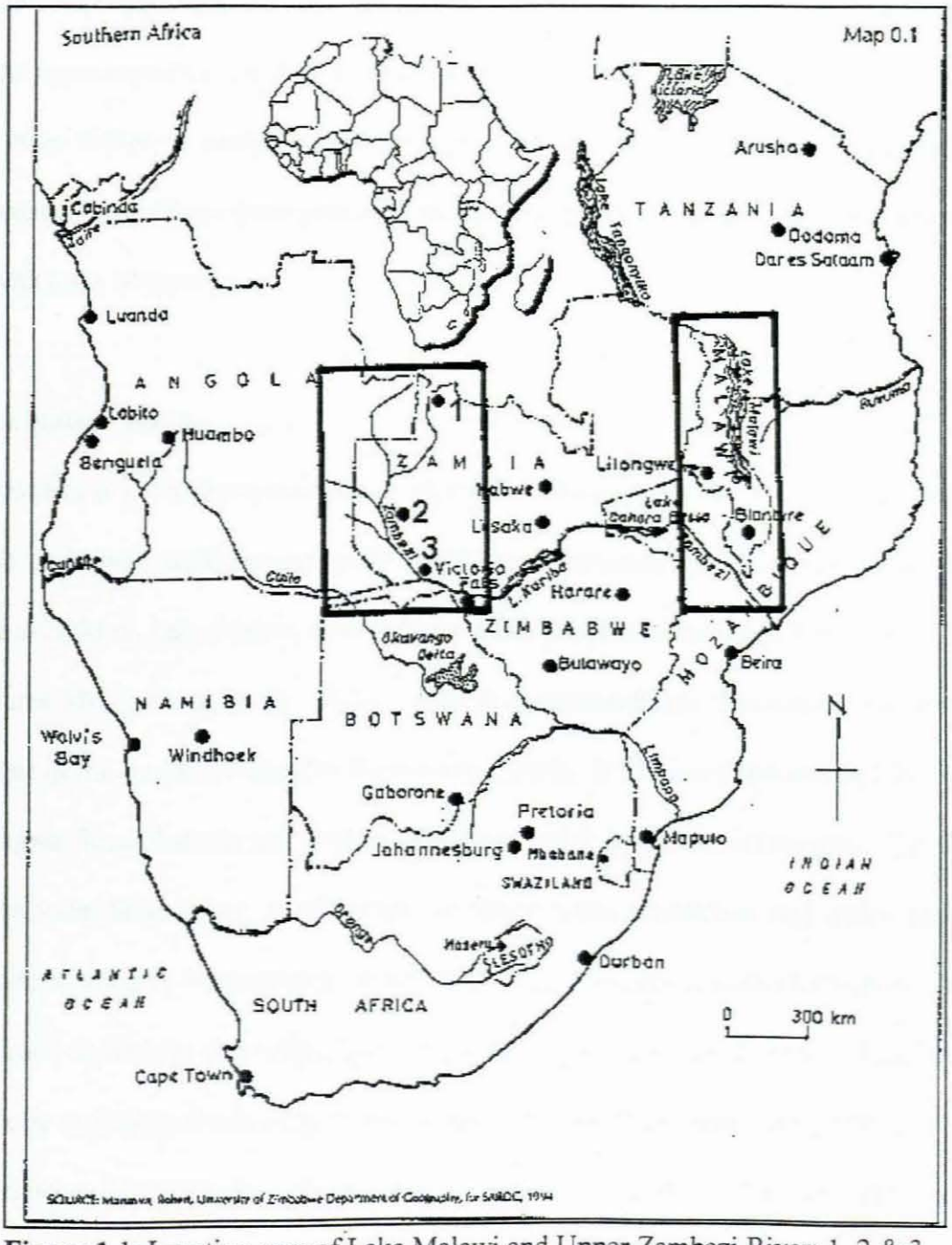

Figure 1.1: Location map of Lake Malawi and Upper Zambezi River; 1, 2 & 3 are Mwinilunga, Mongu & Sesheke respectively

Lake Chilwa.

Mandeville (1990) classifies the topography of Malawi into four zones: the plateau, highland, rift valley plains and the escarpment. The plateau is at an altitude between 900 and 1200 m with a broad undulating plain while the highland is at 2100 to 3000 m. The plains are mostly along the lakeshore and the upper Shire valley lying at about 600 to 100 m above sea level.

Lake Malawi is one of the major natural lakes in southern Africa and has a number of rivers which feed Lake Malawi. For example the Bua River is the second largest feeder with a catchment area of 6970 km^2. It receives mean annual rainfall of 1032 mm, which results in mean annual runoff of 103 mm, 10% of the total precipitation (Malawi Water Department, 1986). Other important feeder rivers are the Rukuru and the Songwe in the North. The Lake Malawi catchment experiences mean annual evaporation rates ranging from 1600 mm in the uplands to 2400 mm in the lowlands. Most of its sub-catchments are characterized by sandy, loam, or alluvial clay soils which are suitable for agriculture. These soil types are prone to erosion and create siltation problems in the catchments, particularly where farming is extensive.

The population in the catchment surrounding Lake Malawi is estimated at 20 million, a density of up to 200 persons km^{-2}. Farming activities range from intensive mixed farming mostly in commercial estates to extensive mixed farming in most subsistence settlement areas. Crops grown include tobacco, tea, maize, groundnuts, rice, sugar and some wheat. Livestock ranching is also common. There is a large sugar estate at the mouth of Dwangwa River which uses some of the inflow waters for irrigation. Lake Malawi contributes a significant amount of total fish landings in the region. The catchment is characterised by four main soil groups (Moyo et al. 1993); the latosols, hydromorphic soils, lithosols and calcimorphic soils. The vegetation is savanna woodland with Brachystegia as the dominant species.

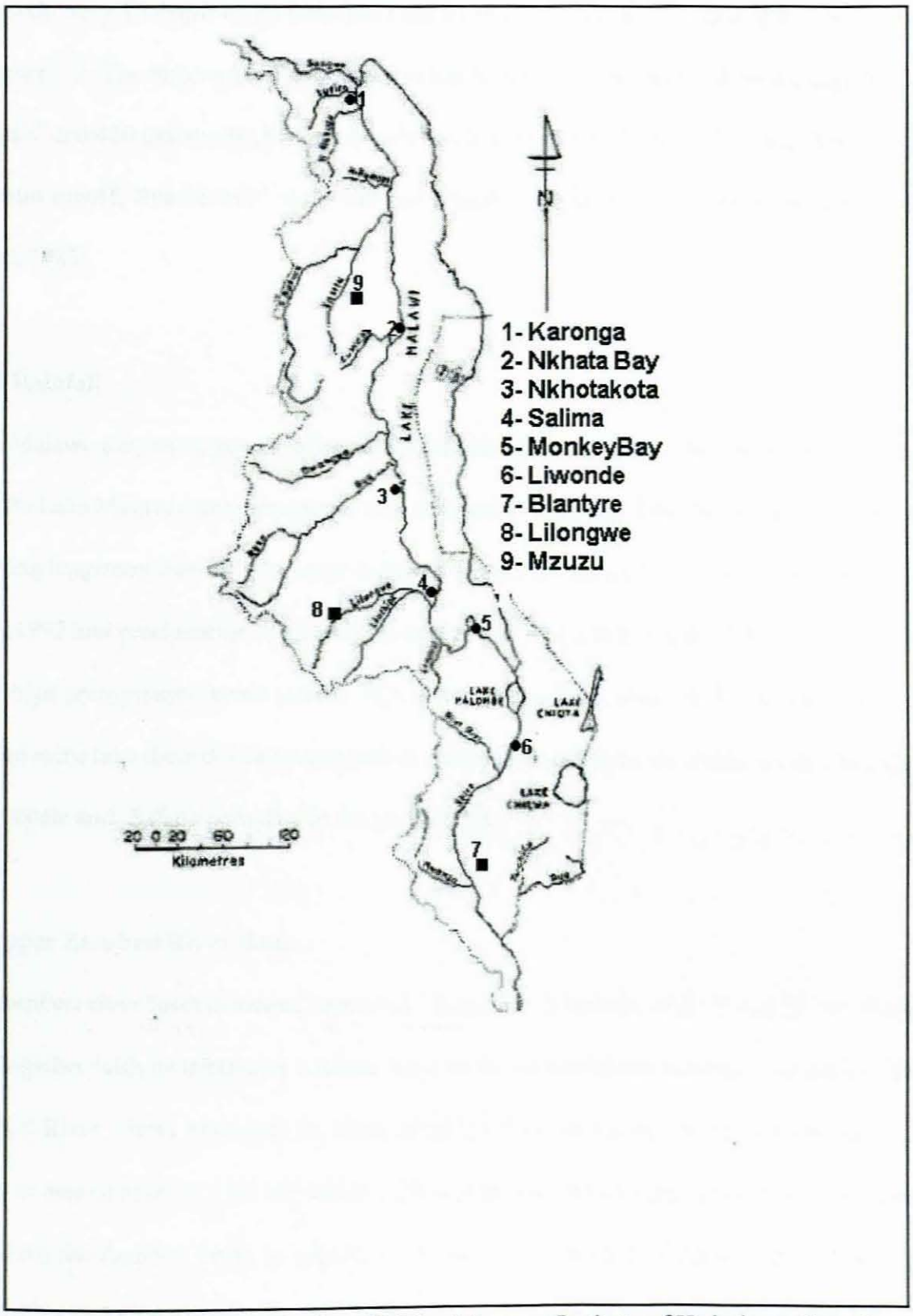

Figure 1.2 Major drainage basins of Malawi (source: Institute of Hydrology, Report no.110)

1.1.3 Major River Inflows

Approximately 10 major rivers flow into Lake Malawi from the 95 750 km^2 basin surrounding it, figure 1.2. The major runoff contributor is the Ruhuhu in Tanzania with an average flow of 193 m^3s^{-1} and 430 mm runoff, Songwe 56 m^3s^{-1} with 410 mm runoff, South Rukuru 38 m^3s^{-1} with 100 mm runoff, Bua 35 m^3s^{-1} with 100 mm runoff, Linthipe 39 m^3s^{-1} with 150 mm runoff (Kidd, 1983).

1.1.4 Rainfall

Lake Malawi climate is greatly influenced by the lake and elevation. The mean annual rainfall over the Lake Malawi catchment ranges from 600 mm to 2500 mm. Rainfall is the primary factor affecting long-term lake inflows hence makes an impact on the lake's levels. In 1949-50, 1972, 1967, 1992 low precipitation levels resulted in very low lake levels while in 1961 - 63, 1978-80, 1989 high precipitation totals yielded high water levels. Particularly in 1979, the peak level flooded some lake shore developments such as Karonga township in the northern part, Dwangwa sugar estate and Salima township in the central area.

1.2 Upper Zambezi River Basin

The Zambezi river basin is located between 8° S and 20° S latitude, 16.5° E and 36° E , Figure 1.1. Together with its tributaries it drains most of the southeast-central region of Africa. The Zambezi River flows eastwards for about 3000 km from its source into the Indian Ocean. It drains an area of about 1.3 10^7 km^2 which is 23% of the total area for the surrounding countries. In Malawi the Zambezi basin covers 93% of the country, while in Zambia and Zimbabwe it covers 72% and 64% respectively, and in Namibia and Tanzania only 3%. The Zambezi River basin comprises mainly natural and a few artificial water bodies. The natural lakes include Lake

Malawi and the artificial lakes include Kariba. The major tributaries are the Kafue, the Luangwa and the Shire Rivers. The Zambezi itself rises from the Kalene Hills in western Zambia about 1500 m above sea level. It flows through Angola and then back to Zambia and Zimbabwe. The vegetation consists of woodland bush and savanna grasses and scrub

1.2.1 Climate

Climatic conditions in the Zambezi River basin are generally tropical. The seasonal and annual range of temperature, humidity and evaporation are less pronounced (Torrance, 1972). The average rainfall for the whole river basin is 990 mm and the average annual evaporation is 870 mm. Evaporation is highest around Tete province in Mozambique reaching up to 2016 mm per annum.

1.2.2 Geology and Soils

The Zambezi River basin is covered by crystalline and metamorphic rocks. The soil characteristics differ depending on these parent materials and the influence of climate and human activity. The topsoils across the region are generally very shallow and face serious erosion problems. The main erosional agents being rain water and wind.

1.2.3 Surface Water resources

The mean annual runoff for the whole Zambezi basin reaches 106 km^3, it is 3378 m^3s^{-1} at the river mouth; at Victoria Falls the mean annual runoff is 24 km^3, Liebaert (1997). The runoff coefficients are 0.12 to 0.13 in most parts of the basin. The quality of the surface water is influenced by the variations in flow, however most of it is freshwater. Lake Kariba covers about 5.4 10^4 km^2 at about 486.5 m above sea level. It has a length of 280 km by 30 km wide. Lake

Cabora Basssa is 130 km long northwest of Tete with a dam 170 m high and 330 m wide impounding the Zambezi. It has a volume of 2500 km^3.

1.2 Literature Review

1.2.1 Concepts of Lake Dynamics

Lakes are dynamic systems that are sensitive to local and regional climate and to land use changes in the surrounding areas. The history of fluctuations in lake levels provides a detailed record of climate changes taking place in the region, and is useful for regional hydrological investigations, and for a wide range of issues concerning lakeshore land-use. Continued monitoring of lake levels provides a convenient way to monitor changes in climate and hydrological conditions.

The water level of a lake is information on its volume. The rate of change of the lake level is controlled by the rate at which water enters the basin minus the rate at which it is lost through river discharges and evaporation (Chow, 1964). Chow proposed a water balance equation of the form:

$$Az = A(\mathrm{Pr} - Ev) + (A' - A)(\mathrm{Pr}' - Ev') - Aef \qquad \text{Eq. 1.2.1}$$

where Pr= precipitation over the lake

Pr'= mean precipitation over the rest of the basin

ef= mean discharge by any channel per unit of lake area

z= mean rate of increase of depth

A= area of the lake

A'=area of basin including lake

Both lake area, A, and discharge, ef, are dependent on the lake level or depth.

Hutchinson (1957) determined a differential equation of water balance which states that the rate of change of the lake volume V with time t is the difference between water input and output rates:

$$\frac{dV}{dt} = (R + P + G_i) - (D + E + G_o) \qquad \text{Eq. 1.2.2}$$

the rates of change of level and area can be obtained by substituting $dV/dt = Al(dL/dt)$ and $dL/dt = (dL/Al)(dAl/dt)$ giving

$$dL/dt = 1/Al[(R+P+Gi) - (D+E+Go) \qquad \text{Eq. 1.2.3}$$

and $$dAl/dt = dAl/dL\ 1/Al[(R+P+Gi)-(D+E+Go)] \qquad \text{Eq. 1.2.4}$$

where both Al and (dAl/dL) are both functions of time; R and D are surface runoff and discharge rates into and out of the lake respectively. P is precipitation over the lake, E is evaporation from the lake surface; and G is the groundwater seepage into or out of the lake bed.

For open lakes such as Lake Malawi at equilibrium, $\frac{dV}{dt} = 0$ so that equation 1.2.4 reduces

to equilibrium lake level

$$L_e = f(R+A_{le}Pl-E_{le}El) \qquad \text{Eq. 1.2.5}$$

Where L_e is an indicator of climatic conditions both in the catchment and over the lake.

1.2.2 River flows

The nature of factors which condition flow variability can be described according to interval and time unit of the series under study. In hydrology one considers flow variability within the year separately to flow variations from one year to another. To study the variation of annual discharges seasonal influences cannot be modelled explicitly despite their significant impact from year to year (Haidu,1987). Annual mean discharge integrates all the causative factors: time varying factors such as precipitation, temperature and situation of the previous years water reserves. Haidu (1987) confirms that models used for the study of flow variation from year to year have not been based on analysis of causal factors but on the decomposition of the time series into its basic components by means of dynamic series:

$$y(t) = u(t) + v(t)+s(t)+e(t) \qquad \text{Eq. 1.2.6}$$

where:

$u(t)$ = trend due to the action of persistent factors

$v(t)$ = cyclic variations due to the action of rhythmical factors

$s(t)$ = stochastic components assumed to follow an autoregressive moving average process

$e(t)$ = random component, due to the interaction of random factors and other chaotic mechanisms

1.2.3 Evaporation and Latent Heat:

Evaporation occurs when water is converted into vapour. The rate of evaporation is controlled by the availability of energy at the evaporative surface and the ease with which water vapour diffuses into the atmosphere. This energy is called latent heat and is responsible for reducing attractive intermolecular forces. If T_s is the surface temperature of water in degrees C, Chow

(1964) defines latent heat of vaporisation as

$$\lambda=2.501- 0.002361\ T_s \qquad \text{Eq. 1.2.7}$$

There are a number of methods to estimate evaporation from the water surface. These include water budget method, energy budget method, mass transfer method, and evaporation formulae. The water budget method uses the continuity equation which simply states that Inflow - Outflow = Change in storage. The energy budget method assumes that the water surface receiving energy from the sun and atmosphere is balanced by the energy stored in water and related surroundings. By the use of latent heat of evaporation the total amount of evaporation can be calculated. In the mass transfer method, evaporation is taken to be proportional to the difference of vapor pressure, and the wind speed. The empirical evaporation formula is based on aerodynamic distribution of vapor pressure:

$$E = [e_g-e_d]\ F(u) \qquad \text{Eq. 1.2.8}$$

where E is the evaporation

e_g is the saturation vapor pressure at the temperature of the evaporating surface in mm of mercury

e_d is the saturation vapor pressure at dew point temperature of the atmosphere

F(u) is a function of wind velocity

The Penman method comprises of the energy budget (based on solar budget) and the aerodynamic component based on the wind (Mandeville et. al.,1990). In many cases the potential evaporation is estimated from evaporation pans, the class A pan consists of galvanised iron, 120 cm in diameter and 25 cm deep. The change of water level in 24 hours is the evaporation.

The majority of evaporation methods used in Malawi dwell on estimating open water evaporation and potential evapotranspiration which are intended to estimate evaporative losses from large open water surfaces such as lakes (Mandeville, 1990). The Penman method is

prefered because of the availability and quality of meteorological data used to analyse potential evaporation in relation to lake outflows.

1.2.4 Runoff

Runoff is defined in simple terms as that depth to which a given drainage area would be covered if all the rainwater for a given time period were uniformly distributed over it. It can be computed by the following expression (Malawi Water Resources Book, 1986):

$$RO = (\text{Average flow } m^3s^{-1} * 86.4 * n)/(\text{Catchment Area } (km^2)) \qquad \text{Eq. 1.2.9}$$

where n = the number of days in a month, flow = a measure of streamflow in cubic metres per second. In most cases for a big basin, runoff is computed from the water balance equation such as Equation 1.2.1.

1.2.5 Climatic Variability of Southern Africa

The area under study; Lake Malawi and the Zambezi River (figure 1.1) are situated on a plateau, dissected by numerous rivers such as Luangwa in Zambia, Shire in Malawi, and Sabi in Zimbabwe. Air pressures rise and fall in resonance with the seasons and respond to changes further south. The amplitude of variation decreases equatorwards. The winter anticyclonic pattern is replaced in summer by a weak pressure trough near the Zambezi valley with persistent easterly winds to the south. Fluctuations in the position and intensity of this trough account for most weather changes (Torrance, 1972).

In winter when the high pressure belt moves further north, the divergent southeast trades are dominant and originate from Madagascar. Apart from the lowest layers there is little moisture in the air and the temperature inversion at 600-700 hPa is strong, persistent and extremely dry. With the southward movement of the sun, surface winds tend to back and strengthen as pressure falls

over the interior of the continent. About mid September recurved southeast trades from the tropical Atlantic appear in the extreme northwest of Zambia. These are moister and lead to isolated thunderstorm development. By October/ November a portion of the south east trades from the Indian Ocean reaches Malawi via Madagascar and become appreciably moister. If the air has an oceanic track, it is much moister and yields more thunderstorms. During January to February the rainy season is at its height and the ITCZ becomes distinct over Malawi.

The confluence of Indian ocean trades and recurved Atlantic air are known as the Congo air mass. The rainy season usually comes to an end in early April due to the northward withdrawal of the ITCZ. In Malawi the strengthening of the southeast trade winds intensifies orographic rainfall. The wettest month of the year is usually March in the southern highlands and on the windward escarpments in the north of Malawi in April or May.

The rainfall regime of the southern Congo basin is divided into two, a dry season and a rainy season. The dry season commences in April and continues through October in most areas. The earliest thunderstorms start in Gabon, and spread southeast to Zambia. Moist air replaces the dry regime with falling pressure and closed lows creating a northerly winds. The ITCZ is fed by recurved Atlantic southeast trades which pick up moisture over Congo rain forests. The Northeast monsoon of the Indian Ocean reaches Malawi/ Zambia during summer. It feeds considerable moisture into the ITCZ along its usual position around 15-17° S.

In addition to seasonal variations, low and high pressure systems pass eastward over South Africa in a rhythm, causing intra-seasonal variation of rainfall. Explanations of rainbearing weather systems are not usually found in the study of mean circulation patterns. Harrison (1984a) found that much of the rain over South Africa came in the form of cloud bands. He determined this using surface and upper tropospheric circulation and rainfall patterns in principal component analysis. Tyson (1986) offered an alternative approach using circulation types. One such postulate is that

over the interior of the continent. About mid September recurved southeast trades from the tropical Atlantic appear in the extreme northwest of Zambia. These are moister and lead to isolated thunderstorm development. By October/ November a portion of the south east trades from the Indian Ocean reaches Malawi via Madagascar and become appreciably moister. If the air has an oceanic track, it is much moister and yields more thunderstorms. During January to February the rainy season is at its height and the ITCZ becomes distinct over Malawi.

The confluence of Indian ocean trades and recurved Atlantic air are known as the Congo air mass. The rainy season usually comes to an end in early April due to the northward withdrawal of the ITCZ. In Malawi the strengthening of the southeast trade winds intensifies orographic rainfall. The wettest month of the year is usually March in the southern highlands and on the windward escarpments in the north of Malawi in April or May.

The rainfall regime of the southern Congo basin is divided into two, a dry season and a rainy season. The dry season commences in April and continues through October in most areas. The earliest thunderstorms start in Gabon, and spread southeast to Zambia. Moist air replaces the dry regime with falling pressure and closed lows creating a northerly winds. The ITCZ is fed by recurved Atlantic southeast trades which pick up moisture over Congo rain forests. The Northeast monsoon of the Indian Ocean reaches Malawi/ Zambia during summer. It feeds considerable moisture into the ITCZ along its usual position around 15-17° S.

In addition to seasonal variations, low and high pressure systems pass eastward over South Africa in a rhythm, causing intra-seasonal variation of rainfall. Explanations of rainbearing weather systems are not usually found in the study of mean circulation patterns. Harrison (1984a) found that much of the rain over South Africa came in the form of cloud bands. He determined this using surface and upper tropospheric circulation and rainfall patterns in principal component analysis. Tyson (1986) offered an alternative approach using circulation types. One such postulate is that

tropical disturbances in the easterlies over southern Africa are often associated with heavy rainfall. Tropical easterly lows are associated with the ITCZ and driven by warm humid easterly winds from the subtropical high pressure belt (Taljaard,1985).

Rainfall variation across southern tropical Africa has become a critical socio-economic issue particularly considering that much of the subsistence farming is rain-fed. Current research has shown that the prevailing patterns of the SST, the atmospheric winds and the surrounding ocean-atmosphere climate variability are the major influencing factors. Africa's climate is governed by monsoon circulations that cover much of the Atlantic and Indian Oceans, Jury (1997). The interannual variation in rainfall is thus determined by the circulation regimes that affect the mean position of the ITCZ. El Nino - Southern Oscillation (ENSO) warm events in the equatorial Pacific and Indian Ocean are associated with warm dry conditions over much of Africa (Jury 1997). A strengthening of upper westerly flow during these events results in a decrease in moisture convergence over southern Africa, Hastenrath et al, (1993). The stratospheric Quasi-Biennial Oscillation (QBO) may play a role in modulating rainfall in the region, (Mason and Tyson, 1992). The Walker circulation connecting Africa and the Indian Ocean may interact with the QBO causing rising motion over Africa during its westerly phase while during the QBO easterly phase, convection increases significantly over Madagascar (Jury, 1995) according to statistical evidence. Generally, year to year fluctuations over Southern African are influenced by circulation regimes that alter the location of the tropical convection and the ITCZ (Harrison,1986).

1.2.6 Previous studies on Regional Climatic Variation

Earlier research findings provided evidence of relationships amongst hydrometeorological variables which led to numerous exploratory studies. Global and regional patterns of SST

anomalies have been investigated (Rocha, 1992). In addition the behavior of ENSO (Nicholson, 1986), the QBO (Trenberth, 1980), and convective anomalies (Lau and Chan, 1983) have been investigated to provide physical explanations for climatic variations. Year to year rainfall variability has been examined in relation to regional circulation forcing (Tyson and Dyer 1975, Tyson 1986, Lindesay 1984). Tyson et al (1975) suggested that southern Africa has distinct spatial and temporal patterns in rainfall. Dyer (1975) found that rainfall processes over southern Africa are modulated with quasi-periodicities of about 20, 3.6, and 2.3 years. Hasternrath (1986) examined the distribution of precipitable water and found relatively low values over southern Africa in early summer (< 30 mm) but an increase in February. Greatest amounts of precipitable water (PW) occur over the equatorial Atlantic Ocean with a tongue into the Congo basin. The Indian Ocean also experiences PW >50 mm which extends into the Mozambique channel in association with the advance of the monsoon and marine ITCZ.

Studies have been done on the influence of Indian monsoon and SST of the Indian and Atlantic Oceans on southern African rainfall. In sub-Saharan Africa climatic patterns have been linked to spatial anomalies of SST (Jury,1993), and ENSO phase (Lindesay 1988). A warmer equatorial central and western Indian Ocean is associated with dry conditions over Southern Africa (Tyson, 1986). Observational evidence shows that strengthening of the convection and latent heat release over these warmer ocean areas occur at the expense of convergence over Africa (Jury, 1992). Atlantic influences appear to resemble those of El Nino events of the Pacific, (Nicholson and Entekhabi, 1987) and affect rainfall distribution over the western half of southern Africa, (Jury,1997). The variations of rainfall with altitude, slope and exposure have been documented (Schulze, 1995). Nicholson (1986), states that variations in rainfall are generally related to changes in intensity of the rainy season rather than to its onset and duration as the ITCZ hypothesis would require. Makarau (1997) illustrated that summer rainfall may be on the decline

for Zimbabwe up to 1992. Lindesay (1988) found that rainfall in a NW-SE band through central South Africa was associated most closely with ENSO. Rocha (1992) showed that Zimbabwe rainfall correlated significantly with SOI (+0.4) at lead times of 4-5 months.

Jury (1992) outlined how a Walker-like circulation may link reduced convection over the tropical south west Indian ocean to increased convection over southern Africa. Pathack (1993) determined that the South Atlantic SST are positively correlated with early summer rains over much of South Africa. Recent atmospheric numerical modelling simulations by Jury et al (1997) have demonstrated that composite tropical Atlantic conditions influence late summer rainfall. Long et al (1998) examined local and large scale contributions to the initiation and maintenance of drought over Africa. They considered rainfall, moisture flux, and vertical motion and found that Saharan rainfall is accompanied by land surface forcing. Berndtsson (1987) analysed the variability of rainfall and potential evapotranspiration in Tunisia and found a 1 to 5 relation with cycles of 10 to 15 years.

The relationships of climatic variations with surface water availability have been conducted globally and regionally. Farquharson et al (1989) examined the relation between SST and annual flows over some selected rivers of Africa. The Zambezi at Kariba gave the poorest correlation (r = 0). They explain that the regional circulation has an important role in regulating rainfall and hence runoff. They conclude that the SOI and ENSO patterns may be indicators of annual runoff for some rivers in Southern Africa. Nordenson (1968) noted a carryover of runoff from season to season but found little significant effect on annual stream flow variability. Moss et al (1994) examined the relation of Southern Oscillation Index (SOI) with streamflows in New Zealand and found that the probability of nonexceedance of seasonal streamflow varies by a factor of more than 5 as a function of the SOI. Aguado et. al. (1992), Cayan and Peterson (1989) analysed effects of precipitation, temperature in Western United States using regression models to expain

streamflow variability and note control by atmospheric circulation anomalies.

Sutcliffe (1987) looked at the variability of African water resources through historic flow records. He found that annual runoff is sensitive to rainfall variations using a seven year moving average. Long-term streamflow records represent net rainfall over a basin and provide a valuable indication of climatic variations. Kite (1981) showed that the rise in Lake Victoria in 1961-1964 was similar to rises in Lake Tanganyika, and Lake Malawi. Zaire River levels at Kinshasa were also exceptionally high during the same period. Given that annual evaporation is conservative, a small change in rainfall can lead to marked changes in runoff.

Thiaw et al (1998) used NCEP/NCAR reanalysis data to study the atmospheric circulation over the Sahel during wet and dry years. They found that the mid and upper level easterly jet plays an important role in modulating rainfall. Moisture fluxes from the southern Atlantic Ocean have distinct impact on West Africa climate. Nicholson et al (1998) evaluated the fluctuations of African lakes levels during the last two centuries and showed that numerous lakes in east and central Africa are important indicators of climatic variability. Jury (1998) developed predictive algorithms for forecasting water resources in South Africa and found statistical correlations between antecedent patterns of monthly SST, pressure, surface and upper level winds and El Nino indices.

A number of studies have also dealt with recent and historical floods and droughts in Africa, Farmer and Wigley (1985) looked at their meteorological background, whilst Nicholson (1980) studied Sahel river flows, the Nile and Lakes such as Lake Victoria. The Southern Africa Regional Remote Sensing Project (SADC-RRSP) in Harare, is applying satellite imagery to hydrology and relating estimated rainfall, temperature, evapotranspiration and groundwater flow to Cold Cloud Duration. Sene et al (1994) updated the hydrological information on Lake Victoria and confirmed that the observed lake level can be explained in terms of natural variations in rainfall . Annual

streamflow variability and note control by atmospheric circulation anomalies.

Sutcliffe (1987) looked at the variability of African water resources through historic flow records. He found that annual runoff is sensitive to rainfall variations using a seven year moving average. Long-term streamflow records represent net rainfall over a basin and provide a valuable indication of climatic variations. Kite (1981) showed that the rise in Lake Victoria in 1961-1964 was similar to rises in Lake Tanganyika, and Lake Malawi. Zaire River levels at Kinshasa were also exceptionally high during the same period. Given that annual evaporation is conservative, a small change in rainfall can lead to marked changes in runoff.

Thiaw et al (1998) used NCEP/NCAR reanalysis data to study the atmospheric circulation over the Sahel during wet and dry years. They found that the mid and upper level easterly jet plays an important role in modulating rainfall. Moisture fluxes from the southern Atlantic Ocean have distinct impact on West Africa climate. Nicholson et al (1998) evaluated the fluctuations of African lakes levels during the last two centuries and showed that numerous lakes in east and central Africa are important indicators of climatic variability. Jury (1998) developed predictive algorithms for forecasting water resources in South Africa and found statistical correlations between antecedent patterns of monthly SST, pressure, surface and upper level winds and El Nino indices.

A number of studies have also dealt with recent and historical floods and droughts in Africa, Farmer and Wigley (1985) looked at their meteorological background, whilst Nicholson (1980) studied Sahel river flows, the Nile and Lakes such as Lake Victoria. The Southern Africa Regional Remote Sensing Project (SADC-RRSP) in Harare, is applying satellite imagery to hydrology and relating estimated rainfall, temperature, evapotranspiration and groundwater flow to Cold Cloud Duration. Sene et al (1994) updated the hydrological information on Lake Victoria and confirmed that the observed lake level can be explained in terms of natural variations in rainfall . Annual

total inflows are 10-25% of the annual rainfall.

It is seen from previous studies that the magnitude of climatic variability still remains to be fully determined. This lack of complete understanding of climatic variability makes it difficult to arrive at a quantitative assessment of major factors responsible for the observed behaviour (Diaz, 1986).

1.3 Lake Malawi Inflow and Outflows: Water Balance Components

Lake level fluctuations vary with the water balance of the lake and its catchment. Table 1.1 is the summary of the lake's long term annual water balance components :

Table 1.1: Annual Water Balance Summary for Lake Malawi

Direct Rainfall	+1414 mm
Catchment Inflow	+1000 mm
Evaporation	-2264 mm
Shire Outflow	-418 mm
Storage Increase/Decrease	+112 mm

(source: Advancement of Water Resources in Malawi, Kidd 1983)

The major input components to the lake are the rainfall over the lake and the runoff from river basins while the Shire River and evaporation are the main water loss components. The majority of the catchment runoff and associated inflow occurs in the northern end of the lake, outflow being in the south (Kidd 1983).

Approximately 10 major rivers flow into Lake Malawi within the 95 750 km^2 basin surrounding, figure 1.2. Measurements of river levels and flows began as early as 1954, (ref. Water Department, 1986).

1.4 Evaporation

The mean seasonal distribution of evaporation over the Lake Malawi from January to December is shown by figure 1.3. Evaporation rates are in the range of 170 to 300 mm a month. The annual total is 2042 mm. Evaporation is conservative with CoV values of 1.26% to 7.43% while inter-annual range is 3.27% in the period 1970-78 (Mandeville et al1990). Generally the evaporation peaks during the October and is low from January to June.

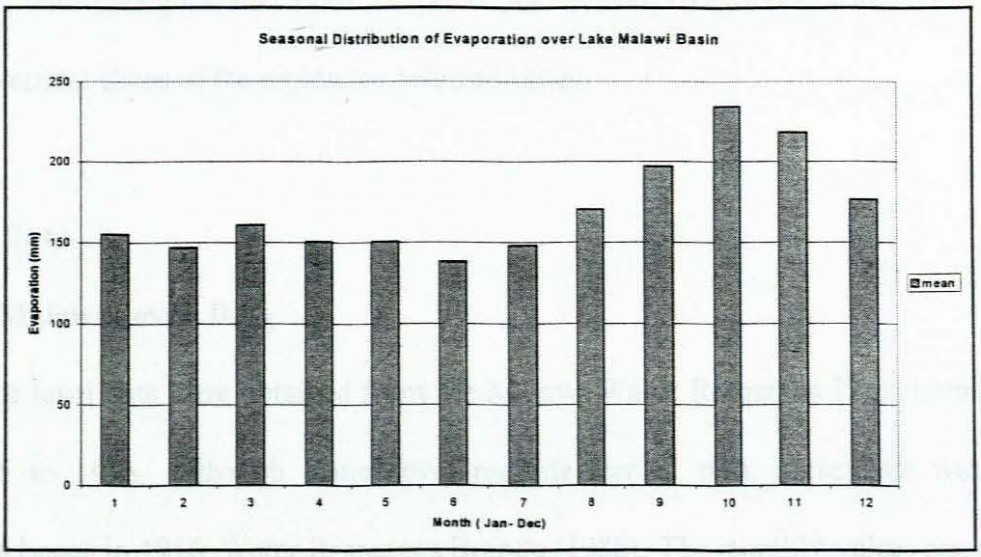

Figure 1.3: Seasonal Distribution of Evaporation

CHAPTER 2: DATA AND METHODOLOGY

2.1 Introduction

This section presents the sources and formats of data and the methods used to process and analyse it. The locally-derived data are monthly for Lake Malawi and annual stream-flow totals for the Zambezi. Monthly rainfall data for stations along the lakeshore and within the upper river basin are utilised. Some records extend from as early as 1896. This chapter is divided into two parts; station data from particular points including lake levels, rainfall and stream-flow data. The other section deals with data generated from NCEP/NCAR reanalysis sources, which are typically spatial and vertical slices of the region for selected times.

2.2 Station Data

2.2.1 Lake Malawi Levels Data

Monthly lake level data were obtained from the Malawi Water Resources Department for the period 1896 to 1995. Although water level records started then, systematic water level observations began in 1916, Water Resources Branch (1986). The monthly values are averages of observations made at three stations Chilumba (10° 26 S and 34° 16' E), Nkhata Bay (11° 38'S and 34° 17'E) and Monkey Bay (14° 04'S and 34° 55' E) Figure 1.2. The average removes some wind effects on lake level. The hydrological year in Malawi starts on November 1st and continues until October 31st of the following year. This is the convention used in this study for the time series where for instance 1958/59 means water year from November 1958 to October 1959. Lake levels are measured in metres with reference to the national datum called the Shire Valley Datum to remove irregularities in a lake base of varying bathymetry.

2.2.2 Rainfall data

Monthly rainfall data were obtained from the Malawi Meteorological Department for stations along the lakeshore; Karonga, Nkhotakota and Salima, for varying periods. Monthly rainfall data for Mongu, Mwinilunga and Sesheke, Zambia was obtained from the United States Geological Survey (USGS) web site for the period 1950-1988. For the purposes of this study only annual rainfall totals have been used to relate them to Zambezi annual flows.

2.2.3 Zambezi Stream flow data

Annual stream flow totals were obtainable from the Namibian Department of Hydrology for period the 1915 - 1996 as measured at Livingstone near Victoria Falls. Victoria Falls stream flow data is used for assessing inflows to Lake Kariba. Annual standardised departures from the mean (1937-95) were computed.

2.2.4 Other Station Data

Evaporation Data: Penman computed evaporation data were obtained from the Malawi Meteorological Department for the period 1970 to 1978. These are mean areal values for the Lake Malawi catchment. Penman estimation method is developed from fundamental physical considerations, thus it provides an index of open water evaporation close to pan data observations with an annual pan factor of 1.02 (Kidd, 1983).Four types of basic data required for using the Penman formula are temperature, humidity, wind speed and sunshine hours. Other data include the Shire River monthly discharges (1948-1997) as measured at Liwonde, and monthly temperature data as recorded at Karonga, Khotakota, Salima along the lakeshore. Data is manually checked and quality controlled using consistency, completeness and double analysis methods by meteorological and hydrological personnel respectively before archiving.

streamflow records is by percentiles, ranking the data above 85 th percentile and below the 15 th percentile. To distinguish the variations of lake inflow and streamflow which are associated with high and low seasonal fluctuations, composites of grouped monthly standardised anomalies were examined.

2.4.2 Computation of Lake Inflow and Outflow Index

Mathematically, at any point in time, the water balance expression for the lake level change, δh is:

$$\delta h = \sum I - \sum O \qquad \text{Eq. 2.3}$$

Where I is the total inflow (rainfall and runoff), and O is the total outflow (discharge and evaporation etc). Lake level data were processed to determine an inflow and outflow index. Considering that a water year starts from November to October of the following year, the inflow index is the difference of seasonal peak (usually occuring about April-May) minus the preceding minimum usually about November to December of the previous year, refer figure 3.1.

i.e. Inflow Index, $I_I = L_{\max} - L_{precedingMin}$ Eq. 2.4

The Outflow Index, I_o, is formulated by subtracting the minimum following the peak of the same year.

Outflow Index, $I_o = L_{max} - L_{\text{min after peak}}$ Eq. 2.5

2.4.3 Determination of River flow index

The Zambezi annual river flow index is computed as departures from the mean for the period

1937 to 1995. These departures were standardised using the equation

$$Z = (X - \mu)/\sigma \qquad \text{Eq. 2.5}$$

Where X is the annual streamflow total, μ is the mean, σ is the standard deviation.The standard deviation is based upon 1937-95 annual data. The data is a complete processed series as extracted from the Namibian Water Resources data, Langenhove et al (1998).

2.4.4 Correlation

Correlation is a measure of the degree of association between two data sets. It is defined by formula

$$r = \frac{\sum xy}{\sqrt{(\sum x^2)(\sum y^2)}} \qquad \text{Eq. 2.7}$$

where $x = X - \overline{X}$ and $y = Y - \overline{Y}$

Correlation is the most commonly used statistical measure in hydroclimatic analysis. This can further be written in terms of their variances if

$$s_{XY} = \frac{\sum xy}{N} \quad \text{, where } s_X = \sqrt{\frac{\sum x^2}{N}} \quad , \; s_Y = \sqrt{\frac{\sum y^2}{N}}$$

so that using the covariance of X and Y, s_{XY},

$$r = \frac{s_{XY}}{s_X s_Y} \qquad \text{Eq. 2.8}$$

Coefficient of Variation is the relative dispersion for a standard deviation s and the average $\overline{X}$, then

$$\text{CoV} = \frac{s}{\overline{X}} \qquad \text{Eq. 2.9}$$

This is one of the dispersion measures particularly for comparison of distributions where units are different such as lake levels and stream-flow.

2.4.5 Autocorrelation

One way of checking persistence in a series is simply by the Covariance between consecutive values in the series, x_t and x_{t+k}. It is called the auto-covariance at lag k and is given by, Salas et al (1980):

$$C_k = Cov[x_t, x_{t+k}] = \frac{1}{N}\sum_{t=1}^{N-k} (x_t - x)(x_{t+k} - x) \qquad \text{Eq. 2.11}$$

Where C_k is the lag -k autocovariance, k represents the time lag between correlated pairs (x_t, x_{t-k}), N is the sample size.

When k=0 equation 2.11 becomes the variance σ^2, referred to as C_o. a dimensionless measure of linear dependence is obtained by dividing C_k by C_o which gives r_k, the autocorrelation function.

$$r_k = \frac{\sum_{t=1}^{N-k} (x_t - x)(x_{t+k} - x)}{\sum_{t=1}^{N} (x_t - x)^2} \qquad \text{Eq. 2.10}$$

Where x is the mean of the sample, and x_t are individual values. The plot of r_k versus k is the correlogram.

2.4.6 Spectrum analysis and filtering techniques:

The spectrum of annual time series may be determined by transforming the correlogram r_k, Salas et al (1980) as

$$g(f) = 2(1 + 2\sum_{k=1}^{m} D_k r_k \cos 2\pi f k) \qquad \text{Eq. 2.11}$$

where g(f) is the smoothed sample spectral density, f= j/2m (j=0, 1, ...,m) is the frequency, k is the lag , m is the maximum number of k's used (N/6 or N/4), D_k is the smoothing function. For different values of k, the following relationships of D_k are obtained:

$$D_k = 1 - 6(\frac{k}{m})^2 + 6(\frac{k}{m})^3, \quad \text{for } k \le m/2 \qquad \text{Eq. 2.12}$$

$$= 2-(k/m)3 \quad , \text{for } m/2 < k \le m$$

$$= 0 \qquad , \text{for } k > m$$

The periodogram estimates a frequency spectrum for a time series, decomposing the variance of

the data into contributions over a range of frequencies. The analysis represents the series as a sum of sinusoids at fourier frequencies. This procedure is useful for testing nonrandom periodic effects in a time series.

Both the autocorrelation and the spectral analysis are computed and plotted using the Statigraphics and Excel spreadsheet software.

2.4.7 Hydrological Analysis

2.4.7.1 The Probability Theory

The probability that seasonal lake levels or streamflow will be less than a critical amount can be estimated from the lake level or streamflow data by

$$P = n / N \qquad \text{Eq. 2.13.}$$

where p is the estimate of probability, n is the number of data points for which the seasonal stream-flow is less than L_c or Q_c, and N is the total number of data points; L_c and Q_c are threshold values for the lake and river flows respectively.

2.4.7.2 Frequency analysis of extremes

There are several distributions used to estimate hydrological extreme values which include the normal, lognormal, type I, II, III extremal, Pearson III and log Pearson III, exponential etc. The frequency analysis of extremes of Lake Malawi levels used in this study is generally based on the annual maxima series. The type I extremal has been used as recommended by Sevruk et al (1981) who proposes the use of lognormal and type I extremal distributions in the analysis of annual maxima. The procedure for computing this is given in appendix A.

CHAPTER 3.0: VARIABILITY OF LAKE MALAWI LEVELS AND ZAMBEZI RIVER FLOWS

3.1 Introduction

Lake Malawi receives water mainly from precipitation and runoff. The Lake 's only outlet, the Shire River, has a barrage some 60 km down stream. The barrage operations have little effect on the Lake's mean water levels (Kidd , 1983). It is therefore possible to interpret lake level changes as climatic variations with a view to formulating predictands important for water resources management. This section covers the lake's level variability and determination of wet and dry years therefrom.

3.2 Lake Level Variability

3.2.1 Seasonal Lake Level Variability

The lakes' annual hydrological cycle is shown in figure 3.1. Lake Malawi undergoes a unimodal

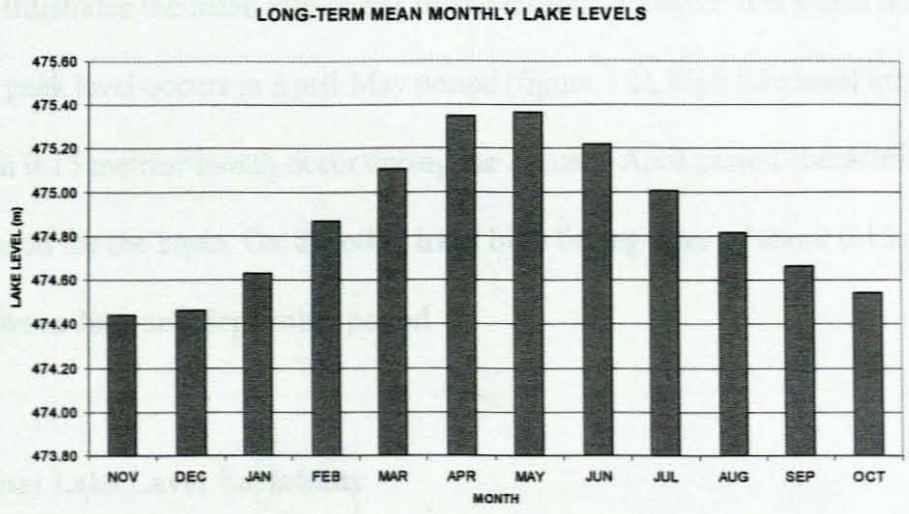

Figure 3.1 : Seasonal distribution of long-term mean monthly Lake Malawi levels

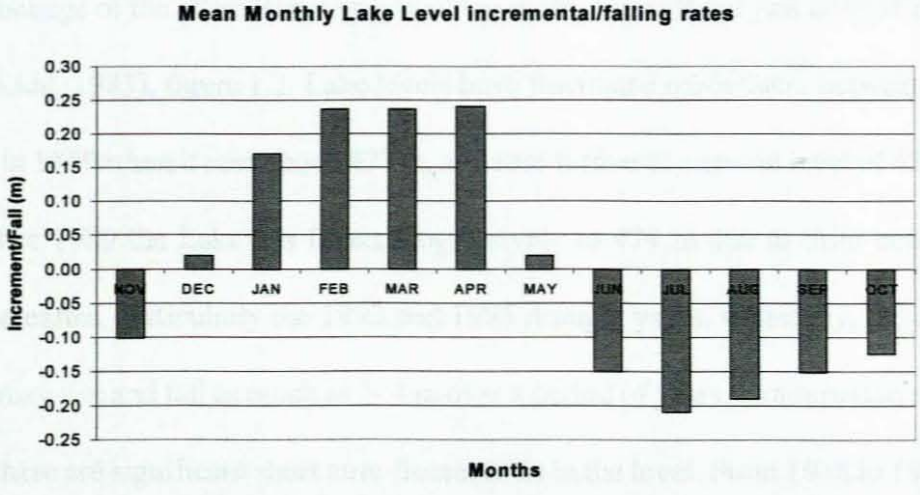

Figure 3.2 : Long-term average monthly Lake Malawi level Incremental/ Fall rates

seasonal cycle. It is characterised by net inflow in the summer months of January to March. Hence the lake peaks in April-May and falls in Nov- December due to relative outflows and evaporation from June to November. The lake level fluctuates between 474 and 475 metres. This pattern is so regular that the mean seasonal variation can be described adequately by the normal distribution function. The normal seasonal range of the lake level is 1.09 m for period 1937-95. The extreme range is 1.77 m.

Figure 3.2 illustrates the mean rate of rise or fall month by month. It is worth noting that even though the peak level occurs in April-May period (figure 3.1), high lake level incremental rates greater than 0.15 metres/ month occur during the January-April period characterising the main rainfall season for the basin. On the other hand high falling rates of about 0.15 metres/ month appear between June and September period.

3.2.2 Annual Lake Level Variability

The storage changes in any lake water balance are accounted for by the observations in lake levels (Mason,1994). The plot shown in figure 3.3 is the historical behaviour of Lake Malawi for

the period 1937-95. Prior to 1937 there was a progressive lake level rise from about 468 m to 474 m due to blockage of the Shire River by a sand bar in the Nkasi River just downstream of Lake Malombe (Kidd, 1983), figure 1.2. Lake levels have fluctuated moderately between 472 m and 474 m until in 1979 when it rose above 477 m, and rose further to a record level of 477.16 metres in 1980. After 1980 the Lake has fallen progressively to 474 m due to drier conditions that followed thereafter, particularly the 1992 and 1995 drought years. Generally, the inter-annual water level may rise and fall as much as 3- 4 m over a period of years. Examination of the record shows that there are significant short term fluctuations in the level. From 1938 to 1952 the most common cycle was 3 years, during 1955 to 1963 2 years was more common and in the later years most prominent was of 8 year period. Table 3.1 is a summary of lake statistics over the 1938-95 period. A 2- year moving average fit (figure 3.3) is considered as the best fit for this series.

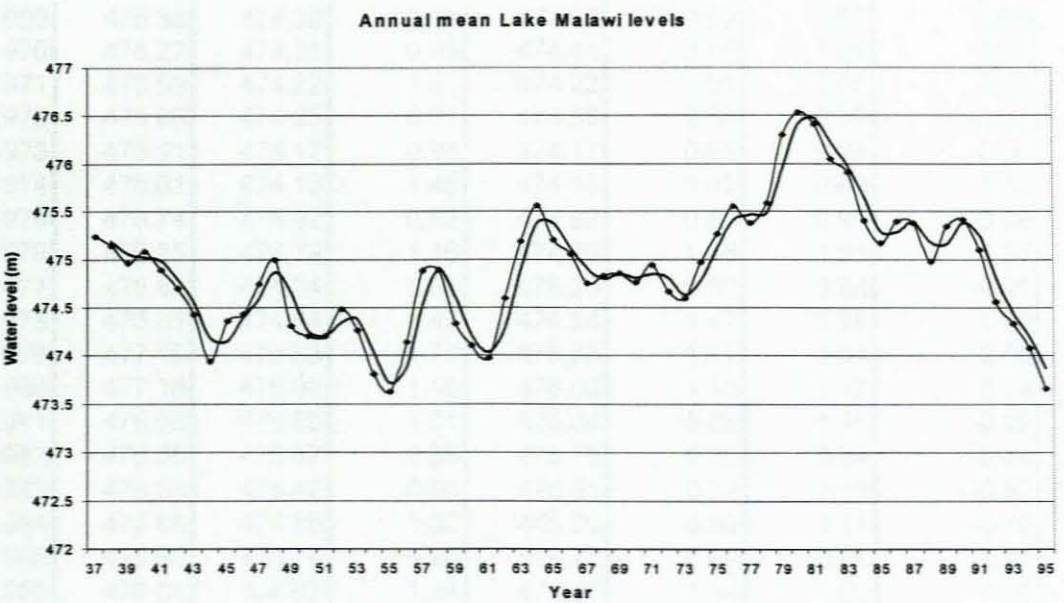

Figure 3.3: Lake Malawi levels historical series for 1937-1995 period

Table 3.1: Lake Malawi Annual Levels, Inflows and Outflows

Year	Annual Max	Annual Min	Annual Range	Min Prior Peak	Inflow	Outflow	Normalised Inflow
1938	475.57	474.81	0.76	474.86	0.71	0.96	-0.68
1939	475.40	474.61	0.79	474.61	0.79	0.89	-0.47
1940	475.73	474.51	1.22	474.51	1.22	1.10	0.65
1941	475.37	474.48	0.89	474.63	0.74	0.94	-0.60
1942	475.02	474.43	0.59	474.43	0.59	0.77	-0.99
1943	474.79	474.00	0.79	474.30	0.49	1.15	-1.25
1944	474.72	473.47	1.25	473.64	1.08	1.36	0.29
1945	475.02	473.36	1.66	473.36	1.66	0.84	1.80
1946	474.94	474.10	0.84	474.18	0.76	0.99	-0.55
1947	475.37	473.95	1.42	473.95	1.42	0.79	1.17
1948	475.55	474.58	0.97	474.58	0.97	1.07	0.00
1949	474.56	473.69	0.87	474.53	0.03	1.09	-2.45
1950	474.81	473.47	1.34	473.47	1.34	0.92	0.96
1951	474.69	473.87	0.82	473.89	0.80	0.99	-0.44
1952	475.07	473.70	1.37	473.70	1.37	0.86	1.04
1953	474.67	473.70	0.97	474.21	0.46	1.09	-1.33
1954	474.26	473.28	0.98	473.58	0.68	1.13	-0.76
1955	474.11	473.13	0.98	473.13	0.98	0.90	0.03
1956	474.84	473.21	1.63	473.21	1.63	0.80	1.72
1957	475.58	474.04	1.54	474.04	1.54	0.93	1.48
1958	475.38	474.34	1.04	474.65	0.73	1.21	-0.63
1959	474.80	473.79	1.01	474.49	0.31	1.11	-1.72
1960	474.63	473.69	0.94	473.69	0.94	1.04	-0.08
1961	474.47	473.59	0.88	473.59	0.88	0.89	-0.24
1962	475.24	473.58	1.66	473.58	1.66	0.85	1.80
1963	475.83	474.39	1.44	474.39	1.44	0.79	1.22
1964	476.08	475.04	1.04	475.04	1.04	1.22	0.18
1965	475.73	474.84	0.89	474.86	0.87	0.99	-0.26
1966	475.51	474.66	0.85	474.74	0.77	0.95	-0.52
1967	475.16	474.40	0.76	474.56	0.60	0.86	-0.96
1968	475.32	474.30	1.02	474.30	1.02	0.93	0.13
1969	475.38	474.39	0.99	474.39	0.99	0.97	0.05
1970	475.27	474.31	0.96	474.41	0.86	1.05	-0.29
1971	475.53	474.22	1.31	474.22	1.31	1.03	0.88
1972	475.06	474.25	0.81	474.50	0.56	0.89	-1.07
1973	475.11	474.17	0.94	474.17	0.94	0.98	-0.08
1974	475.61	474.13	1.48	474.13	1.48	0.69	1.33
1975	475.74	474.92	0.82	474.92	0.82	0.95	-0.39
1976	476.25	474.79	1.46	474.79	1.46	1.05	1.27
1977	475.82	474.94	0.88	475.20	0.62	0.98	-0.91
1978	476.31	474.84	1.47	474.84	1.47	0.98	1.30
1979	477.10	475.33	1.77	475.33	1.77	1.04	2.08
1980	477.16	476.06	1.10	476.06	1.10	1.12	0.34
1981	476.90	475.89	1.01	476.04	0.86	1.15	-0.29
1982	476.55	475.67	0.88	475.75	0.80	0.94	-0.44
1983	476.38	475.42	0.96	475.61	0.77	1.18	-0.52
1984	475.88	474.86	1.02	475.20	0.68	1.11	-0.76
1985	475.66	474.76	0.90	474.77	0.89	0.99	-0.21
1986	476.01	474.67	1.34	474.67	1.34	1.00	0.96
1987	475.94	474.88	1.06	475.01	0.93	1.30	-0.11
1988	475.50	474.54	0.96	474.64	0.86	1.08	-0.29
1989	476.11	474.42	1.69	474.42	1.69	0.95	1.87
1990	475.84	474.88	0.96	475.16	0.68	1.22	-0.76
1991	475.68	474.62	1.06	474.62	1.06	1.10	0.23
1992	474.90	473.94	0.96	474.58	0.32	1.08	-1.69
1993	474.93	473.82	1.11	473.82	1.11	1.06	0.36
1994	474.56	473.58	0.98	473.87	0.69	1.14	-0.73
1995	474.12	473.22	0.90	473.42	0.70	1.02	-0.70

3.3 Spectral Characteristics of the Lake Malawi Levels

Figures 3.4 and 3.5 are the periodograms for particular time periods for Lake Malawi Levels and Inflows respectively. During the 1937-95 period (figure3.4) peaks appear at 14.5, 8.3, 5.8 years. When this period is divided into segments the Lake Malawi levels depict sharp spectral components which are different from one period to another. During the 1938-1976 period a single peak of 9.58 years occurs. In the 1976-95 period there is a lower frequency of 19.2 year peak. The more stationary inflow series (figure 3.5) depicts higher frequency peaks at 5.57, 2.6, 2.44, 2.05 years. During 1937 - 1995 a descernible spectral peak occurs at 5.8 years which agrees with Nicholson's (1986) analysis of the southern oscillation. Tyson (1986) reports peaks in Southern African rainfall at about 2-3, and 18-20 years.

The persistence within the record of annual peaks shows the expected decrease with lags, table 3.2. The correlation is significant (>= 0.4) for lags < 3 years for lake levels. However for inflows the persistence is lower (r = -0.21at 2 years).

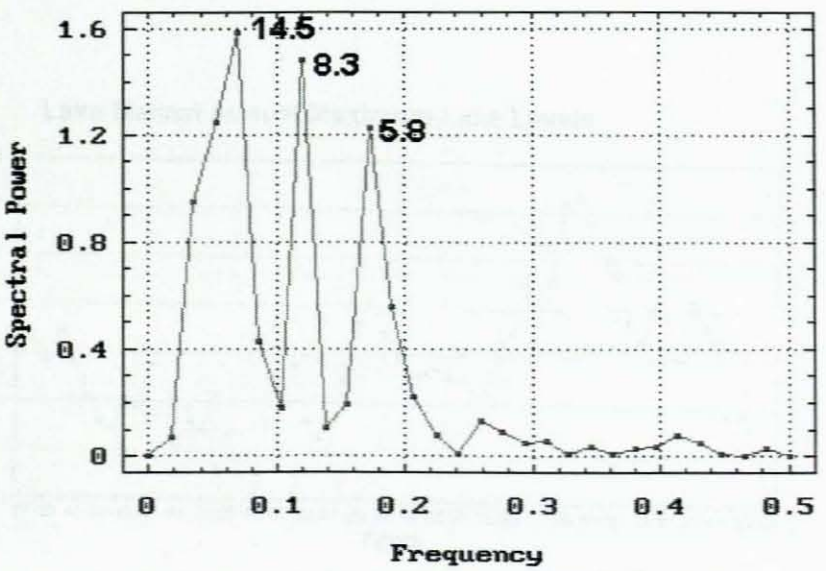

Figure 3.4 Periodogram for Lake Malawi levels for period 1937-95

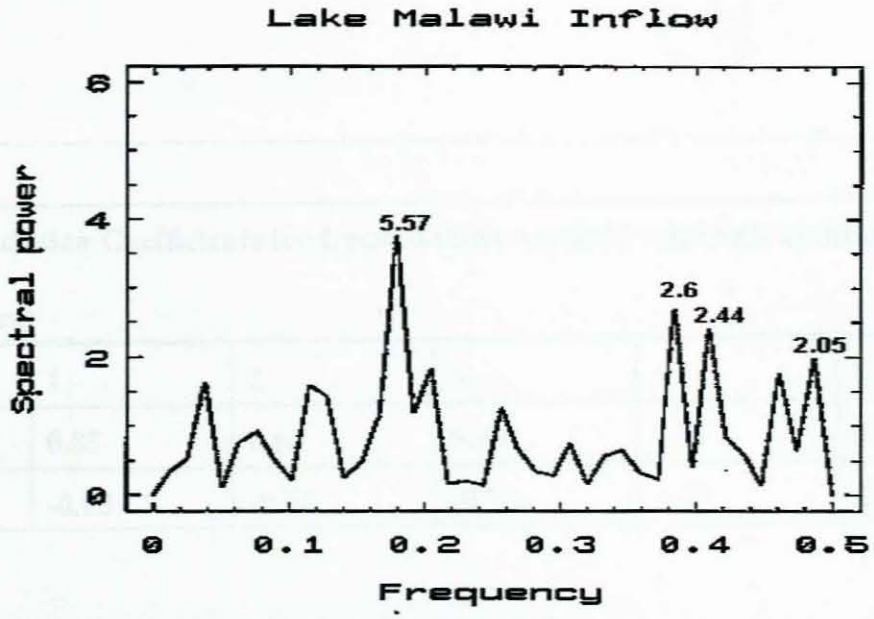

Figure 3.5: Periodogram of Lake Malawi Inflows

3.4 Hydrological analysis of the Annual Maximum Levels

The hydrological statistical summary of the annual peak levels during the 1937-95 period is shown by table 3.3. The CoV and C_s are coefficients of variation and coefficient of skewness respectively. The annual peaks have oscillated about 475.41 m with a coefficient of variation of 0.14 but a stronger positive skewness coefficient of 0.43. The annual maximum series (figure 3.7) follows the mean annual lake level trend (figure 3.1). Using the Extremal Type I pattern shows that the peak which occured in 1980 has a 50- year return period and a probability of non-exceedance of about 0.9.

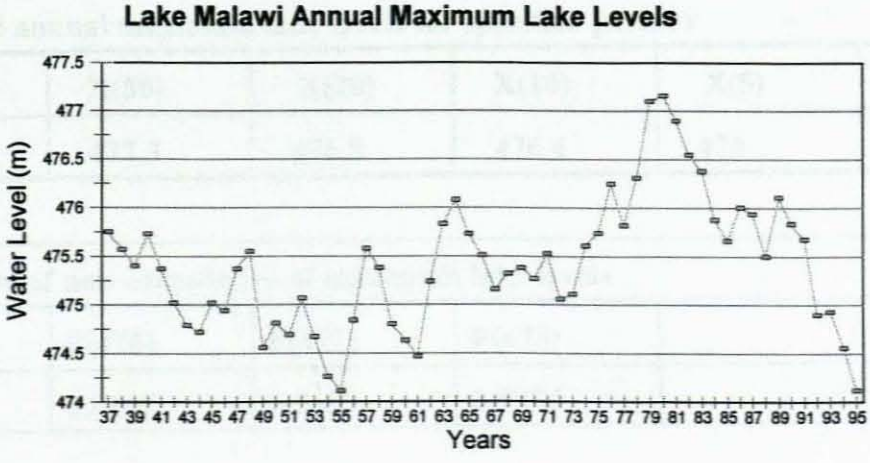

Figure 3.6 Lake Malawi peak water level fluctuations for period 1937-1995

Table 3.2:					
Serial Correlation Coefficients for Lake Malawi Annual Peak levels at different time lags (in years)					
	1	2	3	4	5
Peaks	0.85	0.63	0.46	0.38	0.38
Inflow	-0.03	-0.06	-0.22	-0.21	0.16

Table 3.3: Summary of statistical parameters for lake Malawi annual peaks				
Parameter	Mean (m)	Std Deviation	CoV(%)	Cs
Peak Levels	475.41	0.682	0.14	0.43

TABLE 3.4: Extreme analysis of maximum lake levels using Extremal Pearson Type I

Extreme analysis of annual maximum Lake Malawi levels					
Period	No. of Yrs	Extr. Max	Avg Max		
1937-95	58	477.2	475.4		
Computed annual maximum lake levels for specified periods					
X(100)	X(50)	X(20)	X(10)	X(5)	X(2)
477.8	477.3	476.8	476.4	476	475.3
Probability of non-exceedance of maximum lake levels					
F(475)	F(476)	F(477)	F(478)		
0.317	0.8142	0.9639	0.9934		

3.5 Variability of Lake Malawi Inflows

As noted above, the lake level may not be very sensitive to year to year variations. The net inflows provide a better indication of climatic variability. This study will not dwell on the individual inflow systems but will focus on the lake Inflow Index as described in chapter 2. Figure 3.7 is an illustration on the long-term series of standardised. Using thresholds of percentiles of greater than 85% and less than 15% the years 1971, 1950, 1986, 1952, 1947, 1963, 1976, 1978, 1974, 1957, 1956, 1946, 1962, 1989, 1979 are classified as wet; and years 1995, 1994, 1990, 1984, 1954, 1977, 1967, 1942, 1972, 1943, 1953, 1992, 1959, 1949 are dry, in ascending order of severity. The year 1949 was the driest year with inflow of 0.03 m. The record peak of 1.77 m occurred in 1979. There are short periods of consecutive years with progressive increase/ fall of annual inflows. The Index will be the focus of prediction efforts for climate variability in the region. The frequency distribution of the standardised annual inflows for the same period is shown by figure 3.8. Higher frequencies occur in below normal categories (less than zero).

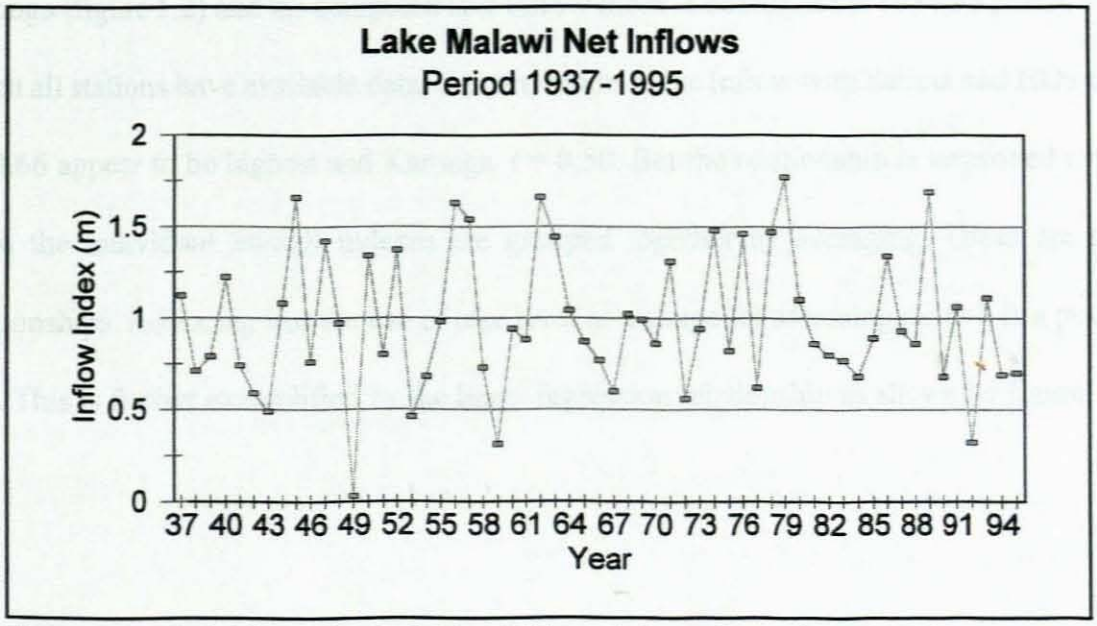

Figure 3.7: Variability of Lake Malawi Water Inflows for period 1937-95

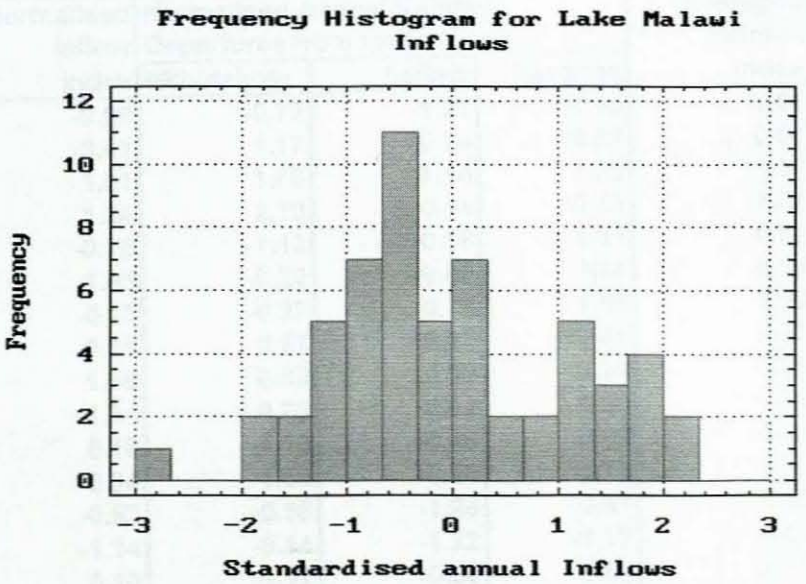

Figure 3.8: Frequency distribution of standardised Lake Malawi Inflows

3.4.2 Lake Malawi Inflows in Relation to Rainfall at Lakeshore Stations

The relationship of Lake Malawi inflows with rainfall is presented in terms of correlation coefficients and regression models. Table 3.5 shows the individual and the grouped standardised annual rainfall departures for period 1954 to 1995 of lakeshore stations; Salima, Nkhotakota and Karonga (figure 1.2) and the computed lake Inflow Index. Looking at the 1954-95 period during which all stations have available data, the correlation of the Inflow with Salima and Nkhotakota $r = 0.66$ appear to be highest and Karonga $r = 0.50$. But the relationship is improved $r = 0.77$ when the individual rainfall indexes are grouped together by averaging. These are strong relationships indicating that the use of lake level as a gauge for assessing rainfall is a powerful tool. This is further exemplified by the linear regression relationship as shown by figure 3.9.

Table 3.5 : Lake Malawi Inflow Index and station standardised rainfall departures

Year	Normalised Inflow Index	Normalised Annual Rainfall Departures from mean			Averaged Rainfall Index
		Nkhotakota	Salima	Karonga	
54	-0.90	-0.72	-1.21	-1.10	-1.01
55	-0.01	1.17	0.74	0.58	0.83
56	1.91	1.66	1.14	1.22	1.34
57	1.64	2.70	0.64	-0.13	1.07
58	-0.75	-1.13	-0.16	-1.61	-0.97
59	-1.05	-0.22	-0.06	N/A	-0.14
60	-0.13	-0.27	-0.75	1.08	0.02
61	-0.31	0.57	0.81	0.41	0.59
62	1.99	0.99	0.60	0.24	0.61
63	1.34	0.70	0.14	0.35	0.39
64	0.16	-0.18	-0.46	0.56	-0.03
65	-0.34	1.04	-0.15	-0.75	0.05
66	-0.63	-0.38	-1.25	0.67	-0.32
67	-1.14	-0.14	-1.22	-1.17	-0.84
68	0.10	-1.17	-0.30	-0.63	-0.70
69	0.02	0.55	0.54	-0.62	0.16
70	-0.37	-0.50	-0.16	0.36	-0.10
71	0.96	0.63	0.92	-0.58	0.32
72	-1.25	1.14	-0.02	-0.57	0.18
73	-0.13	0.99	-0.80	-0.54	-0.12
74	1.46	0.27	1.26	1.41	0.98
75	-0.49	-0.24	-0.78	-0.21	-0.41
76	1.40	2.16	2.08	0.38	1.54
77	-1.08	-0.14	-0.54	-0.76	-0.48
78	1.43	2.00	3.13	0.97	2.03
79	2.32	1.45	0.21	1.66	1.11
80	0.34	0.44	0.12	1.01	0.52
81	-0.37	2.00	0.23	-0.64	0.53
82	-0.55	0.95	-1.38	-1.74	-0.72
83	-0.63	-1.24	-0.32	-1.43	-1.00
84	-0.90	-1.35	-1.16	1.14	-0.46
85	-0.28	0.37	-0.34	0.26	0.10
86	1.05	1.69	0.75	-0.16	0.76
87	-0.16	-0.58	-0.50	0.14	-0.32
88	-0.37	-0.48	1.55	-0.54	0.18
89	2.08	0.79	1.17	-0.87	0.36
90	-0.90	-0.53	-0.47	-1.33	-0.77
91	0.22	-0.06	-0.28	-1.12	-0.49
92	-1.96	-1.51	-0.64	-0.79	-0.98
93	0.37	1.07	0.47	-1.25	0.09
94	-0.87	-1.34	-1.05	-1.86	-1.42
95	-0.84	-1.15	-2.11	-0.80	-1.35
Corr Coeffs	1	0.66	0.66	0.52	0.77

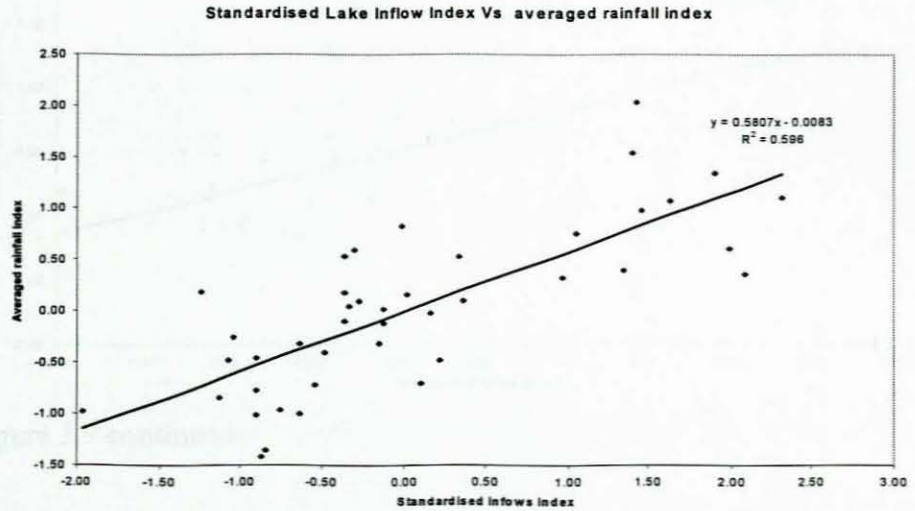

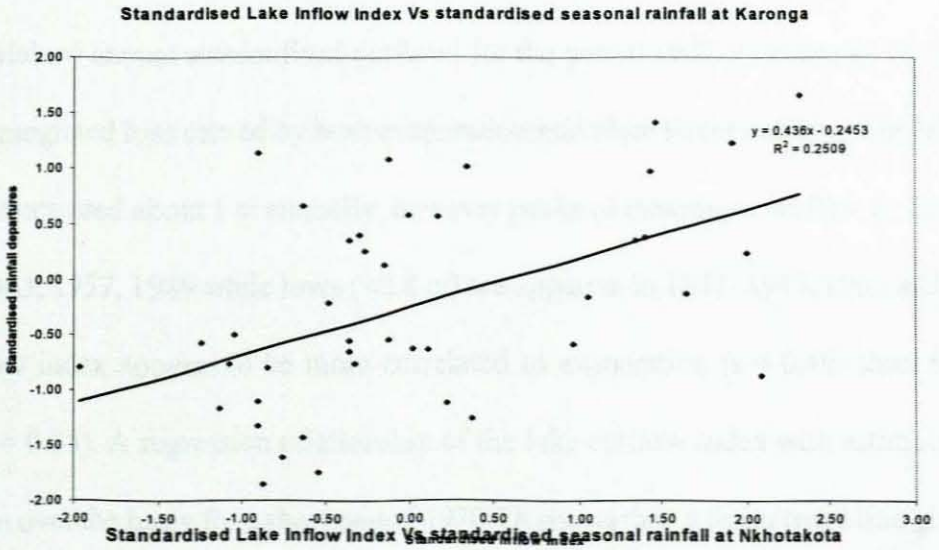

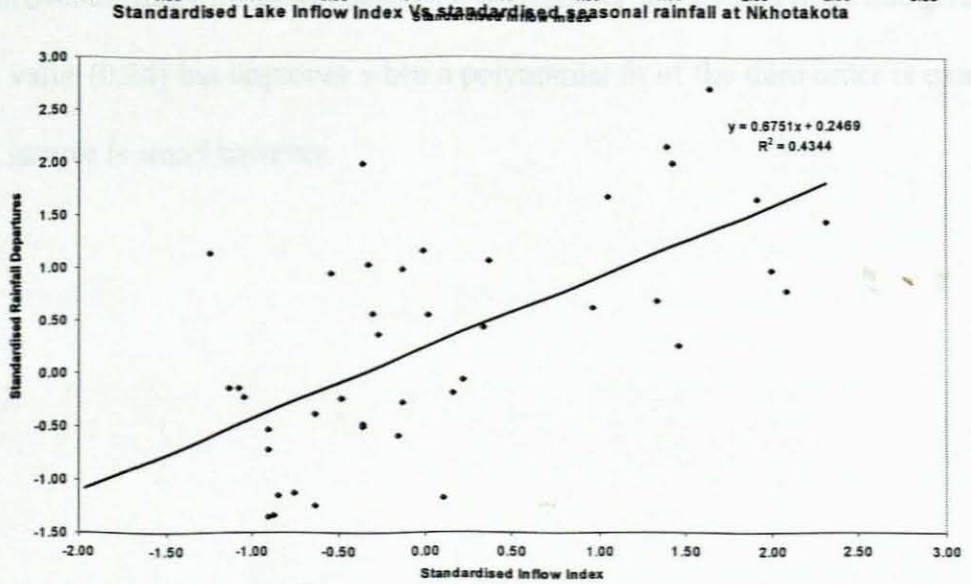

Figure 3.9 Scatter diagrams for lake inflow index versus averaged rainfall, rainfall at Karonga, Nkhotakota, and Salima

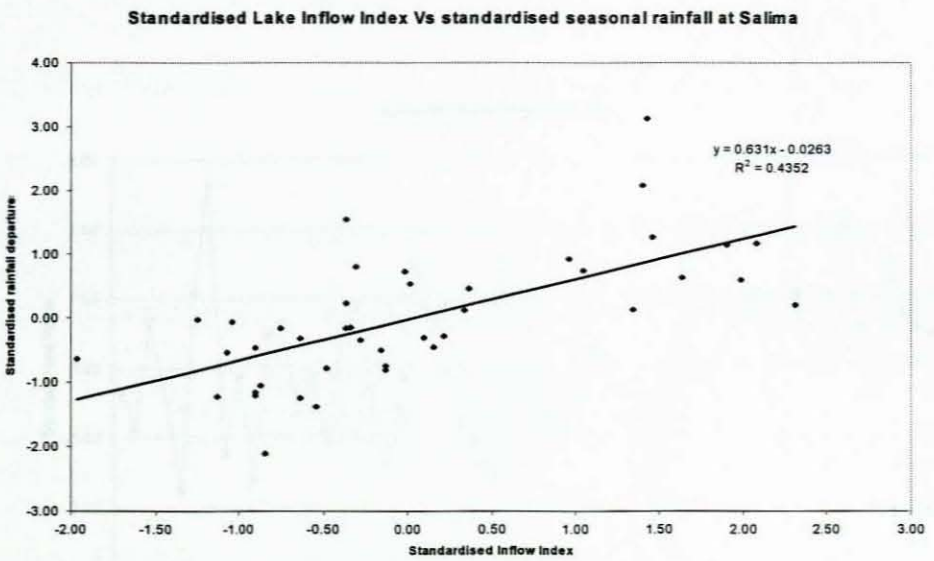

Figure 3.9 continued

3.4.3 Lake Outflows

The Lake Malawi annual standardised outflows for the period 1937-95 is shown by figure 3.10. This is an integrated loss caused by both evaporation and Shire River outflow. The lake outflow index has fluctuated about 1 m annually, however peaks of maximum outflow (>1.2 m) appear in 1943, 1963, 1957, 1989 while lows (<0.8 m) are apparent in 1941, 1947, 1962 and 1973. The lake outflow index appears to be more correlated to evaporation (r = 0.49) than Shire River outflow (r = 0.36). A regression relationship of the lake outflow index with estimated Penman evaporation over the basin for a short period 1970-78 shows that a linear trend line gives a lower R squared value (0.24) but improves when a polynomial fit of the third order is used (Figure 3.11). The sample is small however.

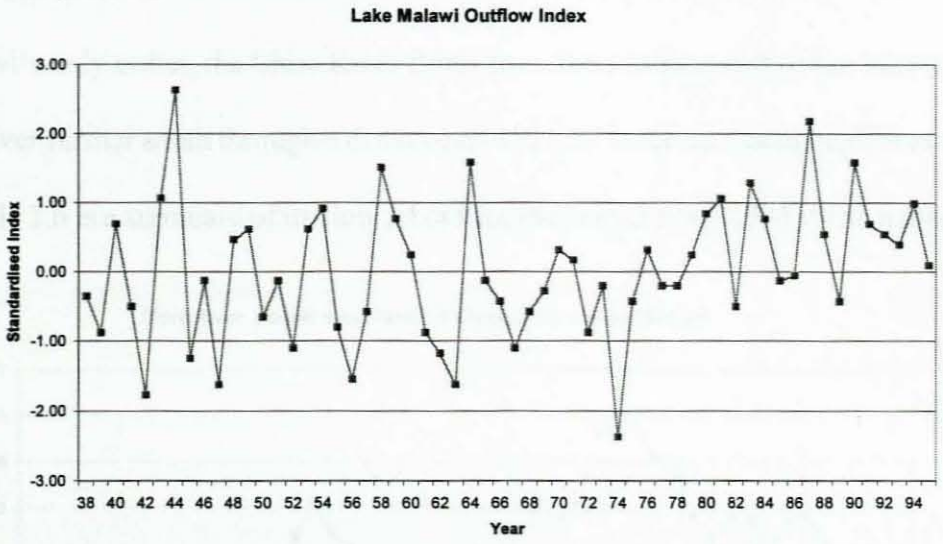

Figure 3.10: Annual series of standardised Lake Malawi Outflow Index

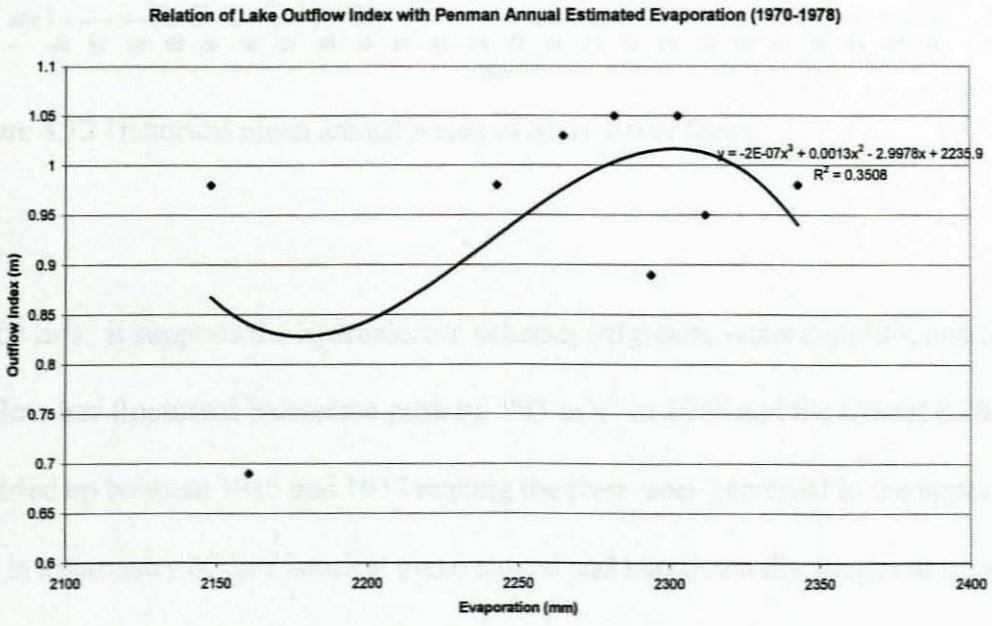

Figure 3.11 Relation of Lake Malawi outflow index with Penman annual evaporation

3.4.4 Shire River flows

Lake Malawi's only outlet, the Shire River flows from the southern end of the lake to join the Zambezi River further south through a distance of 450 km. It serves a catchment area of 1.3 10^5 sq. km. Table 3.6 is a summary of its flow record for the period 1948-1995. With a mean annual

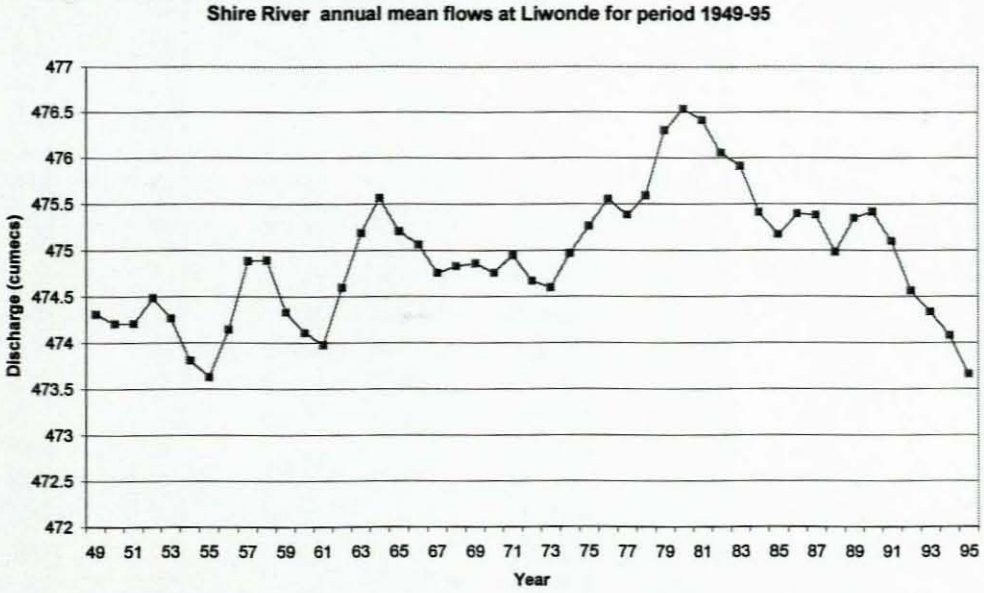

Figure 3.12 Historical mean annual series of Shire River flows

flow of 408 m^3s^{-1} it supports the hydroelectric scheme, irrigation, water supplies, and fisheries. Its daily flow has fluctuated between a peak of 963 m^3s^{-1} in 1980 and the lowest 0.28 m^3s^{-1} in 1957. It dried up between 1915 and 1937 making the river non- perennial in the upper section. Table 3.6 is a summary of the historical mean annual and maximum discharges as measured at Liwonde. Figure 3.11 is the variation of flows as measured at Liwonde from 1948-95. The flows trailed below 500 m^3s^{-1} up to 1973 after which it rose to over 800 m^3s^{-1} in 1979 and dropped down to below 200 m^3s^{-1} by 1994. This is consistent with the Lake Malawi level within the same period. Figures 3.13(a), 3.13(b), 3.13(c) are regressional relationships of the Shire River flows with the Lake Inflow Index, the Lake Annual Maximum Levels, and the outflow Index

respectively. Figure 3.14 is the relationship of Shire River annual maximum flows with peak lake levels which reveals that these are highly correlated with Lake Malawi peak levels with a coefficient of 0.90 . The mean annual flows correlate with the mean annual lake levels with r = 0.88. This is not the same when flows are correlated with the Inflow Index (r = 0.16) however this is stronger with the Outflow Index (r = 0.36).

Table 3.6 : Lake Malawi Levels and Inflows/ Outflows relation with Shire River streamflows

	Lake Mw	Lake Mw	Annual	S h i r e mean	Lake Mw	Shire max
	Annual	Annual	Max Lake	Annual	m e a n annual	annual
Year	Inflow	Outflow	Level	Outflow	Levels	outflows
49	0.03	1.09	474.56	295.92	474.31	340.6
50	1.34	0.92	474.81	294.73	474.21	392.1
51	0.80	0.99	474.69	297.22	474.21	370.3
52	1.37	0.86	475.07	342.40	474.48	434.2
53	0.46	1.09	474.67	296.76	474.26	360.8
54	0.68	1.13	474.26	222.78	473.81	279.1
55	0.98	0.90	474.11	203.55	473.63	259.8
56	1.63	0.80	474.84	229.70	474.14	362.5
57	1.54	0.93	475.58	75.13	474.89	373.1
58	0.73	1.21	475.38	408.50	474.89	483.8
59	0.31	1.11	474.8	321.03	474.33	383.2
60	0.94	1.04	474.63	278.44	474.11	351.3
61	0.88	0.89	474.47	265.77	473.97	330.6
62	1.66	0.85	475.24	354.94	474.60	446.8
63	1.44	0.79	475.83	452.88	475.19	551.5
64	1.04	1.22	476.08	515.00	475.57	608.4
65	0.87	0.99	475.73	357.01	475.20	535.1
66	0.77	0.95	475.51	247.37	475.06	477.1
67	0.60	0.86	475.16	339.73	474.76	382.9
68	1.02	0.93	475.32	402.85	474.83	482.8
69	0.99	0.97	475.38	280.75	474.86	416.7
70	0.86	1.05	475.27	383.09	474.76	486.3
71	1.31	1.03	475.53	341.93	474.95	466.3
72	0.56	0.89	475.06	185.31	474.67	218.0
73	0.94	0.98	475.11	185.31	474.60	218.0
74	1.48	0.69	475.61	274.19	474.97	522.0
75	0.82	0.95	475.74	480.15	475.26	661.5
76	1.46	1.05	476.25	498.54	475.55	702.6
77	0.62	0.98	475.82	518.67	475.38	629.5
78	1.47	0.98	476.31	573.18	475.59	728.4
79	1.77	1.04	477.1	751.48	476.30	930.8
80	1.10	1.12	477.16	821.58	476.54	962.1
81	0.86	1.15	476.9	819.53	476.41	942.9
82	0.80	0.94	476.55	672.63	476.05	702.2
83	0.77	1.18	476.38	598.21	475.91	718.5
84	0.68	1.11	475.88	598.23	475.41	718.5
85	0.89	0.99	475.66	529.51	475.17	672.6
86	1.34	1.00	476.01	601.42	475.39	765.2
87	0.93	1.30	475.94	568.72	475.38	760.2
88	0.86	1.08	475.5	451.46	474.98	659.5
89	1.69	0.95	476.11	607.58	475.35	889.2
90	0.68	1.22	475.84	607.76	475.42	747.8
91	1.06	1.10	475.68	500.70	475.10	720.8
92	0.32	1.08	474.9	322.09	474.56	426.4
93	1.11	1.06	474.93	180.88	474.34	192.9
94	0.69	1.14	474.56	178.68	474.08	185.7
95	0.70	1.02	474.12	183.34	473.66	190.9

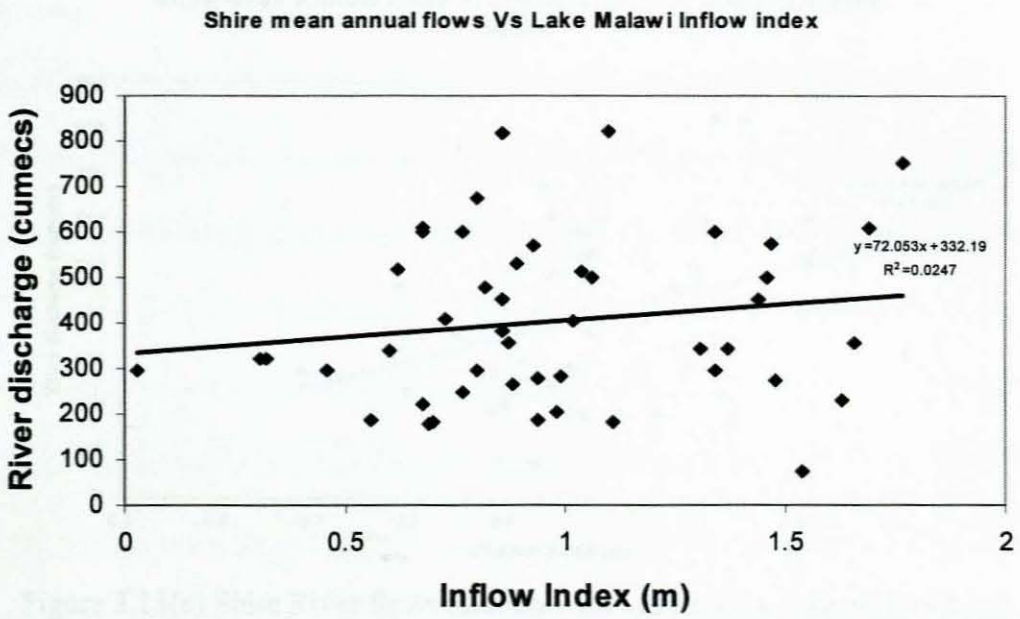

Figure 3.13 (a)

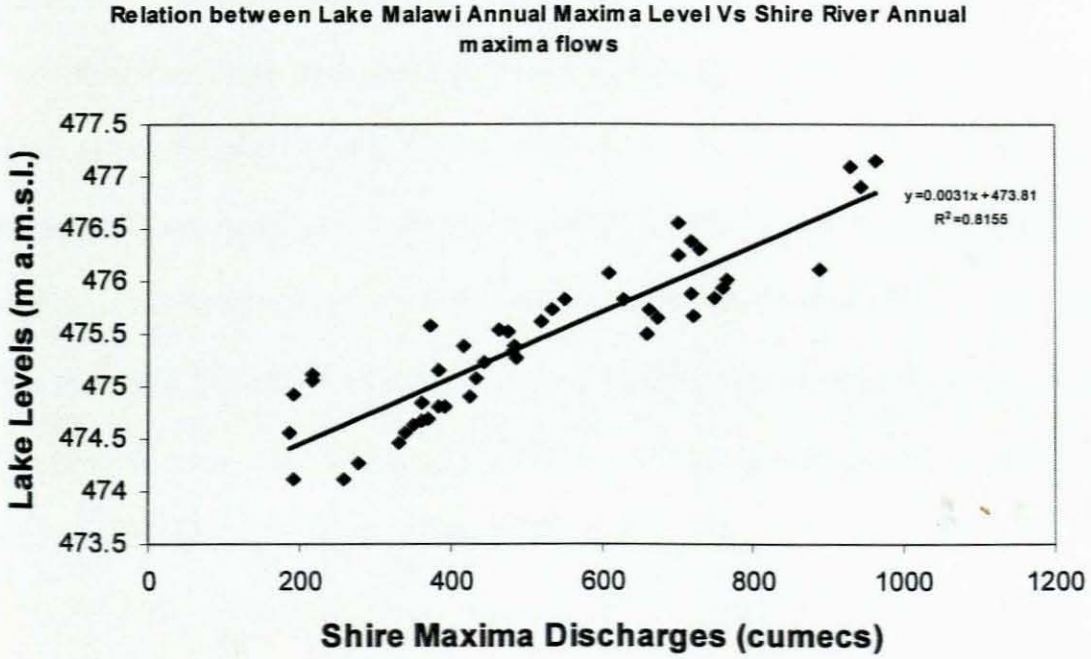

Figure 3.13 (b)

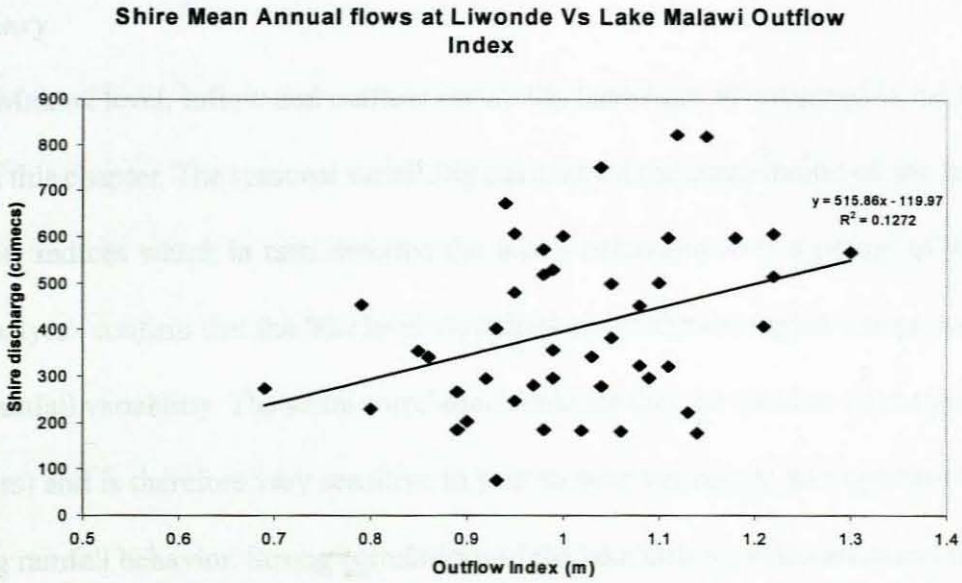

Figure 3.13(c) Shire River flows relation with Lake levels, lake outflows and peak lake levels

3.5 Summary

The Lake Malawi level, inflow and outflow variability have been investigated in the foregoing sections of this chapter. The seasonal variability has enabled the computation of the lake inflow and outflow indices which in turn describe the lake's behaviour over a period of years. The spectral analyses confirm that the lake level variations are within the region's expected spectral bands of rainfall variability. The serial correlations indicate that the lake has short memory (less than 3 years) and is therefore very sensitive to year to year variations; an important aspect for monitoring rainfall behavior. Strong correlations of the lake inflows with catchment rainfall are also indicative of this. Peak levels of greater than 477 m that have caused shoreline flooding, with a return period of just over 20 years, are events to closely monitor and predict. The frequency distribution indicates that many of the annual inflows are below normal which has negative impact on water resources management. The lake's outflows is another aspect to monitor. There is strong association between the lake outflow index and the annual Penman evaporation totals ($r = 0.49$) and the Shire river annual flows ($r = 0.36$) suggesting that the outflow index can be used to extend the lake's integral annual losses series. The relation of Shire flows with the lake peak levels is quite high ($r = 0.90$) but low with the inflow index ($r = 0.16$). This is a typical hydraulic relationship where the flow rates vary directly with variation of the water pressure head in the lake. Thus even if the amount of inflow is high it will not have much impact on the Shire flows if the water level in the lake is still low. This significant relationship is important for water resources management along the Shire River.

3.6 Introduction to Zambezi flows

The variability of river flows and lake levels is one of the main features of hydrology in Southern Africa. River flows in Sub-Saharan Africa are characterised by marked temporal variability and periodicity. Farquharson (1998) suggests two reasons for this; low and variable rainfall and secondly high potential evaporation exceeding rainfall for much of the year. The western Zambezi River basin lies at an elevation over 1000 m and the surface moisture supply is a limiting factor. The annual potential evaporation is relatively conservative, so small changes in rainfall lead to significant changes in runoff. In this section the Zambezi River flow variability is explored and compared with the rainfall distribution as recorded at Mongu, Mwinilunga and Sesheke meteorological stations (figure 1.1) and Lake Malawi to check for regional concurrence of climatic trends.

3.7 Zambezi River flow Variability

3.7.1 Seasonal and Interannual Variability.

The streamflow for the Zambezi River is gauged at Livingstone near Victoria Falls. Annual peaks typically occur between April and May. The peak is a response to summer rainfall during the December to March period.. The discharge at the Falls returns to base flow in the October - November period, similarly to Lake Malawi.

The interannual variation of the Zambezi River during the 1907 - 1996 period is shown in figure 3.15. From as low as 14 10^9 m^3 in 1915 the annual totals peaked to a maximum of 73 10^9 m^3 in 1958. It has oscillated down to 13 10^9 m^3 in 1996. The period between 1952 to 1982 was mostly above 35 10^9 m^3. An upward trend up to 1958 and downward trend after 1958 is apparent. Years with below normal annual flows($< 22\ 10^9\ m^3$, $< 15^{th}$ percentile) include 1995, 1992, 1990, 1973, 1982, 1983, 1994, 1984 while years with above normal annual flows($> 51\ 10^9\ m^3$, $> 85^{th}$

percentile) include 1975, 1962, 1968, 1978, 1969, 1963, 1958.

A summary of statistics for the annual series is provided by table 3.7 while the frequency distribution is shown by figure 3.16. The frequency distribution shows that many of the values are negatively skewed indicating frequent occurrences of below normal flows.

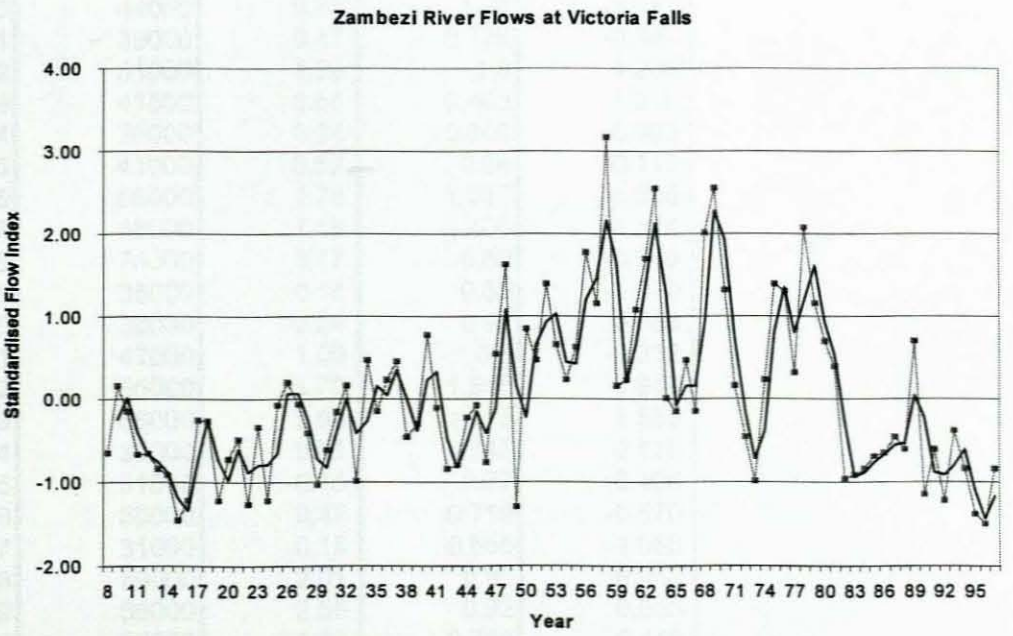

Figure 3.15 Historical series of Zambezi river flows at Victoria Falls fitted with a 2 year moving average trend line

Table 3.7 : Zambezi Annual Total Flows as recorded at Victoria Falls compared with Lake Malawi Annual Levels and Inflows

Year	Zambezi Annual Flows (10^6 m^3)	Zambezi Flow Index	Lake Mw Annual Inflow (m)	Normalised Lake Inflows
1938	27000	-0.46	0.65	-0.767
1939	29000	-0.30	0.725	-0.539
1940	43000	0.78	1.18	0.842
1941	31500	-0.11	0.635	-0.812
1942	22000	-0.84	0.45	-1.374
1943	22500	-0.80	0.34	-1.708
1944	30000	-0.22	0.73	-0.524
1945	32000	-0.07	1.455	1.676
1946	23000	-0.76	0.61	-0.888
1947	39900	0.54	1.33	1.297
1948	54000	1.62	0.945	0.128
1949	16000	-1.30	0.01	-2.709
1950	44000	0.85	1.26	1.084
1951	39000	0.47	0.775	-0.387
1952	51000	1.39	1.3	1.206
1953	41500	0.66	0.405	-1.510
1954	36000	0.24	0.605	-0.903
1955	41000	0.62	0.94	0.113
1956	56000	1.78	1.515	1.858
1957	48000	1.16	1.405	1.524
1958	74000	3.17	0.69	-0.645
1959	35000	0.16	0.55	-1.070
1960	36000	0.24	0.92	0.053
1961	47000	1.09	0.8	-0.312
1962	55000	1.70	1.545	1.949
1963	66000	2.55	1.415	1.555
1964	33000	0.01	0.945	0.128
1965	31000	-0.15	0.77	-0.403
1966	39000	0.47	0.715	-0.570
1967	31000	-0.15	0.555	-1.055
1968	59000	2.01	0.92	0.053
1969	66000	2.55	0.92	0.053
1970	50000	1.32	0.755	-0.448
1971	35000	0.16	1.205	0.917
1972	27000	-0.46	0.54	-1.101
1973	20000	-0.99	0.875	-0.084
1974	36000	0.24	1.315	1.251
1975	51000	1.39	0.785	-0.357
1976	49900	1.31	1.405	1.524
1977	37000	0.32	0.565	-1.025
1978	59800	2.07	1.46	1.691
1979	48000	1.16	1.67	2.328
1980	42000	0.70	1.04	0.417
1981	38000	0.39	0.795	-0.327
1982	20500	-0.96	0.75	-0.463
1983	21000	-0.92	0.71	-0.585
1984	22000	-0.84	0.59	-0.949
1985	24000	-0.69	0.845	-0.175
1986	24500	-0.65	1.26	1.084
1987	27000	-0.46	0.84	-0.190
1988	25000	-0.61	0.765	-0.418
1989	42000	0.70	1.635	2.222
1990	18000	-1.15	0.635	-0.812
1991	25000	-0.61	0.975	0.219
1992	17000	-1.23	0.265	-1.935
1993	28000	-0.38	1.065	0.493
1994	22000	-0.84	0.565	-1.025
1995	15000	-1.38	0.645	-0.782

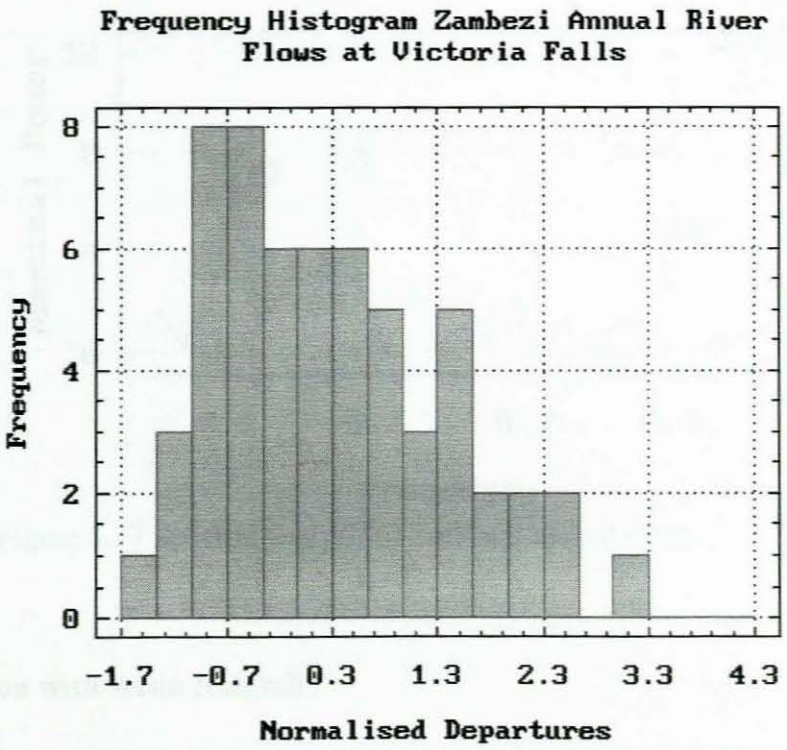

Figure 3.16 Frequency distribution of Normalised departures of Zambezi annual flows at Victoria Falls for 1937-95 period

3.7.2 Spectral Analysis

The Zambezi river annual variation for the period 1937-95 depicts periodicities similar to those produced by climatic parameters in the region. The 1937-95 period displays peaks at 9.67, 5.8, and 2.52 years, figure 3.17. These cycles fall in the range 2-10 years typical of most of the variance of the southern oscillation (Tyson, 1986). All of them are close to spectral peaks obtained from Lake Malawi analyses.

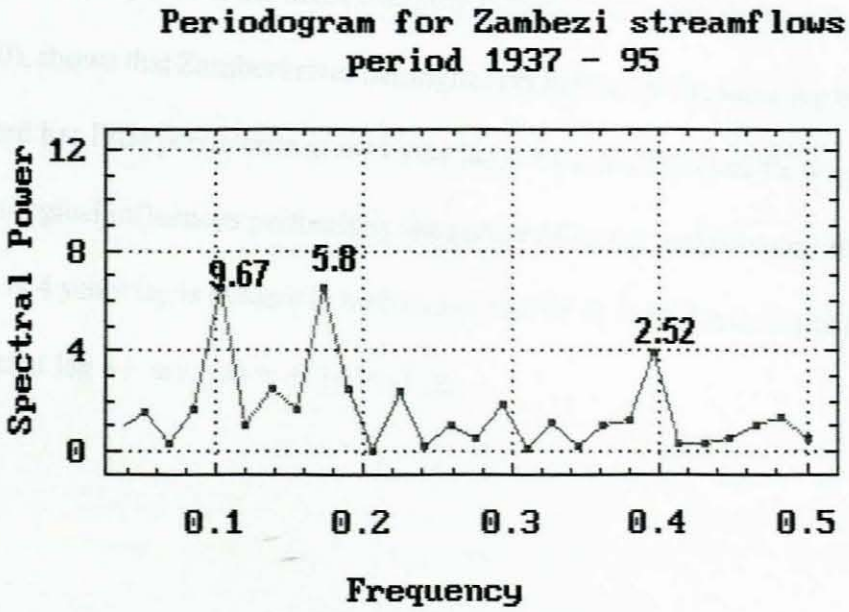

Figure 3.17 Spectral analysis of Zambezi annual flows

3.8 Relation with Basin Rainfall

Table 3.8 is the rainfall index computed from annual rainfall totals for Mongu, Mwinilunga and Sesheke and the Zambezi standardised flow index as recorded at Victoria falls for period 1958-1992. Figure 3.18 is a regression relationship of the area rainfall index and the river flow index. There is a strong relationship with correlation coefficient of 0.74 ($r^2 = 0.53$) indicating that rainfall is a major influence on the river's interannual variability, as expected. The upper Zambezi lies at the centre of the Angola low which forms part of the ITCZ, hence the river flows may describe the behaviour of this low in terms of intensity and position relative to the catchment in addition to other forcing factors such as the moisture flux.

3.9 Relation of Zambezi annual river flows to Lake Malawi levels and inflows

Figure 3.19 is a regression relationship between Zambezi River annual flows and Lake Malawi annual inflows for the period 1937-95. There is a correlation of 0.53 indicating a strong

association on interannual scale. However the association is weaker with peak lake levels r =0.14. This is mainly due to the lakes damping effect. Comparing the correlograms of the two (figure 3.20), shows that Zambezi river has higher persistence at the same lag times. The Malawi inflow record has little persistence at a +1 year lag, whilst the Zambezi flow r > 0.4. This is due other physiological influences particularly the nature of feeder and tributary rivers. The drop to a minimum at 4 years lag is evident in both cases. The 95 % confidence limits for both the Lake and Zambezi at lag +1 are r(k) = -0.74 to -1.26.

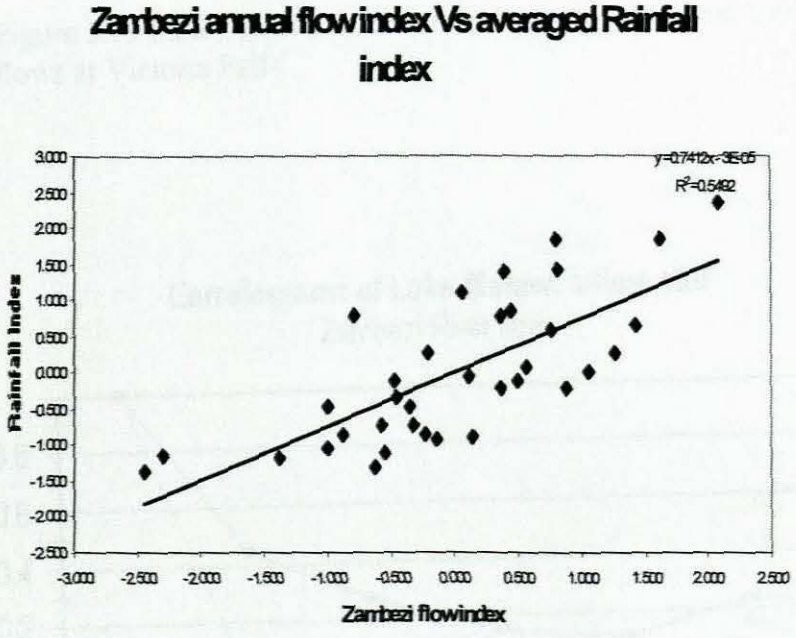

Figure 3.18 Regression relationship of the Zambezi flow index with area rainfall index

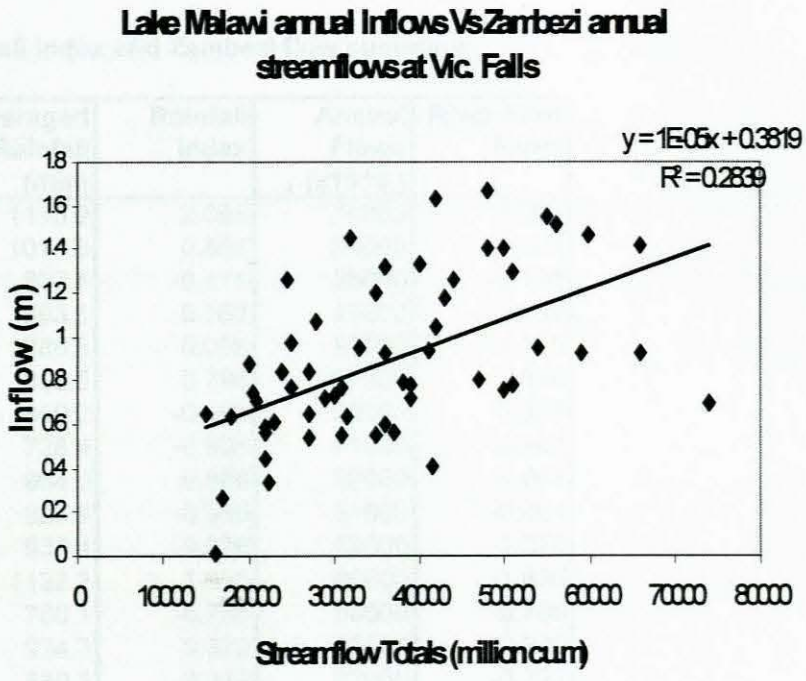

Figure 3.19 Lake Malawi Annual Inflows versus Zambezi annual flows at Victoria Falls

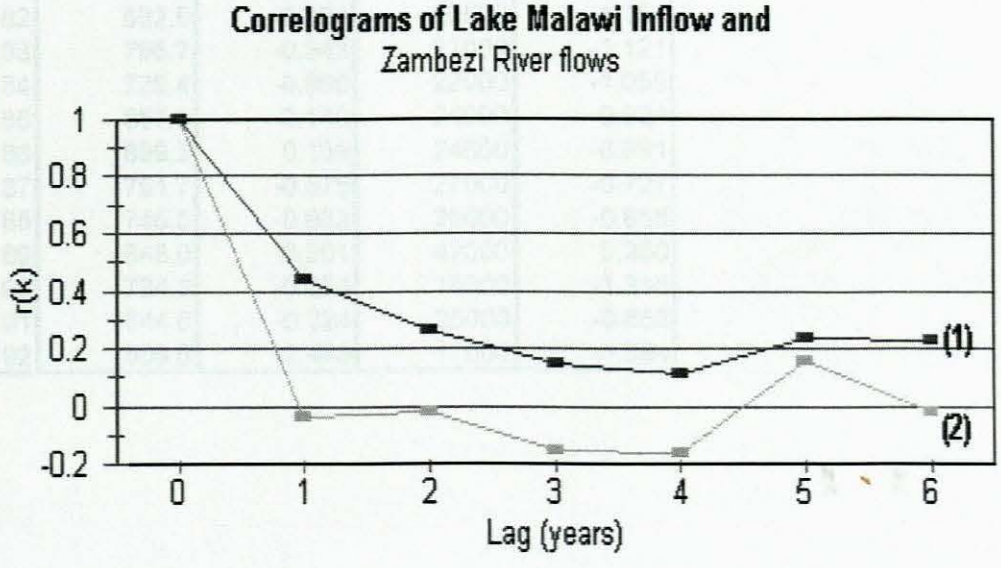

Figure 3.20 Autocorrelation functions for Lake Malawi Inflows (2) and the Zambezi flows at Victoria Falls (1)

Table 3.8 Rainfall Index and Zambezi flow summary

Year	Averaged Rainfall (mm)	Rainfall Index	Annual Flows (x10^6)	River Flow Index
58	1193.9	2.095	74000	2.364
59	1011.8	0.886	35000	-0.200
60	807.4	-0.471	36000	-0.135
61	993.1	0.762	47000	0.589
62	888.5	0.068	55000	1.115
63	998.5	0.798	66000	1.838
64	809.2	-0.459	33000	-0.332
65	728.4	-0.995	31000	-0.464
66	964.0	0.569	39000	0.063
67	825.9	-0.348	31000	-0.464
68	938.4	0.399	59000	1.378
69	1122.2	1.620	66000	1.838
70	760.1	-0.785	50000	0.786
71	934.3	0.372	35000	-0.200
72	830.3	-0.319	27000	-0.727
73	669.8	-1.385	20000	-1.187
74	953.2	0.497	36000	-0.135
75	946.0	0.449	51000	0.852
76	932.6	0.361	49900	0.779
77	895.0	0.111	37000	-0.069
78	1000.5	0.811	59800	1.430
79	1092.2	1.420	48000	0.654
80	1069.5	1.270	42000	0.260
81	1037.8	1.059	38000	-0.003
82	532.8	-2.294	20500	-1.154
83	796.7	-0.542	21000	-1.121
84	728.4	-0.995	22000	-1.055
85	857.3	-0.140	24000	-0.924
86	899.3	0.139	24500	-0.891
87	791.7	-0.575	27000	-0.727
88	745.5	-0.882	25000	-0.858
89	848.0	-0.201	42000	0.260
90	784.3	-0.624	18000	-1.318
91	844.6	-0.224	25000	-0.858
92	509.6	-2.448	17000	-1.384

3.10 Summary

Zambezi River flows at Victoria Falls have been analysed to establish coherence of climatic fluctuations in tropical southern Africa. The association of inter-annual variation obtained in this analysis is one of the striking features. The wet or dry years are often matched, the periodicities conform and Lake Malawi annual Inflows are associated. Thus the years selected for composite analysis in the next chapter reflect the climatic patterns during and prior to wet years as experienced across the tropical southern African region.

CHAPTER 4: COMPOSITE AND ANOMALY ANALYSIS OF WET CLIMATE FIELDS

4.1 Introduction

Spatial and temporal composite analysis is a useful tool in analysing many hydro-climatic parameters. These can be generated using models from the European Community Medium Range Weather Forecast (ECMWF) and the National Centre for Environmental Prediction (NCEP). In this chapter the NCEP reanalysis data are used to investigate the atmospheric circulation associated with the inter-annual variability of Lake Malawi Inflows for the period 1958-1995. In chapter 3, years with high and low annual inflows were identified; the years with high inflows included 1962,1963,1974,1978,1979, and 1989. Composites were constructed for this group of wet years and the long-term mean (1968-1996) was subtracted to produce anomaly patterns. Composite analysis is performed for surface pressure, lower (850 hPa, 1.5 km) and upper level (200 hPa, 12 km) winds, sea surface temperatures, outgoing long-wave radiation, runoff and precipitable water varying within the region 50°S to 10°N and 30° W to 90° E.

4.2 The Pressure Field

The surface pressure field is characterised by large semi permanent high pressure cells : the South Atlantic cell and the South Indian cell. Their interannual changes in positions and intensity have some influence over the sub- continent's climate. Anomaly pressure patterns characterising wet years are analysed below.

4.2.1 Composite Pressure patterns:

The JJA period (lag -6) prior to a wet season, figures 4.1 show negative values both over the

Atlantic and the Indian Ocean with higher values in the Mozambican channel and South east of Madagascar. This pattern is unlike JJA periods prior to dry years where there are positive anomalies in the Atlantic and negative values in the Indian Ocean.

Looking at the SON (lag -3) composite shows that there is a marked division of negative and positive anomalies. The Indian Ocean and the subcontinent show marked negative values with centre around 5° S and 45° E which is about the mean position of the South Indian High. Much of the South Atlantic has positive anomalies.

The DJF (lag 0) composite anomaly for wet years depict a similar pattern but with negative pressure anomalies appearing north off 25° S. Greater negative values are centred over the sub continent around Malawi, Botswana, Mozambique depicting lower pressure patterns than normal during the wet years. This is different from dry composite years where the whole of 20° W - 90° E and 50° S - 5° S is under negative anomalies.

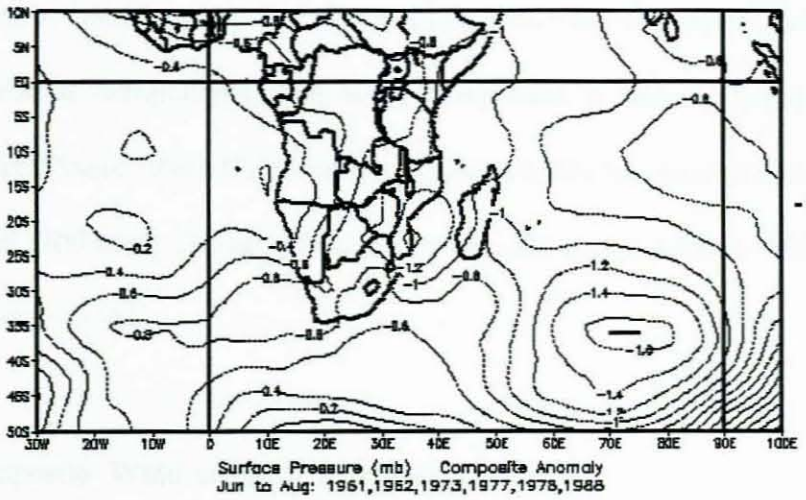

-6 lag

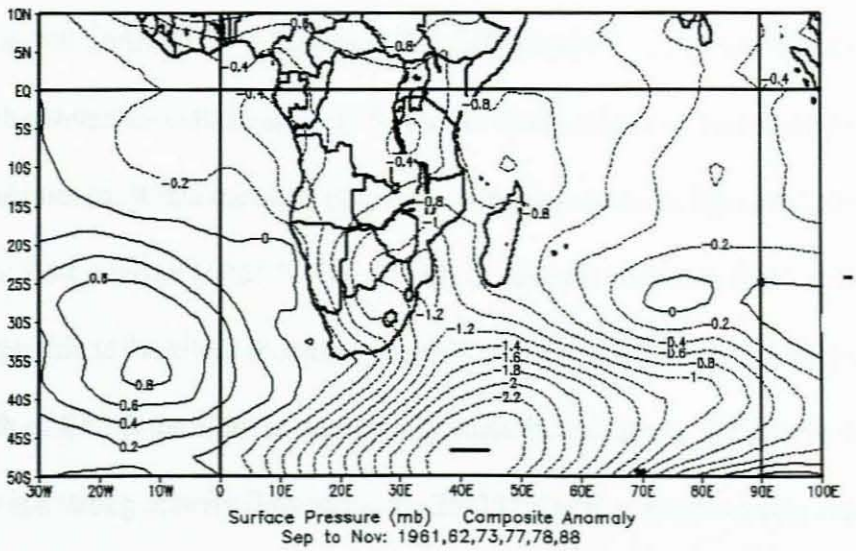

-3 lag

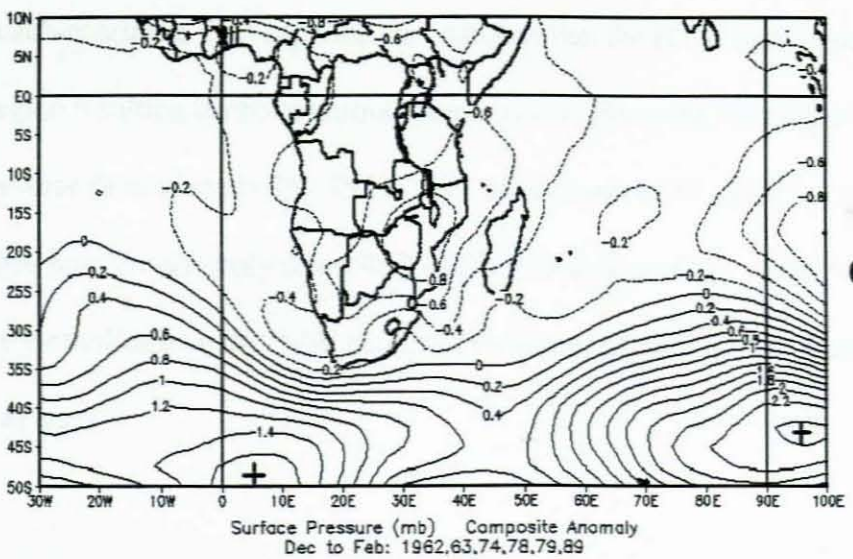

0 lag

Figure 4.1 Composite pressure anomaly charts for wet years

4.3 Wind Field

Winds may be considered by directly examining the wind vectors or resolving them into zonal and meridional components. The zonal component is usually larger than its meridional counterpart (Tyson, 1986). Here vector winds have been considered at lower level (850 hPa) and upper level (200 hPa). The same periods are considered the summer (DJF), spring (SON) and winter months (JJA).

4.3.1 Composite Wind anomaly at 850 hPa Level

The -6 lag composite shows a cyclonic flow anomaly centred around 37° S 65° E over the Indian Ocean but north of 15° S the flow is easterly, figure 4.2. There is westerly flow along the 30° S which converges with an easterly flow over South Africa into a southerly flow over much of the sub-continent. While the SON (lag -3), composite anomaly, figure 4.2, indicates a marked anticyclonic flow centred at 35° S 10° W which extends southerly flow over the west half of the continent; this is the about the mean position of the southern Atlantic High. Over the Indian Ocean north of 25° S the flow is dominantly easterly and along 35° S it is easterly. At lag 0 (DJF) there is a strong easterly flow along the 25-35° S with some moderate westerly flow north of 20° S over the Atlantic and easterly flow from the Indian Ocean converging over the southern African sub-continent. This supports the postulate that the ITCZ is more active and is confined in the region resulting in above normal precipitation. From lag -6 to lag 0 the subtropical zonal winds reverse from westerly 25 - 35S to easterly anomalies (30 - 35S) in response to the change in surface pressure anomaly along 45S which becomes positive within the same period.In all cases the westerlies over the Sahel exist, but these are stronger for lag -6 and lag -3 and become weaker at lag 0.

4.3.2 Composite Winds at 200 hPa

The -6 lag anomaly chart figure 4.3 shows a marked westerly flow south of 25° S which is a prominent feature for the presence of the sub tropical Jet. Stronger easterly flow anomalies appear north of 15° S, especially in the Atlantic. The lag -3 composite anomaly shows a strong westerly flow that recurves about 25° S 60° E over the Indian Ocean into an easterly flow north of 12° S. An area of shear is apparent over the continent along 20-25° S and 20-40° E. At lag 0 there is dominant easterly flow along the 15-20° S. An intrusion of a northerly flow from the equator reaching 10° S along the 25-38° E is apparent. An anticyclonic flow anomaly exists south of Madagascar over the Indian Ocean. Centred at 25° S 30° E is a diffluence pattern within the easterly flow over the sub-continent. This is a region of divergence that enhances ascent and convection beneath (Tyson, 1986).

In summary, the lower westerly flow north of about 20° S and the upper level easterlies are indicative of the effects of an Atlantic Walker Circulation over Africa and suggests that the location of zone of maximum convection and latent heat release occurs from 10- 20° S which is about the southern limit of the summer migration of the Inter Tropical Convergence Zone (Tyson, 1986). Interaction between the zonal Walker and Hadley circulations is likely in the area of maximum convection over the continent where latent heat release provides the energy and momentum to drive both circulations.

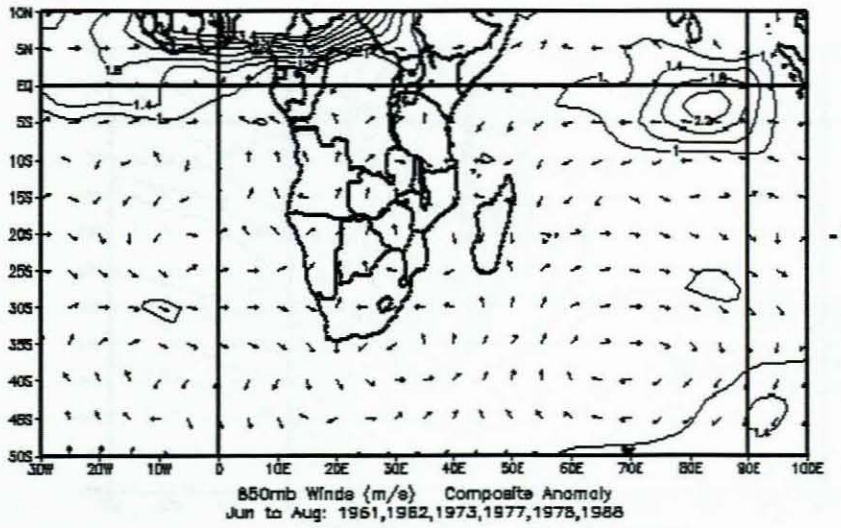

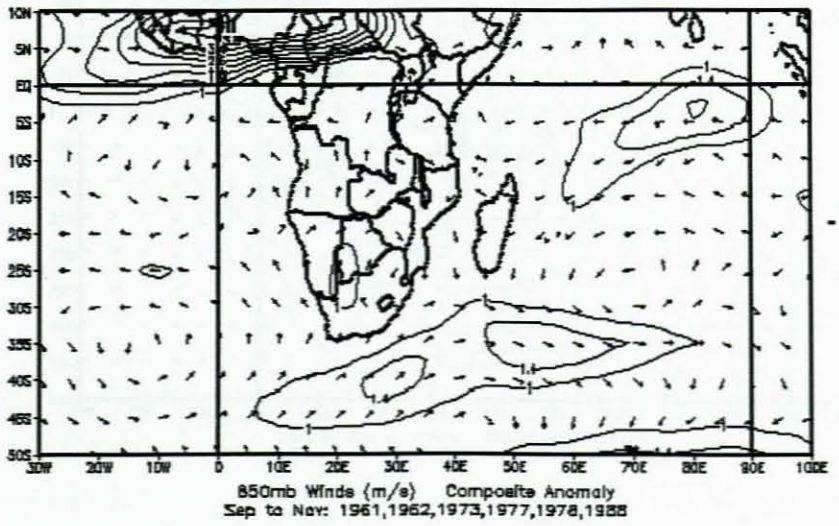

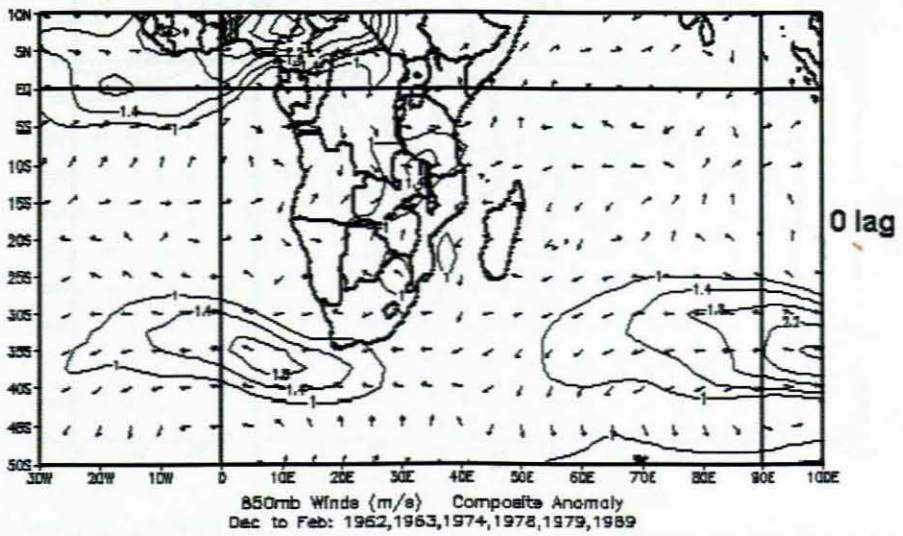

Figure 4.2 850 hPa Wind anomaly charts for wet years for JJA (-6), SON (-3) and DJF (0)

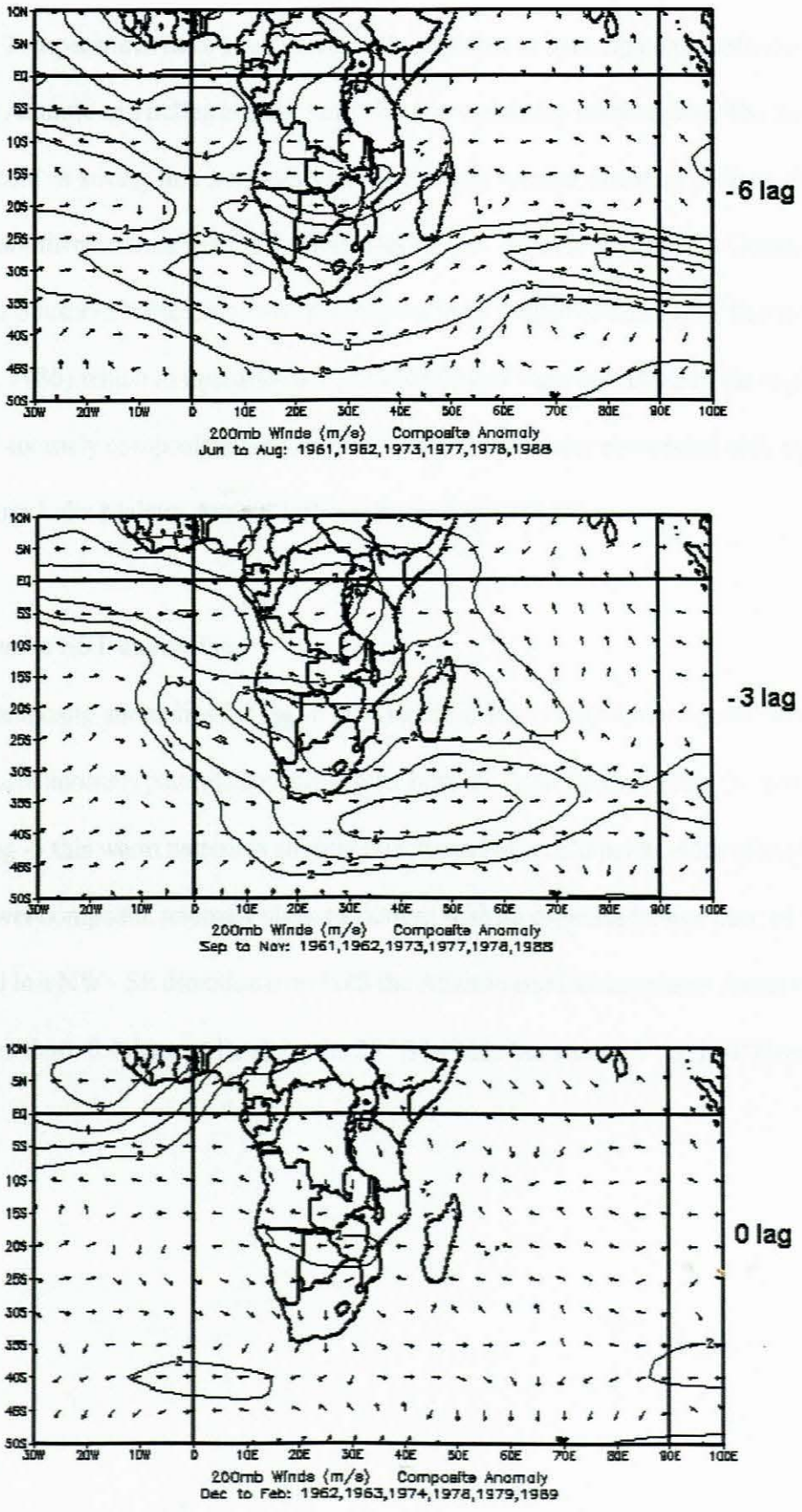

Figure 4.3 200 hPa Wind anomaly charts for wet years for JJA (-6), SON (-3) and DJF (0)

4.4 Sea Surface Temperatures (SSTs)

Sea Surface Temperatures have been extensively explored to investigate the relationship of the surrounding Atlantic and Indian oceans, with climatic variability in the region. The past research studies indicate a strong link between various climatic related disasters such as droughts or flooding in southern Africa and SST anomalies in the Atlantic and Indian Oceans. Rainfall variability in Southern Africa, for example, appear to be related to these SST fluctuations (Hastenrath, 1986) which in turn affects the availability of water resources in the region. In this section SST anomaly composites are analysed to examine patterns associated with wet years as classified from Lake Malawi Annual Inflows for period 1958-94.

4.4.1 Composite SST anomalies

The SSTs composite anomalies for lag -6 (JJA) and the lag -3 (SON) are consistent with weak (< 0.2°C) warm anomaly patterns appearing over both the Atlantic and Indian Oceans. However during the lag -3 this warm pattern is slightly punctuated by a cold patch south of the Cape. The lag 0 (DJF) wet composite anomaly shows a pattern with an organised wave train of warm then cold oriented in a NW - SE direction over both the Atlantic and Indian oceans. Areas with colder anomalies less than -0.4 degrees lie along the 25° S latitude but around 0° and 80°E respectively.

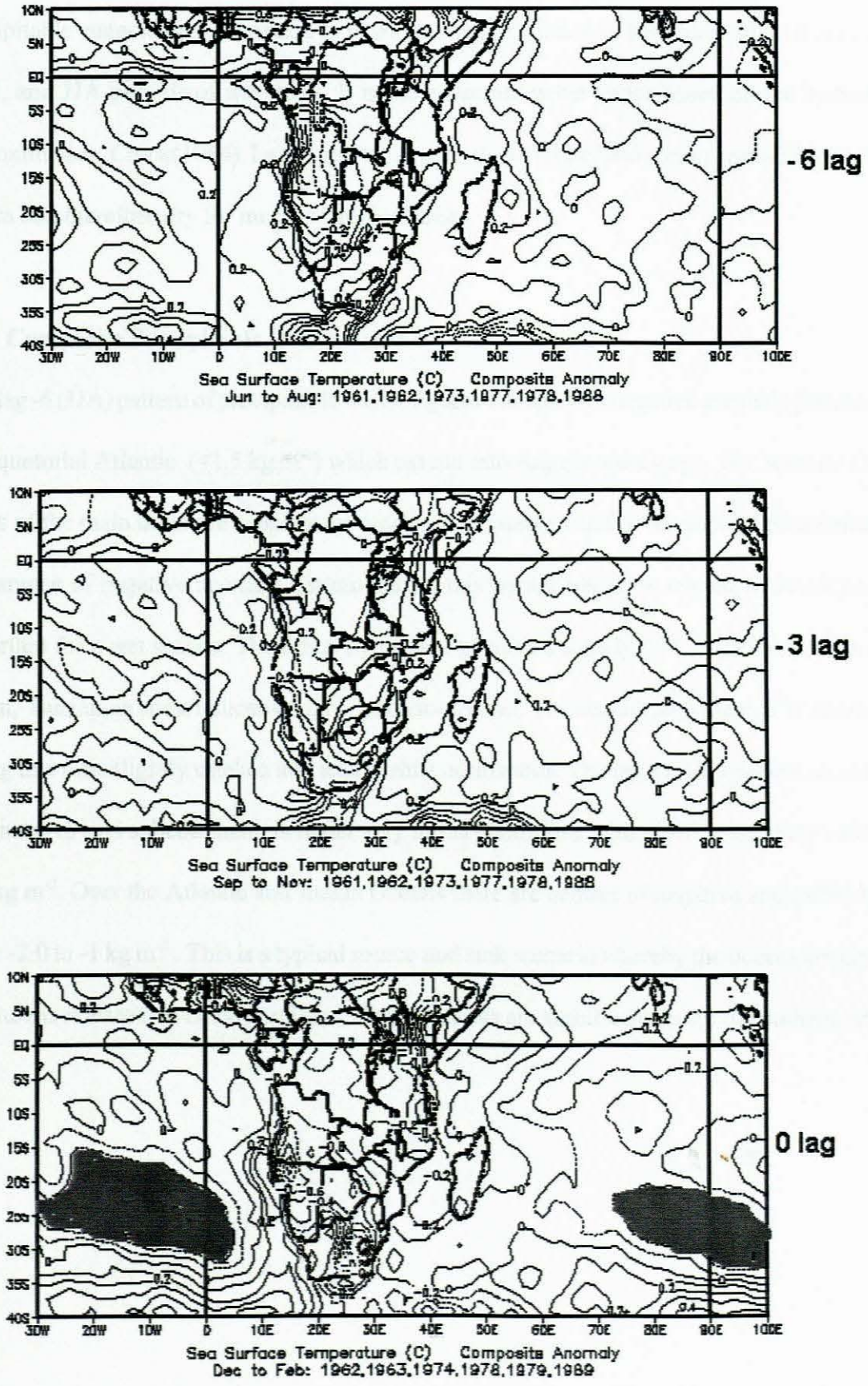

Figure 4.4 Composite sea surface temperature for lag -6 (JJA), lag -3 (SON) and lag 0 (DJF), shaded is < -2 °C

4.5 Precipitable Water

Precipitable water is here examined to illustrate the distribution of moistness of air during DJF, SON, and JJA periods of wet years. It is the columnar water vapor based on the hydrostatic approximation, Chow(1964). Lag -6 and lag -3 periods are winter and spring periods for southern Africa and therefore dry for much of tropical areas.

4.5.1 Composite Precipitable Water Anomaly

The lag -6 (JJA) pattern of precipitable water, figures 4.5, shows a negative anomaly pattern over the equatorial Atlantic (<1.5 kg m^{-2}) which extend into Angola and Congo. The Atlantic Ocean is one of the main moisture supplier for much of the western half of Southern Africa hence the appearance of negative anomaly pattern during this period might be related to developments important for a wet season. There is a significant positive anomaly (> 1.5 kgm^2) over the west Indian, Tanzanian coast indicative of N.E monsoon onset. The equatorial Atlantic PW anomalies during this time slightly weaken and tend to shift northwards. The lag 0 (DJF) pattern shows that Southern African subcontinent is under very moist conditions with positive anomaly values of 1- 2 kg m^{-2}. Over the Atlantic and Indian Oceans there are centres of negative anomalies in the range -2.0 to -1 kg m^{-2} . This is a typical source and sink scenario whereby the oceans are dry and moisture is released over the continent. These patterns are significant for all of southern Africa.

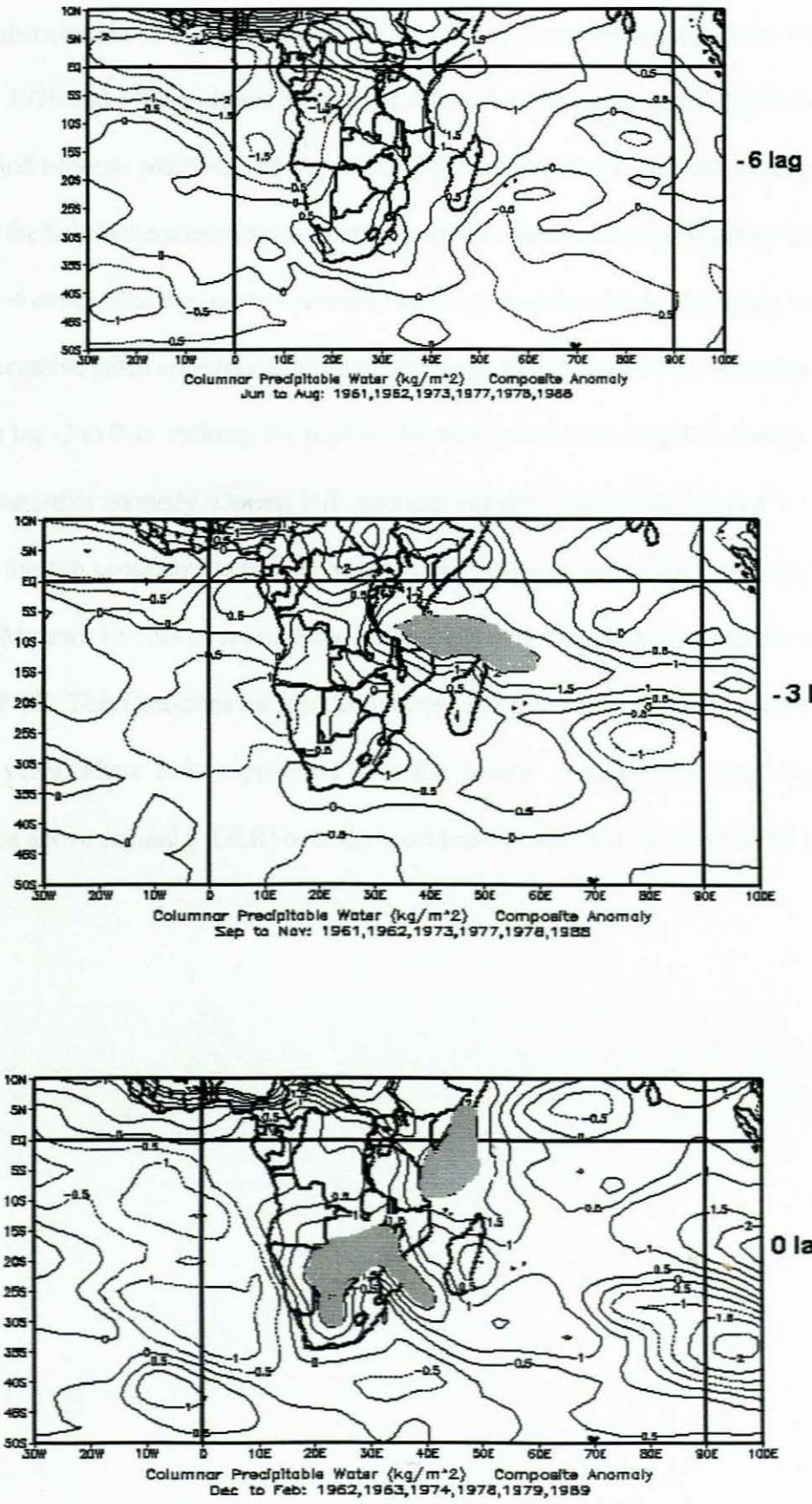

Figure 4.5 Composite anomaly patterns for wet years at lag -6 (JJA), lag -3 (SON) and lag 0 (DJF), shaded is > +2 kg m^{-2}

4.6 Outgoing Longwave Radiation (OLR)

The spatial distribution of OLR for lag -6, lag -3 and lag 0 periods for wet years 1962, 1963, 1974, 1978, 1979 and 1989 is shown by figure 4.6. Much of the Indian and Atlantic Ocean start off neutral and become positive. The lag -6 (JJA) pattern shows a (convective) negative axis portion over the Sahel extending eastwards over the Indian Ocean. The lag -3 pattern is consistent with the lag -6 except that the positive anomaly cell over Angola widens extending to Namibia. A stronger negative patch appears on the equatorial east Atlantic around the Angolan area. The change from lag -3 to 0 is striking; the positive anomaly patch over Angola is totally displaced by a strong negative anomaly. During DJF stronger negative anomalies (shaded < -12 W/m^2) appear over the sub continent centred on South Africa, Botswana, Namibia, Angola, Tanzania and parts of Malawi. Patches of positive anomalies exist over the Atlantic and Indian oceans but oriented NW-SE. This illustrates the high convective activity over the southern African region during wet years where it is suppressed over the oceans in agreement with Jury (1997). Convection is above normal (- OLR) over the west Indian coast and the Sahel at all lags.

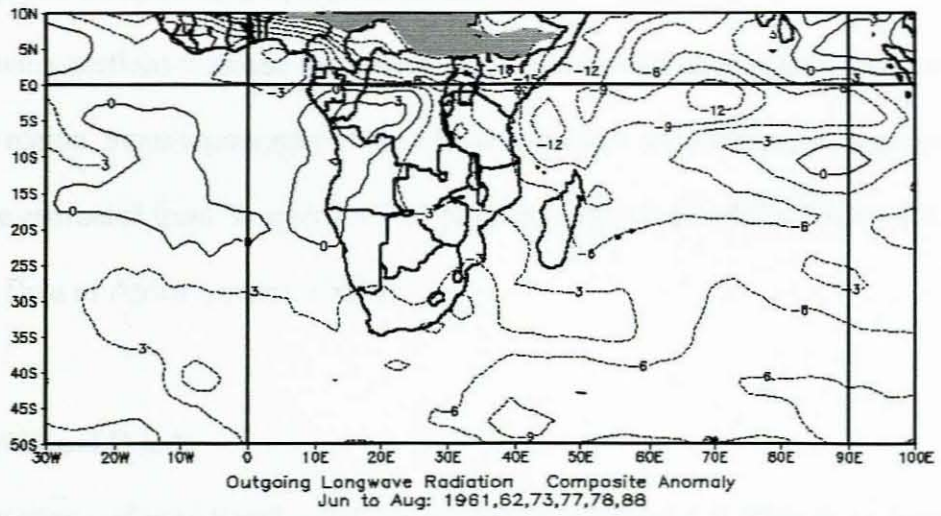

-6 lag

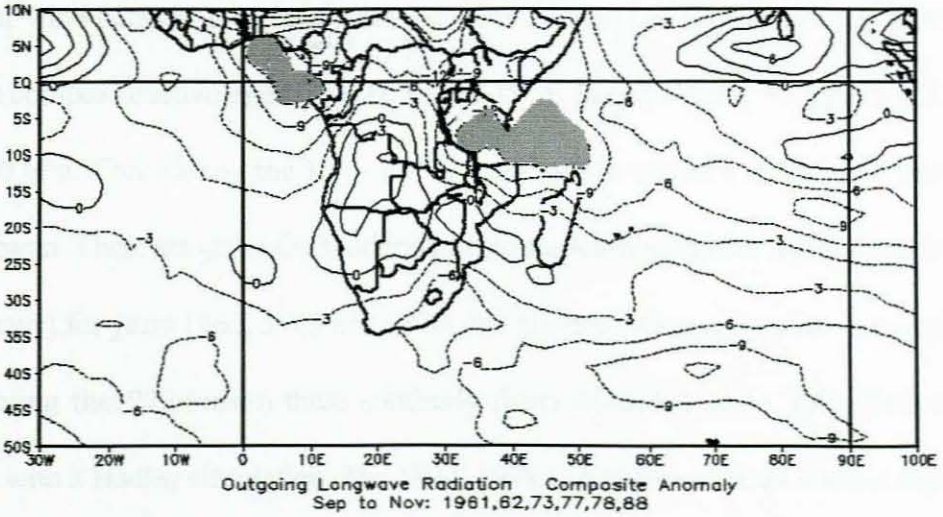

-3 lag

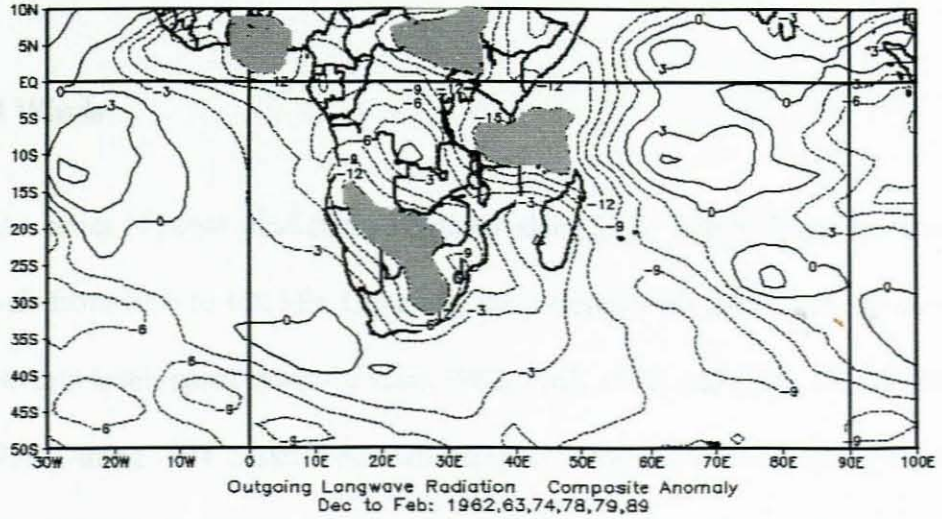

Figure 4.4 Composite Longwave Radiation anomaly charts for lag -6 (JJA), lag -3 (SON) and lag 0 (DJF), shaded is < -12 Wm^{-2}

4.7 Composite analysis of the Meridional and Zonal Winds

The following sections examine the vertical distributions of both meridional and zonal winds across the region. Some topography of the African continent and Madagascar are superimposed, these were estimated from Southern Africa physical map (source: Map Studio, RSA) and the Elevation Data of Africa (source: USGS).

4.7.1 Meridional Winds

Vertical sections of meridional wind are presented in figure 4.7. This is to investigate the meridional wind patterns associated with wet years over the Lake Malawi Basin. The meridional wind slice composite is averaged over 22.5° and 35° E longitude and 50° S to 5° N, from 1000 hPa to 100 hPa. Considering the 10° - 20° S band which covers Lake Malawi and the upper Zambezi basin. There are generally moderate to strong southerly flows in the lower levels (up to 700 hPa level) for years 1962, 1963 and 1979, and northerly flow anomalies in the mid to upper levels. During the1979 season these southerly flows extended up to 500 hPa level. This is consistent with a Hadley circulation. The 1974, 1978 and 1989 wet years show a slight different pattern where there are northerlies deep northerly anomalies particularly north of 30° S.

4.7.2 Zonal Winds

Figure 4.8 is a series of zonal wind slices averaged along 22.5° S to 5° S and run from 0° E to 50° E at levels from 1000 to 100 hPa. Generally the patterns show dominance of westerly flow from lower to mid levels particularly for years 1962, 1963, 1978, and 1989. This is different for 1974 and 1979. During 1974 easterly anomalies appear in the mid levels reaching 100 hPa level. While during 1979 the anomalies in the lower levels are weak, however stronger positive anomalies (westerlies) appear above 500 hPa level.

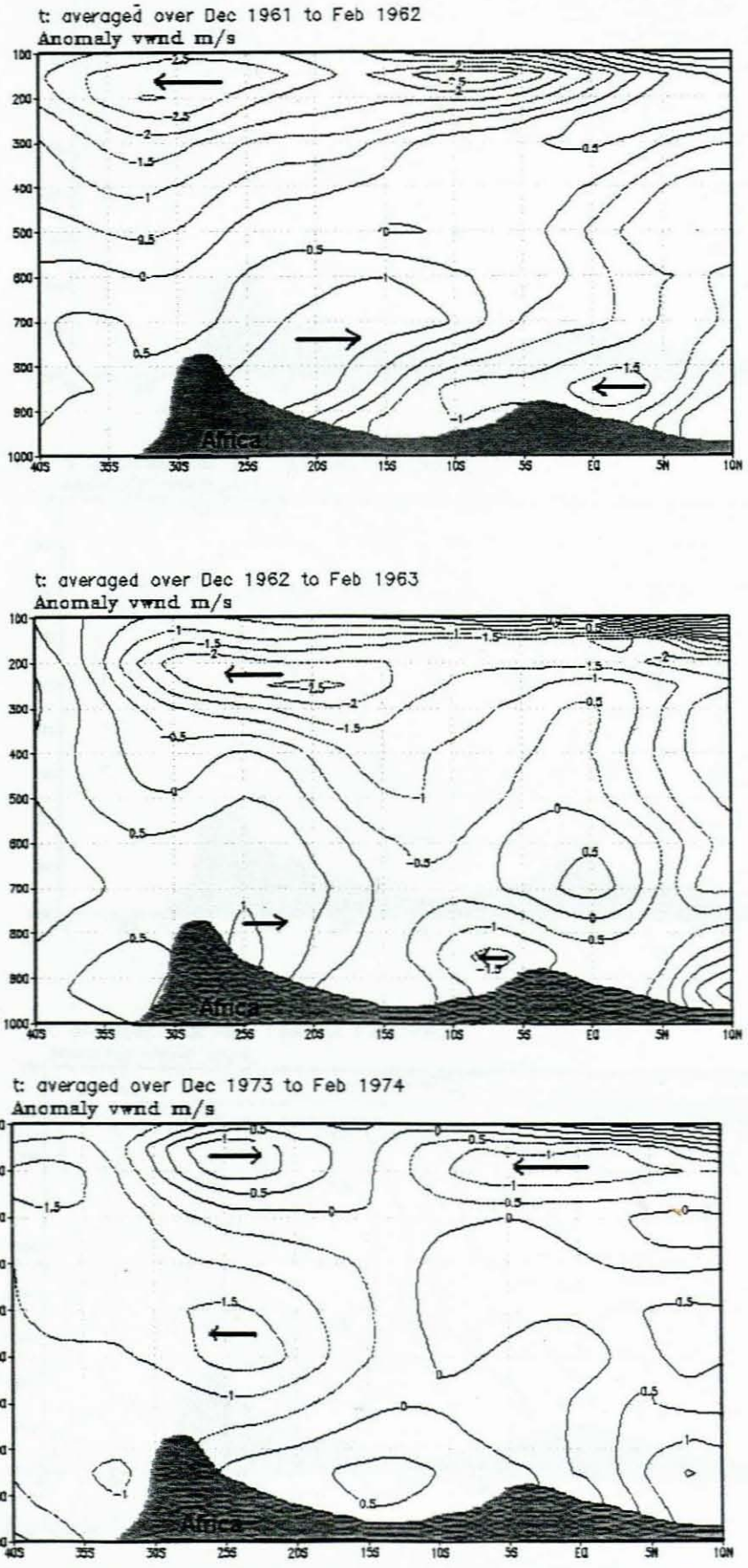

Figure 4.7 Vertical meridional wind charts for 1962, 63, 74, 78, 79 and 89 years along 22.5 - 35°E

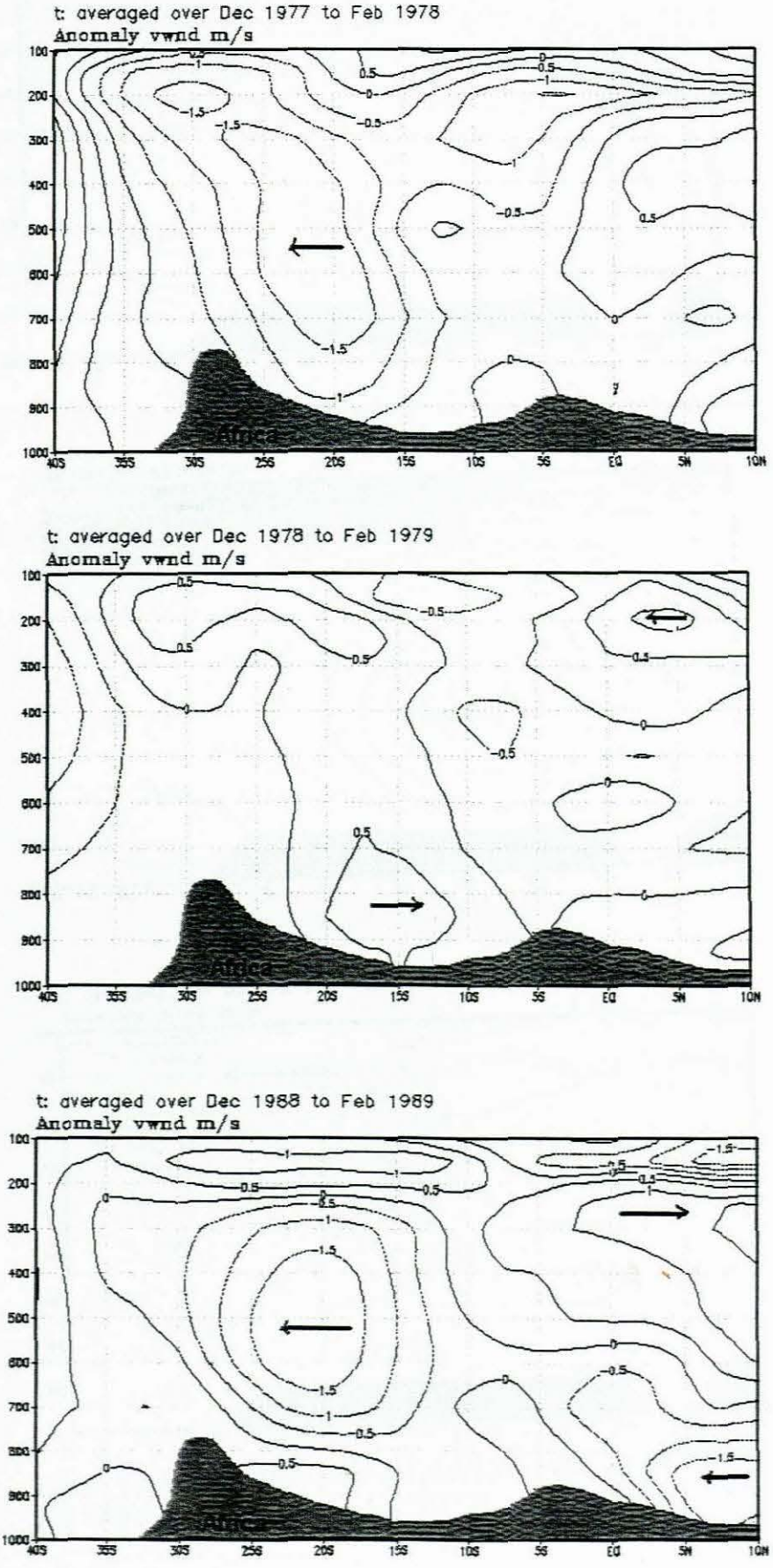

Figure 4.7 contined

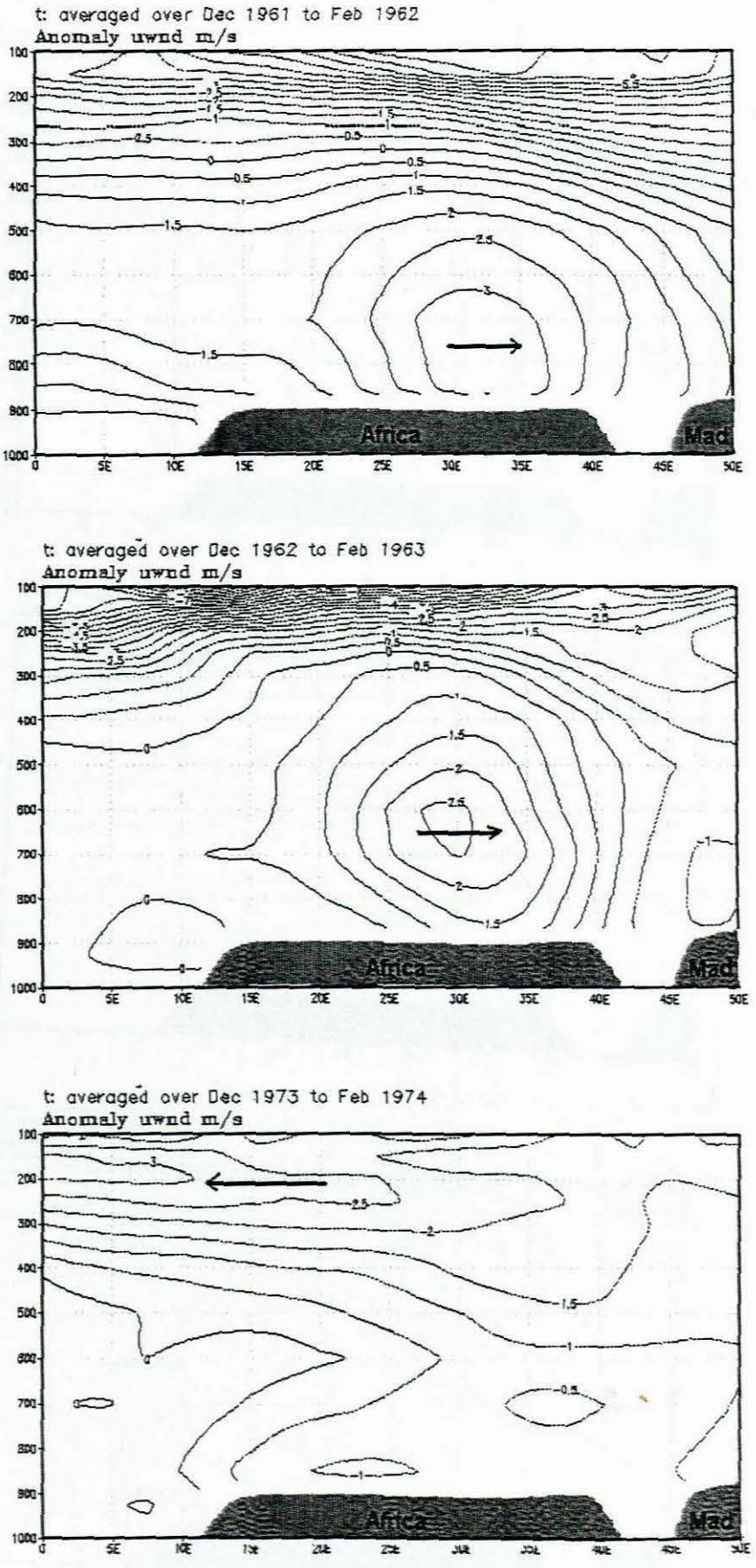

Figure 4.8 Composite zonal wind slices for 1962, 63, 74, 78, 79 and 89 years averaged along 5 - 22.5° S

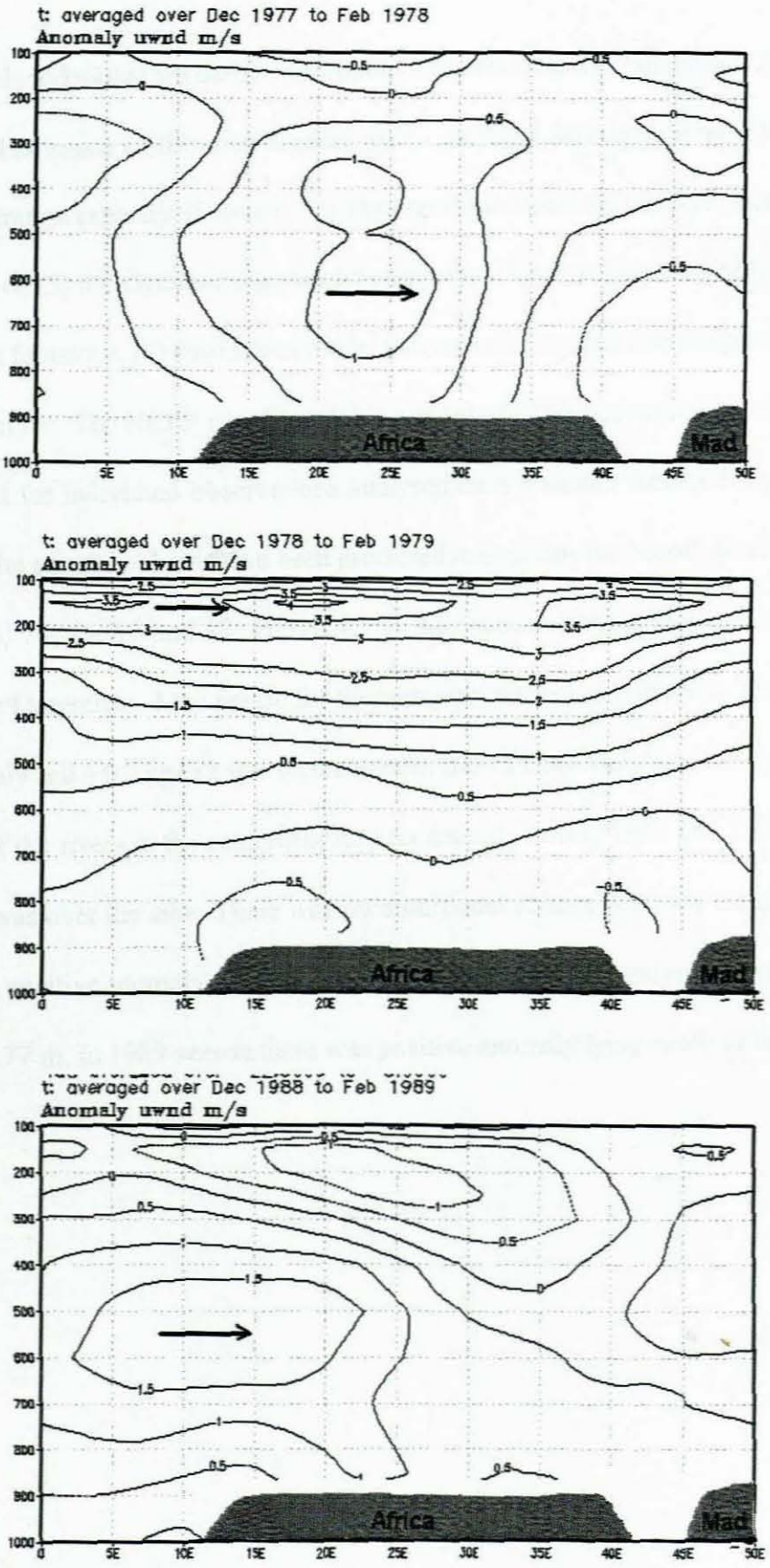

Figure 4.8 Composite zonal wind slices for 1962, 63, 74, 78, 79 and 89 years averaged along 5 - 22.5°S

4.8 Runoff Anomalies

There are several models that are used to estimate surface runoff and its anomalies. Some of them include (1) the Hortonian (infiltration excess) where overland flow is generated when rainfall intensity > infiltration capacity of the soil. (2) Throughflow: which accounts for storm flow with no overland flow, (3) the Dynamic area model similar to 2 but considers variable areas of soil saturation at the footslope. (4) Partial area model that considers spatial and temporal variation in infiltration capacity. The NCEP runoff model is a result of daily accumulation of rainfall in a "bucket" model for individual observations analysed on a gaussian surface for period 1958 - 1999. Composite anomaly charts have been produced to examine the runoff distribution during years 1962, 63, 74, 78, 79 and 89. Figure 4.9 is the spatial distribution of composite runoff anomalies over December - May period for the wet years under consideration. During 1962 the positive anomaly cell > 0.2 kg m-2 was on the eastern side of Lake Malawi while the western side where many of the rivers in the catchment lie was neutral. During 1963 and 1974 the positive anomaly cell was over the lake. There was no significant change from the mean during 1978. During 1979 a positive anomaly cell (> 0.2 kg m^{-2}) lay over the lake and supports the strong lake level rise of 1.77 m. In 1989 season there was positive anomaly lying south of the lake.

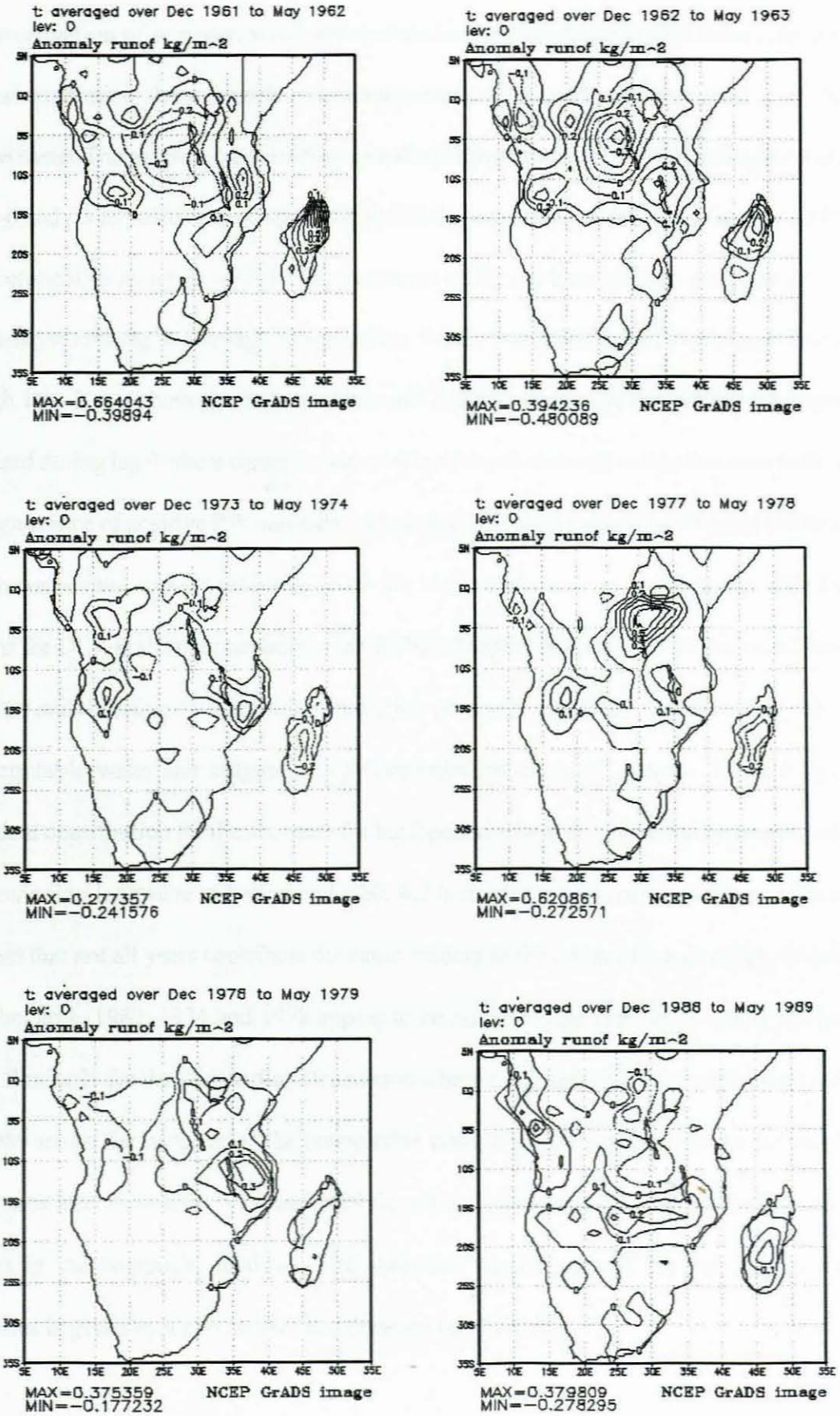

Figure 4.9 Composite runoff anomaly patterns for wet years

4.8 Discussion and Summary

The investigation of pressure, wind, sea surface temperature, precipitable water, and outgoing longwave radiation show remarkable characteristics associated with wet years over the Lake Malawi basin. The pressure pattern show a marked change along the 45°S from negative anomaly at lag -6 and -3 to positive anomaly at lag 0. Similar noticeable changes also appear on 850 hPa wind composites along 25 - 35°S. The existence of the subtropical jet is apparent on 200 hPa wind analyses for lag -6 and lag -3 composites. Weak warm SST anomalies persist from lag -6 through lag -3 over both the Indian ocean and Atlantic ocean but the pattern becomes more organised during lag 0 where there is a wave train of warm and cold anomalies over both oceans. The appearance of positive PW anomaly values along the west Indian Ocean coast is also an area of high convective activity associated with the N.E monsoon onset in the region. The anomaly patterns for OLR is strongly negative over the Sahel region and the west Indian coast during lag -6 period and therefore important for prediction purposes. Persistent significant signals appear in precipitable water and outgoing longwave radiation anomaly patterns. Table 4.1 presents individual contribution for the six cases for lag 0 period where I.O. is the Indian ocean and OLRa is the outgoing longwave radiation and table 4.2 is the description of the areas considered. It is apparent that not all years contribute the same amount to the composite anomalies. Considering the Sahel area, 1962, 1974 and 1978 appear to be on the higher side while only 1989 is on the lower. Similarly for the west Indian Ocean area where 1962 and 1963 are on the upper and 1974 and 1989 are on the lower side. The precipitable water anomaly contribution for the west Indian Ocean area also show that 1974 and 1989 do not contribute much to the positive anomaly that appears in the composite analysis. The statistical significance of the wet years composite anomalies is given by a two tailed t test done on lag 0 values:

$$t = (s/\sigma)*(N-1)^{1/2}$$

where s is the average of the composite anomalies, σ is the standard deviation of the entire sample (1959-1995), and N-1 is the number of degrees of freedom. The wet year composite anomalies show greater significance at 95% confidence level (t = 5.63) for pressure but not for SSTa.

Table 4.1 Intra-composite contributions for PW and OLR anomalies at 0 lag

Year	West I.O. PW	Sahel OLRa	West I.O. OLRa
1962	4.5	-21	-9
1963	3.5	-18	-15
1974	-1.5	-21	-15
1978	2.5	-21	-9
1979	2.0	-12	-21
1989	0.5	-6	-21
composite mean	2.0	-12	-1
σ	2.2	6.22	5.37

Table 4.2 A description of areas used for intra-composite analysis

Area	**Description (Lat / long.)**
West I.O.	3 S - 12 S, 32 E - 52 E
Sahel	2 N - 10 N, 10 E - 42 E

CHAPTER 5.0: DISCUSSION AND SUMMARY

5.1 Introduction

With increasing concern about climatic variability, it is widely acknowledged that the global measurement of climate-related variables is of great importance both for monitoring the climate changes as they occur and as input for predictive climate models (Mason et al.,1994). Such climate fluctuations can be measured either directly or indirectly, by proxy. Lakes and rivers are important proxy indicators of climatic changes in several ways. Analyses of Lake Malawi Levels and Zambezi annual River flows at Victoria falls, chapter 3, have shown interannual variation consistent with the climatic fluctuations in the region. In Chapter 4 composites for different climatic parameters have been examined to investigate patterns associated with wet years as determined from chapter 3.

5.2 Summary on Lake Malawi Levels and Zambezi River flow Variability

The Lake Malawi level series and the Zambezi annual river flows have demonstrated very significant trends in the southern tropical African climate fluctuations. Both water bodies show marked spectral periodicities falling within 2 - 10 year cycles. The 9.58 yrs in the 1938-76 period may be associated with the solar cycle, the lower frequency oscillation of 19.16 years during the recent decades 1976-1995 can be attributed to luni-solar tide. More secondary oscillations at of 14.5 years, 8.3 years, 5.8years (ENSO), 2.05 years (QBO) are apparent on the Lake Malawi series while the Zambezi shows similar periodicities at 20.4yrs, 9yrs, 2.5yrs, 6yrs, 3yrs.This association with global periodicities is an important phenomenon when it comes to seasonal prediction. The interannual lake levels and the Zambezi river flow fluctuations show strong relationship with rainfall as recorded at stations within the respective catchments. Lake Malawi inflows correlate

very strongly with individual station annual rainfall along its shores ranging from r = 0.52 for Karonga in the north, r = 0.60 for Nkhotakota, to r = 0.66 for Salima in central Malawi. On the other hand, the relation of Zambezi river annual flows with area rainfall is strikingly high with a correlation coefficient of 0.74. When the lake inflows are regressed with the Zambezi annual flow the correlation coefficient is r = 0.53. This describes a very close association of climatic fluctuations taking place in both catchments. The persistence at +1 year lag is higher for the Zambezi (r_k = 0.44) but lake level changes have little memory (r_k = -0.036). The years 1978,1979, 1974, 1963, 1962,1989 feature very well as wet years from analyses on both the lake and the Zambezi. An examination on the annual lake level shows that the 1979 peak has a recurrence interval of about 50 years. For purposes of water balance assessments in chapter 3, investigation has been made on the relationship of the lake's annual outflow with other water balance components namely evaporation and Shire River discharges. The Lake Malawi outflow index association is stronger with evaporation (r = 0.49) than the Shire river discharges (r = 0.36). This confirms the mean annual water balance components and shows that water losses from the lake occur mainly by evaporation and very little by river outflows. The Shire river discharges tend to peak at the time when lake levels rises such as in 1979, thus mean annual Shire river flows correlate strongly with the mean annual lake levels (r = 0.88); the relationship is stronger with the annual maximum flows compared to the annual lake level peaks. Climatic parameters that have been used in this investigation are based on variables that have shown marked differences during wet years.

5.3 Summary on Composite Analyses

The climatic patterns associated with wet years have been analysed. The parameters used in the analysis are pressure, wind, sea surface temperature, outgoing longwave radiation, and

precipitable water. Vertical slices have been investigated for zonal and meridional wind components. Table 5.1 summarises significant observations noted from the composite anomaly analyses.

Table 5.1 A summary of notable anomaly climatic characteristics associated with wet years

Parameter	Lag 0	Lag -3	Lag -6
SLP	>1.0hPa around 45°S and 5°E, 40-50°S and 60-100°E	<-2.0 hPa: around 45°S and 45°E	<-0.8 hPa: south of 35°S
850 hPa Winds	Easterlies south of 30°S, westerlies (>0.4 s^{-1}) along 15°S over Atlantic, easterlies (>0.8 m s^{-1}) along 10°S over Indian Ocean	Easterlies (>1.0 m s^{-1}) 0-15°S and 70-95°E, 25°S and 30°W-0°E; westerlies 40°S and 10-90°E	Easterlies (>1.0 m s^{-1}) 10°S-5°N and 70°E-92°E
200 hPa Winds	Easterlies (>2 m s^{-1}) along 40°S and 10°W-10°E	Easterlies 10°S-2°N and 20°E-35°E, westerlies south of 20°S	Easterlies north of 20°S, westerlies from 22°S-40°S
SST	Cool centres (<-0.3°C) around 20°S and 10°W-0°E, 20°S and 75°E-95°E	Warm centre (>0.2°C) over 15-35°S and 30°E-65°E	Warm centre (>0.2°C) over 15°S-25°S and 30°E-50°E

PW	>1.5 kg m^{-2} over 20°S-30°S and 20°E-40°E, 10°S-5°N and 32°E-45°E	>1.5 kg m^{-2} 2 over 5S-17°S and 25°E-70°E	<-2.0 kg m^{-2} over 5°S-5°N and 30°W-2°E
OLR	<-12W $^{-2}$:10-30°S and 12-28°E; 5-10°S and 30E-45E	<-12W m^{-2}: 5-12°S and 30-48°E; 3°S-5°N and 0-10°E	<-12W m^{-2}: 10°S-2°N and 32°E-75°E; 0-10°N and 15-40°E
V wind slice	southerly flow in lower and northerly in upper for 1962, 63 and 79 the reverse occurs for 1974, 78 and 89		
U wind slice	dominantly westerlies for all years except 1974		

5.3.1 Lag 0 (DJF) Composite Patterns

The lag 0 period is the summer period where much of the rains are experienced in the tropical southern Africa. The DJF pattern indicates that the wet years are strongly associated with a rise in pressure of both the south Atlantic and south Indian Highs. The south Indian High tends to move further eastwards centred around 45° S 70° E. The wet years DJF composite anomaly shows remarkable pressure falls over the continent with significant lower values centred over Malawi, Zambia, Mozambique and Zimbabwe. These features are important in that the pressure rises of

the Atlantic and Indian oceans creates a stronger pressure gradient thereby strengthening the Hadley cell circulation. Changes in the strength of the Hadley cell have been invoked to account for rainfall changes in African subtropics (Nicholson, 1986). Lindesay (1986) has shown how the cell modulates rainfall in southern Africa and linked it to Walker circulation. The pressure rise of the Indian Ocean High strengthens the easterly flow north of 15° S at 850 hPa level while the Atlantic High anomalous rise strengthens the meridional arm of the ITCZ at lag 0. The pressure falls over the continent ensures widespread uplifting of air, one of the prerequisite conditions for precipitation to take place. The diffluent flow pattern over the continent is an important feature to support the convergence below. The DJF (lag 0) SST analyses have shown alternating cool- warm- cool anomaly patterns over the Atlantic and Indian oceans. The precipitable water anomalies for these wet years show moister air over the continent and drier air over the surrounding oceans. An area of high Precipitable water exists near Madagascar oriented NW-SE reaching parts of Malawi, Zambia and Mozambique. The OLR DJF anomaly composites support the foregoing argument where there is considerable convective activity over the continent including Madagascar but suppressed convective activity over the adjacent tropical and subtropical ocean areas.

5.3.2 Precursor composite patterns

The composite anomaly analyses have been performed for lag -6 (JJA) and lag -3 (SON) periods. The JJA pressure composite anomaly show a general pressure fall over the area; but the area of greater variability (<-0.4 hPa) exists along the subtropical high belt extending a tongue over Madagascar through Mozambique reaching Malawi. During the SON period there is a distinct anomalous fall in pressure over the Indian Ocean High which extends over the sub-continent. The wind field for the JJA and SON follows the behaviour of the pressure patterns. The JJA

composite anomaly shows a strong cyclonic flow around 40°S 70°E. This illustrates that prior to wet years the Indian High is very close to the South African east coast during the JJA period but abruptly moves eastwards during the SON period. At 850 hPa level during the SON period there is anomalous southerly flow south of the Cape. The change from cyclonic anomaly to anticyclonic flow during SON period south east of Madagascar is also an important feature. The winds at 200 hPa level for JJA and SON periods support the patterns as observed at 850 hPa. The existence of the subtropical jet is evidenced by the strong westerly anomalies exiting during both periods. JJA is a winter period and therefore the subtropical jet moves closer to 35°S (Tyson, 1986). The spatial variation of wind anomalies near the surface and in the upper atmosphere over southern Africa suggests that zonal flows vary consistently (Lindesay, 1986) over the east coast, while meridional flow variations are consistent with anomalies of a Hadley cell type (lower equatorward upper poleward flow).

The lag -6 (JJA) and lag -3 (SON) SSTs show neutral conditions over most areas. Precipitable water distributions during lag -6 (JJA) and lag -3(SON) prior to wet summers indicate that the western half of Africa is drier and the eastern half is moister. The appearance of a moist tongue north of Madagascar extending into Tanzania and Malawi is an important feature to be observed before wet years over the Malawi region. The moisture decrease over the eastern equatorial Atlantic reduces local ITCZ activity, while the Indian ITCZ is enhanced. The lag 0 pattern confirms this as southern African cloud bands are enhanced along 40°E and 25°E.

The lag -6 and lag -3 OLR patterns describe a southeast evolution of higher convective activity (< -12 W m^{-2}) from the Sahel to the equatorial Indian ocean and the eastern half of the continent from JJA covering East Africa during lag -3 and finally reaching Malawi, Mozambique and Zambia during mid-summer period. A patch of suppressed convective activity appears over Angola, Congo and Namibia, which disappears later in the DJF period. The precursor OLR

patterns follow the southward movement of the sun when surface winds tend to back and the pressure falls over the interior of the continent. The recurved Indian Ocean southeast trades become appreciably moister and unstable as they pass around the northern end of Madagascar thereby concentrating moisture over the interior of the continent. The appearance of Congo air enhances the ITCZ with moisture and anchors the ITCZ activity over southern Africa.

The vertical structure of winds during the wet years has been examined. The meridional wind patterns show a variable circulation pattern of southerly flow in the lower levels and northerly flows in the upper levels for 1963 and 1978 years. While the zonal flow patterns support the existence of an overturning circulation with a rising arm over the African continent (Tyson, 1986).

5.4 Statistical model for prediction of Lake Malawi inflow

Models are widely applied in pursuit of climate variability. Nested regional models are used for regional studies while global coupled atmosphere/ ocean/ ice general circulation models are used for global change prediction. Several models have been developed for Lake Malawi basin based on the on rainfall-runoff relationship (Kidd, 1983), some on rainfall (Kidd, 1983) and inflow-global indices (Center of environmental Studies, University of Zululand). In this study significant areas with stronger signals associated with high lake inflows and climatic conditions have been formulated for air pressure, winds, precipitable water and outgoing longwave radiation anomaly composites. The predictors are considered for the July to November period prior to the summer rainy season. These will be the focus of further investigation where statistical multivariate regression methods will be used to formulate quantifiable algorithms for operational prediction. Possible candidate predictors for formulation of models as determined from the composite analyses are listed below and defined in Table 5.2: the first relates outgoing longwave radiation

anomaly in the west Indian Ocean area and the eastern Sahel (negative) in the precursor periods of lag -6 and lag -3 of wet years. The second is precipitable water spatial distribution over the eastern Atlantic ocean (positive) and the west Indian Ocean (positive). While the third is the behaviour of the south Atlantic Ocean winds (westerly, 30° S at lag -6 changing to easterly at lag -3) and south Indian Ocean winds (strongly cyclonic) at 850 hPa and the 200 hPa zonal wind along 45°S (westerly). Lastly the fourth refers to the behaviour of surface pressure along 45°S (negative anomaly) and pressure change from lag -6 to lag -3 plus

1. West Indian Ocean and Eastern Sahel OLRa
2. East Atlantic Ocean and West Indian Ocean PW
3. South Atlantic Ocean, South Indian Ocean winds (850 hPa) and South Atlantic Ocean winds(200 hPa)
4. 45° S SLP (Atlantic and Indian Oceans)

5.4.1 Formulation of predictor model

Multivariate linear regression statistical model is developed using Statigraphics software and a predictor data set in a forward stepwise approach. The model is formulated for optimum hindcast fit (r square) 5 candidate predictors are considered, some for 18 year record and another for 35 years. The candidate predictors include air pressure, vector wind, OLR and precipitable water. The lake inflows are fitted by a number of area averaged predictors for the preceding winter and spring using a stepwise method. Predictors with higher partial correlation are selected, at this time only limited to two. The inflow model algorithm includes contributions from olrasahj the convective anomaly across SE Sahel for JJA period and slpaios is a pressure anomaly for SON period in the south Indian Ocean. The model, eq. 5.1, produces a 83 percent correlation (r^2 fit of 0.70) for 1975-92 training period. The Durbin-Watson statistic is 2.4 and lies above the

appropriate threshold, hence forecast misses may be considered random. The model is validated using jackknife skill test, as illustrated in fig 5.1. The forecast "miss" the correct tercile category once every 8 years. The 35 year model, eq. 5.2, has lower perfomance, with an r^2 fit of 0.20 for the period 1958 - 1992. The Durbin Watson value (1.8) is lower than the critical threshold. The third model, eq. 5.3, (Jury et al, 1999) is a combination of SST and Surface air pressure for JAS period. It has an r^2 fit of 0.33 but Durbin Watson value of 2.2.Hence the 18 year model though shorter is prefered. Predictor inputs to this model are available from the National Centre for Environmental Prediction in Washington via the Internet. The model may be used to issue long range forecasts of lake inflows and lake levels with 6-3 months lead time.

$$I_{p18} = -0.586(olrasahj) - 0.602(slpaios) \qquad \textbf{Eq. 5.1}$$

$$I_{p35} = -0.08(olasahj) - 0.437\ (slpios) \qquad \textbf{Eq. 5.2}$$

$$I_{p40} = .03-0.34(aPac1)+0.34a(aSIst)-0.29(aSWp) \qquad \textbf{Eq. 5.3}$$

Table 5.2 Candidate Predictor definition

Predictor abbrev	Parameter	Area	Lat., long.
slpaios	Sfc air pressure	South Indian Ocean	40-50°S, 30-60° E
slpaaos	Sfc air pressure	South Atlantic	25-40 S, 25 ° W-0°
olrasahj	OLR	South east Sahel	5-10° N, 20-45° E
olrawios	OLR	West Indian Ocean	5-10° S, 35-60°E
pwwios	PW	West Indian Ocean	5-10° S, 35-60° E
pweaoj	PW	East Atlantic Ocean	5°S-5° N, 30°W-5° E
vwsaoj	Vector winds(850)	South Atlantic Ocean	20-30°S, 30°W-10° E
vwsioj	Vector winds(850)	South Indian Ocean	25-45°S, 55-90° E
aPac1	SST	Nino 3	5S-5° N, 180 - 90° W
aSIst	SST	South Indian Ocean	5S-20° S, 55-90° E
aSWp	Sfc air pressure	South West Indian O.	25-30°S, 40-55°E

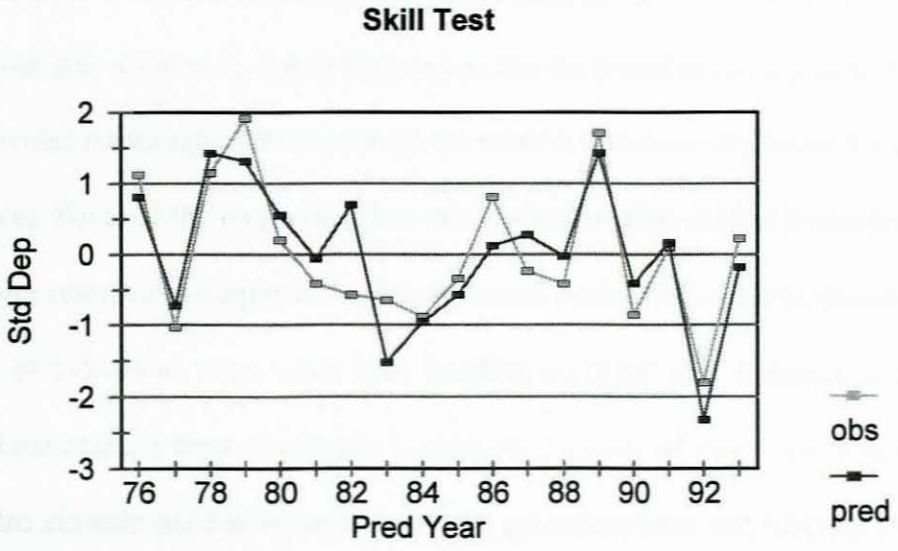

Figure 5.1 Comparison of 3 month lead-time predicted and observed inflows for Lake Malawi

5.5 Concluding Remarks

The main objective of the study was to analyse lake Malawi levels and regional runoff with a view to developing statistical forecast model(s) of summer climatic and hydrological resources over southern Africa. This is a chicken and egg relationship. First the study had to establish that the lake is barometer of climatic (in particular rainfall) variations in the region. This is evidenced in the close relationships between lake inflows and rainfall, and the Zambezi flows, and the association of the lake's outflow with evaporation. The sensitivity to interannual climatic variations is higher when inflows are used than levels hence wet years have been determined based on higher inflow index values. Then climatic patterns characterising wet years were examined. Parameters with large signals especially in the precursor months became a focus for

generating predictor data series required in model formulation. The selected variables are aimed at predicting the inflow index, I_p. It is in this context that the hypothesis is felt to be proved. This study has provided meaningful information on the relative influence of climatic fluctuations on water resources. Some of the issues raised in this research require further examination for the benefit of water resource managers in tropical Southern Africa with specific attention paid to: examination of individual years when lake flooding occurred, use of principal component analysis to pinpoint exact areas of climatic forcing mechanisms related to wet years, inclusion of more hydro climatic parameters to increase the predictors base and formulation of more models to improve forecast reliability. Therefore, further research and numerical modelling will be necessary to explain processes linking statistical indicators of regional circulation and convective processes of climatic variability. This will require continual updating of the statistical models with further predictors and higher quality data sets. This an integrated approach to water balance of Lake Malawi and offers an alternative to climatic variability monitoring in the region meant to improve the socio economic growth potential of the region.

REFERENCES

Abu-Zeid, M.A., and Biswas, A.K., 1992, Climatic Fluctuations and Water Management, Butterworth/ Heinemannn, Oxford, UK.

Aguado, E.,Cayan, D. and Riddle, L., 1993, The Influence of precipitation and temperature on seasonal streamflow in California, Water Resources Research, Vol. 29, No. 4, P1127-1140.

Beran, M., 1986, The water resource impact of future climate change and variability, UNEP/EPA, Washington D.C.

Berndstsson, R., 1987a, On the use of cross correlation analysis in studies of patterns of rainfall variability, Journ. Hydrol.

Berndstsson, R., 1987b, Spatial variation of rainfall and potential evaporation in Tunisia, Paper to be published.

Bjerknes, J., 1966, A possible response of the atmospheric Hadley circulation to equatorial anomalies of ocean temperature, Tellus, 4, 820-829.

Cayan, D.R. and D.H. Peterson, 1989, The influence of North Pacific Atmospheric Circulation on streamflow in the West, American Geophysical Union Monograph 55:375-398

Chow, V.T., 1964, Handbook of Applied Hydrology, McGrow-Hill, Newyork.

deW Rautenbach, C.J. and M.R. Jury, 1997, Atlantic Ocean Peturbation run with the CSIRO-9 GCM, Internal report, Univ. of Pretoria, 34pp.

Diaz, H.F. , 1986, Analysis of twentieth Century Climate Fluctuations in the northern North America, Journal of Climate Appl. Meteorol. Vol 25, p1625 - 1657.

Dyer, A.J., 1975, An international initiative in observing the global atmosphere, Search, 6, 29-33.

Dyer, T.G.T., 1975,The assignment of rainfall stations into homogenous groups; an application of principal component analysis, Quart. J. Roy. Met. Soc., 101, 1005-1013.

Dyer, T.G.T., 1976, On the components of time series, the removal of spatial dependence, Quart. J. Roy. Met. Soc., 102, 157-165.

Farmer, G. & Wigley, T.M.L., 1985, Climatic Trends for tropical Africa, Climatic Research Unit, Norwich.

Frick,D.M, Salas,J.D., 1991, Evaluating modelling strategies for a complex water resource system, proceedings of Vienna Symposium, Aug, IAHS no.201

Gandolfi,C., and Salewicz, K.A., 1991, Water resources management in the Zambezi Valley,

IAHS Publ. No. 201, p13-24.

Haidu, I., 1987, Fourier - Arima modelling of the multiannual flow variation, IAHS publ. No. 168, 281-286.

Harrison, M.S.J., 1984a, A generalised classification of South African summer rain - bearing synoptic systems, Journal of Climatology, 4, 547 - 560.

Harrison, M.S.J., 1986, A synoptic climatology of South African rainfall variability, Unpublished Ph.D Thesis, Univ. of Wits., 341pp.

Hastenrath, S., Merle, J., 1986, Annual Cycle of subsurface thermal structure in the tropical Atlantic Ocean, J. Phys. Oceanogy, 17, 1518-1538.

Hasternrath, S., 1988, Climate and Circulation of the Tropics, D. Rehiel Publ. Co.,Holland.

Hastenrath, S., 1990, Decadal-scale changes of the circulation in the tropical Atlantic sector associated with the Sahel drought. Int. J. Climatology, 10, 459-472.

Hastenrath, S., A. Nicklis and L. Greisher, 1993, Atmospheric-hydrospheric mechanisms of climate anomalies in the western equatorial Indian Ocean, J. Geophys. Res., 98, 20219-20235.

Hirst, A.C. and Hastenrath, S.,1983, Atmosphere-ocean mechanisms of climate anomalies in the Angola-tropical Atlantic sector, Journal of Physical Oceanography, 13, 1146-1157.

Hoskins, B.J., and Pearce, R.P.,1983, Large scale dynamic processes in the atmosphere, Academic Press, UK.

Hutchinson, G.E., 1957, A treatise on limnology, Wiley.

Jury, M.R., 1992, A climatic dipole governing the interannual variability of convection over the SW Indian Ocean and SE Africa region, Trends in Geophysical Research, 1, 165-172

Jury, M.R., Pathack, B. and Sohn, B.J., 1992, Spatial structure and interannual varability of summer convection over southern Africa and the SW Indian Ocean, S. Afr. J Sci., 88, 275-280.

Jury, M.R. 1993, A preliminary study of climatological associations and characteristics of tropical cyclones in the SW Indian Ocean, Meteorology and Atmospheric Physics, 51, 101-115.

Jury. M.R., and Pathack, B., 1993, Composite climatic patterns associted with extreme modes of summer rainfall over southern Africa, 1975-1984, Theor. Appl. Climatol., 47, 137 - 145.

Jury, M.R., 1997, Southeast Atlantic warm events; composite evolution and consequences for southern African climate, S African. J. Marine Science, 17, in press.

Jury, M.R, B.A. Parker, N. Raholijao and A. Nassor, 1995, Varability of summer rainfall over Madagascar: climate determinants at interannual scales. Int. J. Climatology, 15, 1323-1332.

Jury, M.R., 1998, Forecasting water resources in South Africa, IAHS publ. No. 252, p275-279.

Jury, M.R., Mulenga, H.M., and Mason, S.J., 1999, Exploratory long-range models to estimate summer climate variability over southern Africa, J. Climate, (in press).

Kalnay, E., and Coauthors, 1996, The NCEP/NCAR Reanalysis 40 - year Project. Bull. Amer. Met. Soc. , 77, 437 - 471.

Keith, S. & Michael, B.R., 1993, Recent Hydroclimatic fluctuations and their effect on water resources in Illinois.

Kidd, C.H.R., 1983, Advancement of Hydrological Services in Malawi; A Water Resources Evaluation of Lake Malawi and the Shire River, WMO, Geneva.

Kite, G.W., 1981, Recent changes in level of Lake Victoria, Hydrol. Sci. Bull. 26, 233-243.

Krasoviskaia and Gottschalk, 1992, Stability of rivers flow regimes, Nordic Hydrol. 23, 137-154.

Langenhove, G., Amakali, M., and Bruine, B., 1998, Variability of flow regimes in Namibian rivers: natural and human induced causes, Water resources variability in Africa, IAHS Publ. no. 252, p455-462.

Liebaert, 1997, Sharing Resources in Sadc, The Courier ACP-EU No. 161, p4.

Liebman, Brant, and Catherine A. Smith, 1996: Description of a complete Outgoing Longwave Radiation Dataset. Bull. Amer. Soc., 77, 1275 - 1277.

Long M., Entekhabi, D., Nicholson, S., 1998: Interannual Variability in rainfall, water vapor flux, and vertical motion over West Africa, IAHS Publ. No. 252.

Lindesay, J.A., 1984, Spatial and temporal rainfall variability over South Africa, 1963 to 1981, South African Geog. J., 66, 168-175.

Lindesay, J.A., 1986, Relationships between the Southern Oscillation and atmospheric circulation changes over southern Africa, Univ. of Wits.

Lindesay, J.A., 1988, South African rainfall, the Southern Oscillation and a Southern Hemisphere semi-annual cycle. Int. J. of Climatology, 8, 17-30.

Lindesay, J.A., 1988, South African rainfall, the Southern Oscillation and a southern Hemisphere semi-annual cycle. Int. J. of Climatology, 8, 17-30.

Maidment, D.R., 1993, Handbook of Hydrology, Mc GrawHill, Inc.

Mandeville, A.N., and Batchelor, C.H., 1990, estimation of actual evapotranspiration in Malawi, Report No. 110, Institute of Hydrology, UK.

Mason, S.J. and Tyson, P.D., 1992, The Modulation of sea surface temperature and rainfall associations over southern Africa with solar activity and the quasi-biennial oscillation, J. Geophys.Res., 97, 5847-5856.

Mason, I.M., Harris, A.R., Birkett, C.M., Cudlip, W., and Rapley, C.G.,1991, Remote sensing of lakes for the proxy monitoring of climatic change, Proc. 16th Ann. Conf. Remote Sensing Society, 314-324.

Mason, I.M., Guzkowska, M.A., Rapley, C.G., 1994, The response of lake levels and areas to climatic change, Climatic Change 27, p161-197, Netherlands.

Matalas, N.C., 1963, Statistics of runoff - precipitation relation, US Geological Survey, Proffessional paper, 434-D, p9.

Moss, M.E., Pearson, C.P. and McKerchar, A.I., 1994, The Southern Oscillation index as a predictor of the probability of low streamflows in New Zealand, Water Res. Research, Vol.30, No.10, p2717-2723.

Moyo,S., O'keefe, P. and Sill, M., 1993, The southern African environment; Profiles of the SADC countries. Earthscan publications ltd., London. Ch.4.

Nicholson, S.E., 1980, Saharan Climates in historic times, The Sahara and the Nile, M.A.J Williams & H.Faure (eds), 173 - 200.

Nicholson, S.E.,1986, The nature of rainfall variability in Africa south of the equator. J. Climatology, 6, 515-530.

Nicholson, S.E. and D.Entekhabi, 1987, Rainfall variability in equatorial and southern Africa: relationships with sea surface temperatures along the southwestern coast of Africa. J. Climate and Appl. Meteor., 26, 561-578.

Nicholson, S. , Yin , X., 1998, Variation of African lakes during the last two centuries, IAHS publ. no. 252, p181-187.

Nordenson, T.J., 1968, Preparation of coordinated precipitation, runoff and evaporation maps, Report no. 6, WMO, Geneva.

Ojo, O, 1990, Variations in hydroclimatic components and concepts of regionalisation in West Africa, Regionalisation in Hydrology, IAHS Publ. no. 191.

Pathack, B.M.R., 1993, Modulation of South African summer rainfall by global climatic

processes, PhD thesis, University of Cape Town.

Piper,B.S., Plinston, D.T. & Sutcliffe,J.V. , 1986, The Water Balance of Lake Victoria, Hydrol.Sci. J., 31, 25-37.

SADC Regional Remote Sensing Project, 1997, Issue 5.

Salas, J.D., Delleur, J.W., Yevjevich, V., Lane, W.L., 1980, Applied Modelling of Hydrologic Time Series, Water Resources Publications, USA.

Sene, K.J. and Plinston, D.T. 1993, A review and update of the hydrology of lake Victoria in East Africa,

Schulze, R.E., 1995, Hydrology and Agrohydrology, University of Natal, Water Res. Comm.

Sevruk, B., Geiger, H., 1981, Selection of Distribution Types for Extremes of Precipitation, World Meteorological Organisation Rep. No. 15, WMO No. 560, Geneva.

Singh, V.P., 1995, Environmental Hydrology, Netherlands.

Sutcliffe, J.V., and D.G. Knot, 1998, Historical variations in African water resources, Hydrol. Sci. J., 463-475.

Sutcliffe, J.V., and D.G. Knot, 1987, Historical variations in African water resources, In: The influence of climate change and climatiic variability on the hydrologic regime and water resources, IAHS publ. no. 168, 463-475

Taljaard, J.J., 1986, Change of rainfall distribution and circulation patterns over southern Africa. In. J. Climatology, 6, 579-592

Thiaw, W.M., Kousky, J., and Kumar, V., 1998, Atmospheric circulation associated with recent sahelian hydrologic anomalies, IAHS publ. No. 252, p63-67.

Tyson, P.D. and Dyer, T.G.T., 1975, mean annual fluctuations of precipitation in the summer rainfall region of South Africa, South Africa Geog. J., 57, 104-110.

Tyson, P.D., Dyer, T.G.T., and Mametse, M.N., 1975, Secular changes in South African rainfall: 1880-1972, Quart. of Roy. Met. Soc., 101, 817-833.

Tyson, P.D., 1980, Temporal and spatial variation of rainfall anomalies in Africa south of latitude 22 during period of meteorological record, climate change, 2, 363-371.

Tyson, P.D., 1986, Climatic Change and Variability over Southern Africa, Oxford University Press, Cape Town, 220pp

Torrance, J.D., 1972, Malawi, Rhodesia and Zambia, World Survey of Climatology, 10, 409-460.

Water Resources Branch, 1986, Water Year Book, An account of river flows, lake levels, reservoir levels and water quality November 1985 to October 1986.

Xie and Arkin, 1996, Analyses of Global Monthly Precipitation using gauge observations, Satellite Estimates, and Numerical Model Predictions.

Yevjevich, V.M., 1963, Fluctuations of Wet and Dry years, pt.I, research data assembly and mathematical models, Hydrology Paper, No.1, Corolado State University, p55.

Zuming, L., (1987), An analysis of the variation trend of the annual runoff on the eastern slope of Qilian Shan, IAHS Publ. No.168.

.

APPENDIX A

Extreme Value Analysis of Annual Maxima Series

The following analysis concerns the annual maxima series (1937-1994) for Lake Malawi Levels. The analysis is in three parts: parameter estimation of the distribution using Gumbel's method; testing whether the Type I is appropriate compared to Type II extremal; computation of confidence limits.

The following symbols have been used:

c.l. Confidence limits

c, x Scale and location parameters

D Distribution function

i Rank in descending order

k Frequency factor

l Leaps

ln Logarithm natural

N Sample size

n N-1

r Correlation coefficient of l and y_i+1/2

se Standard error of estimate

s_x,s_n Standard deviation

T Return period, (in years)

t Fractil of the standardised normal distribution

x Annual maximum of monthly lake levels, in (m)

x , y Mean

Δx, Δy difference between successive values

α Confidence level

Σ Sum

Parameter estimation of the Type I extremal distribution for the annual maxima series by Gumbel's method

Step No.	Step Description	Formulae and results
Part A		
1	Ranking of x_i in Descending order	
2		Σx_i $\bar{x} = \frac{\sum x_i}{n}$
3		x_i^2 Σx_i^2 $(\sum x_i)^2$ $s_x = \sqrt{\frac{\sum x_i^2 - \frac{(\sum x_i)^2}{n}}{n}}$
4	Calculation of return period using Weibull's formula	$T_i = \frac{n+1}{i}$
5		$y_i = -\ln(-\ln(1-\frac{1}{T_i}))$

$$\sum y_i$$

$$\bar{y} = \frac{\sum y_i}{n}$$

6 y_i^2

$$\sum y_i^2$$

$$s_n = \sqrt{\frac{\sum y_i^2 - \frac{(\sum y_i)^2}{2}}{n}}$$

Part B

Calculation of parameters of $F(x) = e^{-e^{-\frac{x-x}{c}}}$
The Type I extremal D

$$c = \frac{s_x}{s_n}$$

$$x = \bar{x} - c\bar{y}$$

Plot of x against T in Extremal probability paper

The distribution is fitted by a straight line With equation for x:

$$x(T) = x + c.y(T)$$

$$y(T) = -\ln(-\ln(1-\frac{1}{T}))$$ Where

Part C
Test for use of Type I extremal

$$\Delta x_i = x_{i+1} - x_i$$

7

$$\Delta y_i = y_{i+1} - y_i$$

9 Calculation of leaps l_i

$$l_i = \frac{\Delta x_i}{\Delta y_i}$$

10		$\sum l_i$ $\sum l_i^2$
		$y_{i+1/2} = -\ln(-\ln(1-\frac{1}{T_i+1/2}))$
11		$T_{i+1/2} = \frac{n+1}{i+1/2}$ $\sum y_{i+1/2}$ $\sum y_{i+1/2}^2$
13	The test statistic is the Correlation coefficient r of l and $y_{i+1/2}$	
	r Critical	0.22 r<<r_{crit} use of Type I extremal is accepted

Part D
Computation of the confidence limits

14	Calculation of the Frequency factor k	$k_i = (y_i-y)/s_n$ $B_i = \sqrt{(1+1.14k+1.1k2)}$
16	Standard error of estimate	$se_i = (B_i s_x)/\sqrt{n})$
	Assuming normal D, the Confidence limits are	X+- $t(\alpha).se_i$